Calhoun
Institutional Archive of the Naval Postgraduate School

Calhoun: The NPS Institutional Archive

DSpace Repository

Theses and Dissertations | 1. Thesis and Dissertation Collection, all items

1994-12

MATLAB simulation of a distributed feedback (DFB) laser with chirp effects

Espe, Burt Lann

Monterey, California. Naval Postgraduate School

http://hdl.handle.net/10945/30535

This publication is a work of the U.S. Government as defined in Title 17, United States Code, Section 101. Copyright protection is not available for this work in the United States.

Downloaded from NPS Archive: Calhoun

http://www.nps.edu/library

Calhoun is the Naval Postgraduate School's public access digital repository for research materials and institutional publications created by the NPS community. Calhoun is named for Professor of Mathematics Guy K. Calhoun, NPS's first appointed -- and published -- scholarly author.

Dudley Knox Library / Naval Postgraduate School
411 Dyer Road / 1 University Circle
Monterey, California USA 93943

NAVAL POSTGRADUATE SCHOOL
Monterey, California

DTIC
ELECTE
AUG 0 3 1995
S D
F

THESIS

MATLAB SIMULATION OF A DISTRIBUTED FEEDBACK (DFB) LASER WITH CHIRP EFFECTS

by

Burt Lann Espe

December, 1994

Thesis Advisor: John P. Powers
Thesis Co-Advisor Randy L. Borchardt

Approved for public release; distribution is unlimited.

19950802 044

J6K

REPORT DOCUMENTATION PAGE

Form Approved
OMB No. 0704-0188

Public reporting burden for this collection of information is estimated to average 1 hour per response, including the time for reviewing instructions, searching existing data sources, gathering and maintaining the data needed, and completing and reviewing the collection of information. Send comments regarding this burden estimate or any other aspect of this collection of information, including suggestions for reducing the burden, to Washington Headquarters Services, Directorate for Information Operations and Reports, 1215 Jefferson Davis Highway, Suite 1204, Arlington, VA 22202-4302, and to the Office of Management and Budget, Paperwork Reduction Project (0704-0188), Washington, DC 20503.

1. AGENCY USE ONLY *(Leave blank)*	2. REPORT DATE	3. REPORT TYPE AND DATES COVERED
	December, 1994	Master's Thesis

4. TITLE AND SUBTITLE
MATLAB SIMULATION OF A DISTRIBUTED FEEDBACK (DFB) LASER WITH CHIRP EFFECTS

5. FUNDING NUMBERS

6. AUTHOR(S)
Espe, Burt L.

7. PERFORMING ORGANIZATION NAME(S) AND ADDRESS(S)
Naval Postgraduate School
Monterey, Ca. 93943-5000

8. PERFORMING ORGANIZATION REPORT NUMBER

9. SPONSORING / MONITORING AGENCY NAME(S) AND ADDRESS(S)

10. SPONSORING / MONITORING AGENCY REPORT NUMBER

11. SUPPLEMENTARY NOTES
The views expressed in this thesis are those of the author and do not reflect the official policy or position of the Department of Defense or the U.S. Government.

12a. DISTRIBUTION / AVAILABILITY STATEMENT
Approved for public release; distribution is unlimited.

12b. DISTRIBUTION CODE

13. ABSTRACT *(Maximum 200 words)*

A model of a distributed feedback (DFB) laser was implemented in MATLAB and SIMULINK. Using the laser rate equation, the model was simulated to obtain general characteristics of the chirp of the laser's frequency. The simulations were controlled by using different drive current waveforms, based on various bit-patterns, data rates, and drive current values (threshold current and the extinction ratio). Once created, the laser drive current was passed to the SIMULINK DFB laser model. The output of a simulation provided frequency chirp, laser power emitted, photon density, and carrier density data.

Two sets of simulations were conducted. The first set of simulations focused on the data rates and bit-patterns. From these simulations it was determined that the transition from a ZERO bit to a ONE bit caused the greatest frequency excursions. Also, as the data rate increases the maximum frequency excursion increases. Finally, the first set of simulations revealed that the predictability of the chirp decreases as the data rate increases and as the complexity of the bit pattern increases.

The second set of simulations examined the effect of the extinction ratio on frequency chirp. By plotting the maximum frequency excursion against its respective extinction ratio, it was determined that in some cases the maximum frequency excursions in a system could be minimized.

14. SUBJECT TERMS	15. NUMBER OF PAGES
Chirp, Laser Rate Equations, Distributed Feedback Laser	140
	16. PRICE CODE

17. SECURITY CLASSIFICATION OF REPORT	18. SECURITY CLASSIFICATION OF THIS PAGE	19. SECURITY CLASSIFICATION OF ABSTRACT	20. LIMITATION OF ABSTRACT
UNCLASSIFIED	UNCLASSIFIED	UNCLASSIFIED	UL

Approved for public release; distribution is unlimited.

MATLAB SIMULATION OF A DISTRIBUTED FEEDBACK (DFB) LASER WITH CHIRP EFFECTS

By

Burt L. Espe
Lieutenant, United States Navy
B.S., United States Naval Academy, 1987

Submitted in partial fulfillment
of the requirements for the degree of

MASTER OF SCIENCE IN ELECTRICAL ENGINEERING

from the

NAVAL POSTGRADUATE SCHOOL
December, 1994

Accesion For
NTIS CRA&I ☒
DTIC TAB ☐
Unannounced ☐
Justification .....
By .....
Distribution /
Availability Codes
Dist | Avail and / or Special
A-1

Author: [redacted]
Burt L. Espe

Approved by: [redacted]
John P. Powers, Thesis Advisor

[redacted]
Randy L. Borchardt, Co-Advisor

[redacted]
Michael A. Morgan, Chairman
Department of Electrical and Computer Engineering

ABSTRACT

A model of a distributed feedback (DFB) laser was implemented in MATLAB and SIMULINK. Using the laser rate equation, the model was simulated to obtain general characteristics of the chirp of the laser's frequency. The simulations were controlled by using different drive current waveforms, based on various bit-patterns, data rates, and drive current values (threshold current and the extinction ratio). Once created, the laser drive current was passed to the SIMULINK DFB laser model. The output of a simulation provided frequency chirp, laser power emitted, photon density, and carrier density data.

Two sets of simulations were conducted. The first set of simulations focused on the data rates and bit-patterns. From these simulations it was determined that the transition from a ZERO bit to a ONE bit caused the greatest frequency excursions. Also, as the data rate increases the maximum frequency excursion increases. Finally, the first set of simulations revealed that the predictability of the chirp decreases as the data rate increases and as the complexity of the bit pattern increases.

The second set of simulations examined the effect of the extinction ratio on frequency chirp. By plotting the maximum frequency excursion against its respective extinction ratio, it was determined that in some cases the maximum frequency excursions in a system could be minimized.

TABLE OF CONTENTS

I. INTRODUCTION 1
II. LASER CHIRP SIMULATION 5
A. MODEL OF LASER CHIRP 5
1. Laser Drive Current 5
2. Single-mode Distributed Feedback (DFB) Laser 7
B. MATLAB SIMULATION OF CHIRP MODEL 9
1. MATLAB Implementation of the Laser Drive Current 10
2. Single-mode DFB Laser SIMULINK Simulation 14
a. Saturable Gain Coefficient, G(t) 17
b. Derivative of Carrier Density, dn(t)/dt 18
c. Derivative of Photon Density, dp(t)/dt 20
d. Instantaneous Chirp Frequency, Dv(t) 22
e. Optical Power Emitted P(t) 23
III. DATA COLLECTION 25
A. DATA COLLECTION TO FIND CHARACTERISTICS OF CHIRP 25
B. DATA COLLECTION FOR THE EXTINCTION RATIO EFFECTS 28
IV. ANALYSIS OF DATA 31
A. BIT-PATTERN/DATA RATE ANALYSIS 31
1. General Characteristics of the Chirp 31
2. Effects of Increased Data Rates on Chirp 33
3. Predictability of the Effects of Chirp 34
B. EFFECTS OF EXTINCTION RATIO 35
V. SUMMARY 37
APPENDIX A. MATLAB CODE 39
APPENDIX B. BIT- PATTERN PLOTS 55
APPENDIX C. EXTINCTION RATIO PLOTS 121
LIST OF REFERENCES 125
INITIAL DISTRIBUTION LIST 127

LISTS OF FIGURES

1. Dense WDM network model [From Ref. 1]. 1
2. (a) WDM channel without chirp. (b) WDM channel with chirp and crosstalk effects. 2
3. Examples of drive current waveforms. 6
4. Generation of the laser drive current. 12
5. Examples of MATLAB generated laser drive currents. 13
6. Example of a SIMULINK function block. 14
7. Major sections of simulation model. 16
8. Saturable gain coefficient subsystem. 17
9. Derivative of the carrier density subsystem. 19
10. Derivative of the photon density subsystem. 21
11. Instantaneous chirp frequency subsystem. 23
12. Optical power emitted subsystem. 24
13. Display of simulation data. 27
14. Typical frequency versus extinction ratio curve. 29
15. Example of bit transitions. *I_thresh* = 33.5 mA, *I_on* = 62.0 mA, *I_off* = 38.9 mA with an extinction ratio of 0.188. 32
16. Chirp effects at different data rates. *I_thresh* = 33.5 mA, *I_on* = 62.0 mA, *I_off* = 38.9 mA with an extinction ratio of 0.188. 33
17. Maximum frequency chirp (Bit-pattern => 0 111). 35

LIST OF TABLES

1. Definition and values of model/simulation parameters [Ref. 3]. 8
2. Initial conditions used in simulation. 16
3. Bit-patterns used in simulation. 26
4. Largest frequency excursion in GHz for each case. Negative values indicate that the frequency excursion had the largest value in the negative direction. 31

I. INTRODUCTION

Wavelength-division multiplexed (WDM) or wavelength-divison multiple access (WDMA) systems have been proposed to increase the aggregate bit rates of fiber optic systems. Single channel bit rates as high as 10 Gb/s are envisioned to support networks containing multiple channels, producing a combined data rate in the terabits per second (10^{12} b/s) range.

A typical *N*-channel WDM/WDMA system is shown in Figure 1. In this figure a WDM star network is depicted. It consists of fixed or tunable single-longitudinal-mode semiconductor laser diodes (such as the distributed feedback (DFB) laser for the

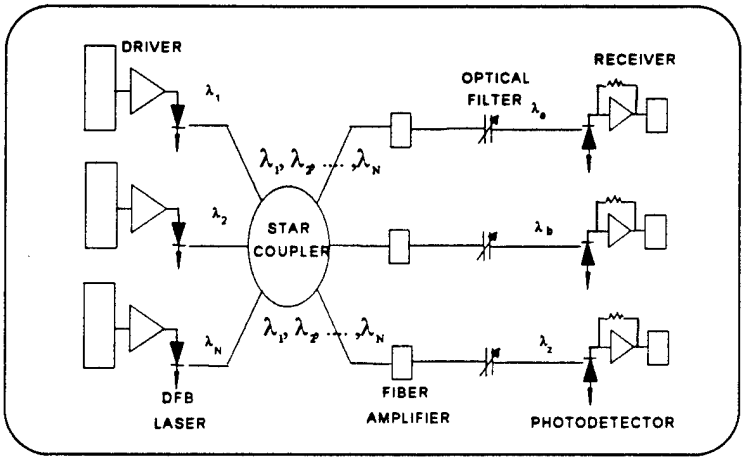

Figure 1. Dense WDM network model [From Ref. 1].

transmitters), a star coupler, optical amplifiers, and optical filters (such as fixed tuned or tunable Fabry-Perot (FP) filters) at the receiver ends [Ref. 1]. In this configuration, each transmitter produces a signal on a different wavelength (λ_1, λ_2, ..., λ_N). The signals are then passed through the star coupler, where the signals are combined and distributed to the receivers. At each of the receiver branches, an optical amplifier amplifies the combined wavelengths (λ_1, λ_2, ..., λ_N). The combined signal is then passed to a direct-detection receiver. The direct-detection receiver uses an optical filter to pass the desired wavelength, isolating the wavelength of interest (λ_a, λ_b, ..., λ_z). In this configuration any

of the source transmitters can talk to any receiver by tuning to the receiver's preasssigned wavelength.

Both ON-OFF keying (OOK) and frequency shift-keying (FSK) are feasible for WDM/WDMA systems. Direct current OOK modulation of the laser transmitter introduces frequency excursions in the laser frequency or "chirp". When passed through the optical filter, the chirped signal experiences significant degradation when the filter bandwidth is smaller than the chirp signal. Figure 2 depicts the filter responses of a multi-channel system. In the ideal system, the optical filters isolate the signal spectra in each channel (Figure 2(a)). However, when the signal is broadened by the chirp, interference from adjacent channels can occur, as in Figure 2(b). This interference is called crosstalk. It is therefore important to be able to predict the amount of frequency broadening produced by the chirp effect. Later efforts will relate the frequency broadening to the crosstalk errors.

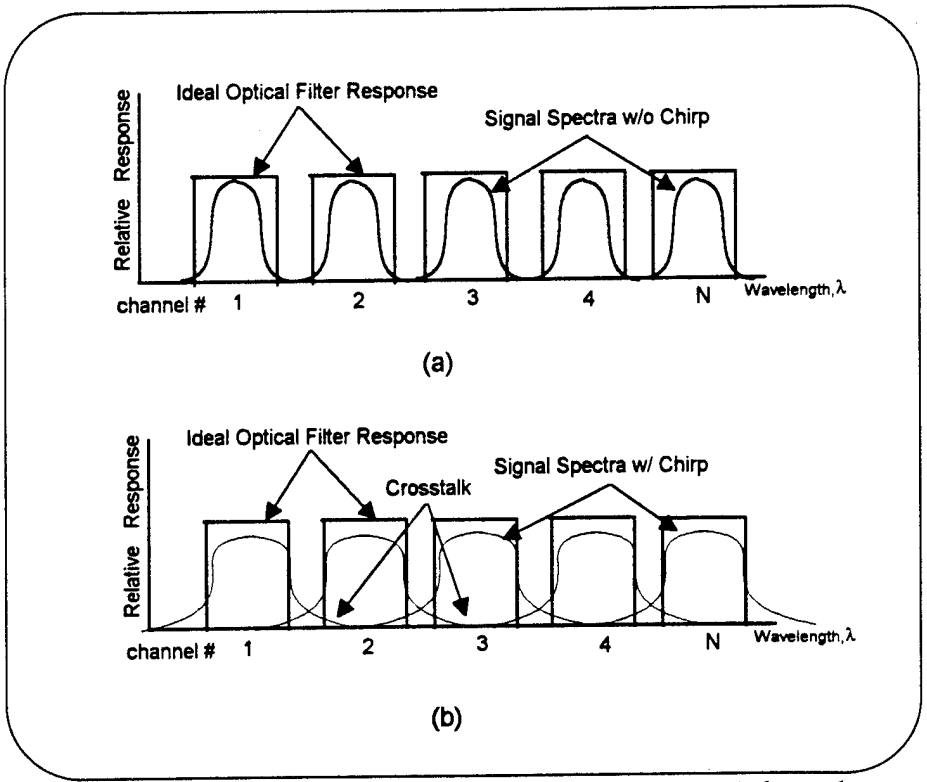

Figure 2. (a) WDM channel without chirp. (b) WDM channel with chirp and crosstalk effects.

Using MATLAB and SIMULINK, this thesis implemented a model of a DFB laser with chirp. The characteristics of chirp were explored by applying different drive currents to the model. The laser chirp model is described in the next chapter, including diagrams explaining its implementation in MATLAB and SIMULINK. The procedures used in collecting data are discussed in Chapter III, followed by an analysis of the data in Chapter IV. Finally, Chapter V reviews the MATLAB/SIMULINK model and summarizes the findings found in Chapter IV.

II. LASER CHIRP SIMULATION

The chirp model is broken into two parts, modeling the laser drive current and modeling the interactions between the charged carriers and photons in a single-mode distributed feedback laser. Both the mathematical expressions for the model and its implementation in MATLAB are discussed in this chapter.

A. MODEL OF LASER CHIRP

The expressions used to model the laser drive current, as well as the laser rate equations were provided from Ref. 1.

1. Laser Drive Current

The current pulse shape, $I_p(t)$, generated from the laser driver is dependent on the present bit and the previous bit. The drive current is characterized by Equation (1) below:

$$I_p(t) = \begin{cases} I_{bias} + I_m\left[1 - \exp\left(-\frac{2.2t}{\tau_r}\right)\right] & \text{if present bit = 1, previous bit = 0} \\ I_{bias} + I_m\left[\exp\left(-\frac{2.2t}{\tau_r}\right)\right] & \text{if present bit = 0, previous bit = 1} \\ I_{bias} & \text{if present bit = 0, previous bit = 0} \\ I_{bias} + I_m & \text{if present bit = 1, previous bit = 1} \end{cases} \quad (1)$$

where I_{bias} is the dc bias current, I_m is the modulation current, and τ_r is the rise time. The fall time is assumed to be equal to the rise time. Figure 3 shows samples of different waveforms created using Equation (1). The waveform at the top of Figure 3 has an alternating bit-pattern of ONEs and ZEROs. When the first ONE is the "present bit", the waveform rises from I_{bias} to I_m. When the next bit, a ZERO bit, becomes the "present bit",

the waveform starts to descend toward I_{bias}. The current continues to ascend and descend in this manner for all of the remaining bits in the bit-pattern. In the bottom waveform of Figure 3, the bit-pattern consists of alternating pairs of ONEs and ZEROs. In the first pair, the first ONE bit causes the waveform to ascend as before. However, since the second bit is also a ONE, the drive current remains at I_m for the second bit period. Similarly, the first ZERO bit causes the current to descend toward I_{bias}, while the second ZERO bit causes the drive current to hold at I_{bias}. The final two ONE bits cause the current to ascend and hold, repeating the actions caused by the first pair of ONE bits. Also note the different horizontal scales in Figure 3. The shape of the drive current is dependent on the bit rate and the scales on the horizontal axes differ to reflect the bit rates used.

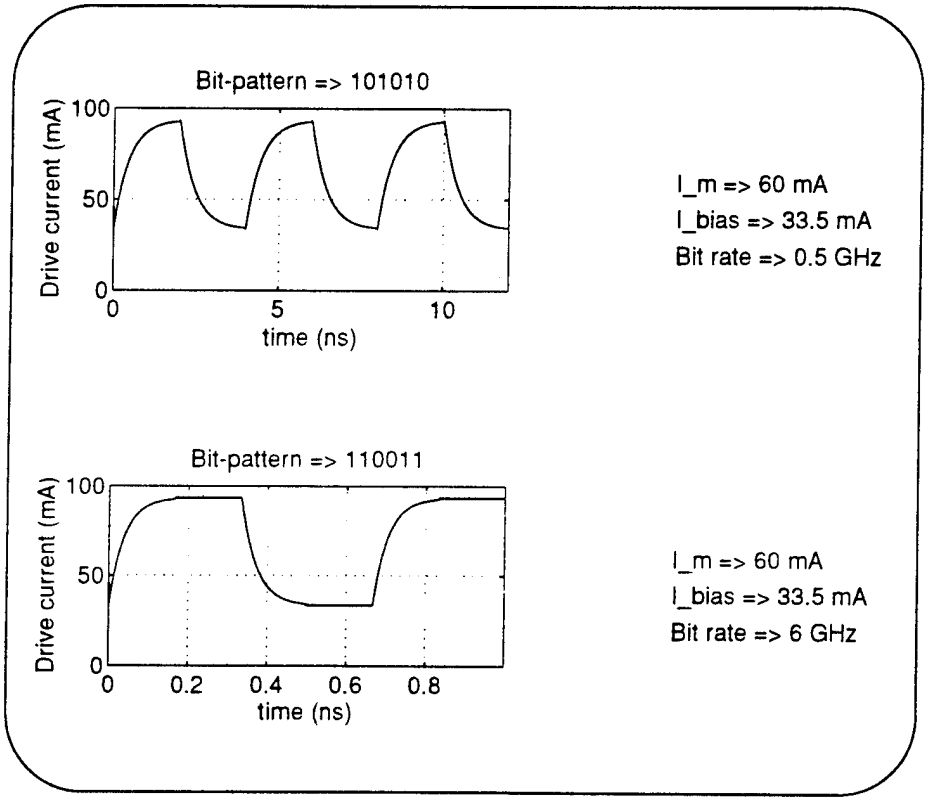

Figure 3. Examples of drive current waveforms.

2. Single-mode Distributed Feedback (DFB) Laser

The laser rate equations [Refs. 2 and 3] were used to model the operation of the DFB laser. These coupled, nonlinear differential equations describe the interactions between the photon density $p(t)$, the carrier density $n(t)$, and the phase of the electric field $\phi(t)$:

$$\frac{dp(t)}{dt} = \Gamma\, G(t)\,[n(t) - n_o]\,p(t) - \frac{p(t)}{\tau_p} + \frac{\beta\Gamma n(t)}{\tau_n} \tag{2}$$

$$\frac{dn(t)}{dt} = \frac{I_p(t)}{qV_a} - G(t)\,[n(t) - n_o]\,p(t) - \frac{n(t)}{\tau_n} \tag{3}$$

$$\frac{d\phi(t)}{dt} = \frac{\alpha}{2}\left(\Gamma\, v_g\, a_o\,[n(t) - n_o] - \frac{1}{\tau_p}\right). \tag{4}$$

Here, Γ is the mode confinement factor, n_o is the carrier density at transparency, τ_p is the photon lifetime, β is the fraction of spontaneous emission coupled into the lasing mode, τ_n is the carrier recombination lifetime, q is the electron charge , V_a is the active layer volume, v_s is the group velocity, a_o is the gain coefficient, and α is the linewidth enhancement factor.

Table 1 lists the parameter values used in the laser rate equations. The values shown are the same values presented in Ref. 3. Table 1 also shows the labels used in the computer simulations for future reference.

The parameter $G(t)$ is the saturable gain coefficient, defined by

$$G(t) = \frac{v_g\, a_o}{1 + \varepsilon\, p(t)} \tag{5}$$

Notation	Definition	Value	SIMULINK label
Γ	mode confinement factor	0.4	Gamma
n_o	electron density at transparency	1018 cm^{-1}	n_0
τ_p	photon lifetime	3 ps	tau_p
τ_n	electron lifetime	1 ns	tau_n
β	spontaneous emission factor	3×10^{-5}	beta
q	electron charge	1.6×10^{-19} C	q
V_a	active volume	1.5×10^{-10} cm^3	V_a
α	linewidth enhancement factor	5	alpha
v_g	group velocity	8.5×10^{9} cm/s	v_g
a_o	gain coefficient	2.5×10^{-16} cm^2	a_0
η_o	total quantum efficiency	0.4	eta_0
ε	gain suppression factor	10^{-17} cm^3	eps

Table 1. Definition and values of model/simulation parameters [Ref. 3].

where ε is the gain compression factor. The value of ε is also given in Table 1.

To find the optical power emitted and instantaneous chirp frequency, Equations (2) - (5) are numerically integrated using the drive current produced from Equation (1). The optical power $P(t)$ is related to the photon density $p(t)$ by

$$P(t) = \frac{p(t)}{2} \frac{V_a \eta_o h\nu}{\Gamma \tau_p}. \tag{6}$$

Similarly, the instantaneous chirp frequency, $\Delta\nu(t)$, is found from

$$\Delta\nu(t) = \frac{1}{2\pi} \frac{d\phi(t)}{dt} \tag{7}$$

where η_o is the differential quantum efficiency of the laser. The value for η_o is also given in Table 1.

Finally, substituting Equations (2) and (4) into Equation (7), the frequency chirp, $\Delta\nu(t)$, can be expressed as:

$$\Delta\nu(t) = \frac{\alpha}{4\pi}\left\{\frac{1}{p(t)}\frac{dp(t)}{dt} + \left[\frac{\varepsilon}{\tau_p} - \frac{\beta\Gamma n(t)}{\tau_n p(t)}\right]\right\}. \tag{8}$$

The "transient chirp", represented by the first term in Equation (8), occurs when the laser is turned off and on. The sudden change in current density disrupts the equilibrium of the system, creating a series of relaxation oscillations on the carrier density signal. This ultimately affects the refractive index of the lasing medium and causes the laser emission wavelength to shift correspondingly.

The "adiabatic chirp", represented by the second term in Equation (8), is the steady state frequency offset between on and off levels which exist because of differences in carrier density and gain compression levels. [Ref. 1]

Several studies have shown the ability to reduce the frequency chirp. For example, the linewidth enhancement factor, α, can be reduced from approximately a value of 5 (in a typical DFB laser) to approximately 3, either by detuning the emission wavelength [Refs. 4-6] or by using a multiple-quantum well (MQW) structure [Refs. 7 and 8]. Additionally, other parameters such as Γ and V_a can have a lesser effect on the size of the frequency chirp [Ref. 1].

B. MATLAB SIMULATION OF CHIRP MODEL

MATLAB and SIMULINK were used to simulate the model. A description of SIMULINK is given later. MATLAB is a computer program that performs mathematical computations. During a MATLAB session, the user performs calculations by executing instructions in a MATLAB workspace. The results of the calculations are stored within the workspace. One of the features of MATLAB is the ability to save a workspace in

computer memory. This allows the user to recall the workspace and restart the MATLAB session using the same variables.

The user can also automate MATLAB by using "m-files". An m-file is a set of ordered MATLAB instructions, including calls to other m-files. An m-file can either be executed to perform a single task or be defined as a function. When defined as a function, an m-file can be used like any other MATLAB function, operating on the inputs provided to it.

The following sections describe the computer implementation of the laser chirp model. The laser drive current was created using MATLAB m-files and is described first. Then, after a description of SIMULINK, the simulation model of the DFB laser is outlined and discussed.

1. MATLAB Implementation of the Laser Drive Current

In Equation (1), the laser drive current for a steady sequence of ZERO bits was I_{bias}. Likewise the drive current for a steady sequence of ONE bits was $I_{bias} + I_m$. In the MATLAB implementation of Equation (1), the drive current for a steady sequence of ONE bits was labeled as *I_on*. The value of *I_on* was defined as 1.85 times the threshold current. (The threshold current, *I_thresh*, is the drive current required for the diode to begin lasing. In this thesis, *I_thresh* is assumed to have the value of 33.5 mA.) Similarly, in the MATLAB implementation of Equation (1), the drive current for a steady sequence of ZERO bits was labeled as *I_off*.

I_off varied in the computer simulations. Its value was a function of the threshold current and the "extinction ratio". The extinction ratio, r, is defined as the ratio of lower optical power to higher optical power in a digitally modulated scheme [Ref. 9]. The following discussion shows the relationship of the MATLAB implementation of Equation (1), with the expressions given earlier. As shown below, the MATLAB implementation of Equation (1) involved the incorporation of the extinction ratio and threshold current.

Equation (9) shows the extinction ratio defined as a function of *I_off*, *I_on*, and *I_thresh*.

$$r = \frac{Power_{OFF}}{Power_{ON}} = \begin{cases} \dfrac{I\_on - I\_thresh}{I\_off - I\_thresh} & \text{for I\_off} \geq \text{I\_thresh} \\ 0 & \text{for I\_off} \leq \text{I\_thresh} \end{cases} \tag{9}$$

Solving Equation (9) for *I_off* and substituting *I_on* with 1.85**I_thresh* results in Equation (10),

$$I\_off = I\_thresh(1 + 0.85r). \tag{10}$$

The following equations relates I_{bias} and I_m with *I_off*, *I_on*, *I_thresh* and *r*. First, we know that

$$I_{bias} = I\_off = I\_thresh(1 + 0.85r). \tag{11}$$

Since

$$I\_on = I_{bias} + I_m = 1.85 * I\_thresh\ , \tag{12}$$

I_m can be put in terms of *I_thresh* and *r* by solving for I_m and substituting for *I_on* and I_{bias},

$$I_m = I\_thresh * .85(1 - r). \tag{13}$$

Finally, substituting for the numerical value of *I_thresh* results in Equation (14) and (15). These expressions relate the I_{bias}. and I_m to the variables used in the MATLAB implementation of Equation (1),

$$I_{bias} = 33.5(1 + .85r)\ \text{mA} \tag{14}$$

and

$$I_m = 28.5(1 - r)\ \text{mA}. \tag{15}$$

The MATLAB implementation of the laser drive current was produced in the main simulation m-file, *chrp_mn.m* (see Appendix A). Created as a data array, the laser drive current, *I_p(t)*, was initialized to hold 1000 elements. Based on the length of the bit-pattern, the elements were divided into three equal increments. As shown in Figure 4, these increments corresponded to the bit period, T_b, of the bit-pattern. The total simulation, therefore, was the number of bits in the bit-pattern times the bit rate. For each bit in the bit-pattern, *chrp_mn.m* determined the value of the present bit and the previous bit and applied the MATLAB implementation of Equation (1). The values for the waveform were calculated for the entire bit period (increment) and, as shown in Figure 4, each increment was appended to the previous increment. To start the creation of the *I_p(t)* data array, an initial bit, *init*, was required. *Init* simulates the "previous bit" for the first bit in the bit-pattern.

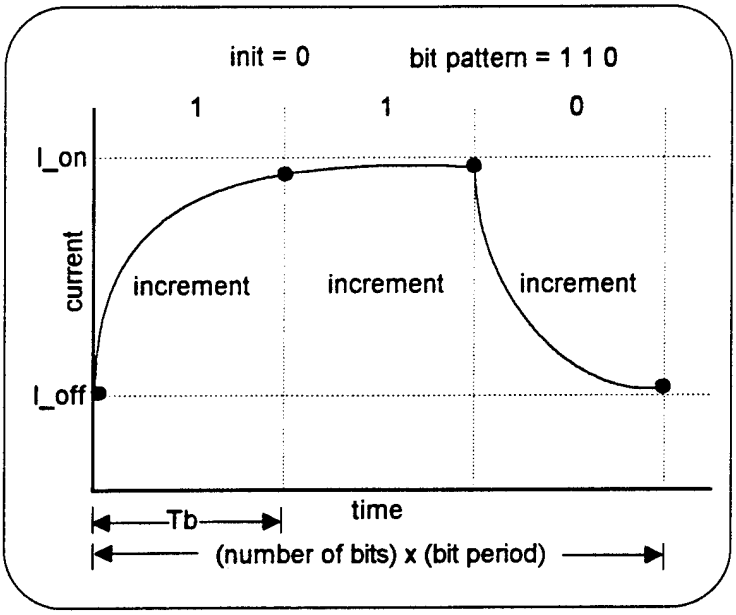

Figure 4. Generation of the laser drive current.

Examples of different drive currents are plotted in Figure 5. Figure 5 shows three waveforms, with different bit rates, bit-patterns and extinction ratios. As in Figure 3, the shape of the drive currents ascend or descend based on the bit-pattern. Additionally, the scales on the horizontal axes reflect the use of different data rates. Figure 5, however, shows the effect of the extinction ratio on the shape of the laser drive current. By holding *I_thresh* (and therefore *I_on*) constant, the value of *I_off* increases when the extinction ratio increases. Although the bottom plot shows an extinction ratio of 0.8235 for illustration purposes, typical values for OOK modulation would be lower. For OOK modulation, I_{bias} is set close to *I_thresh* (i.e., at a low extinction ratio), resulting in higher signal-to-noise ratios or, equivalently, lower bit error rates.

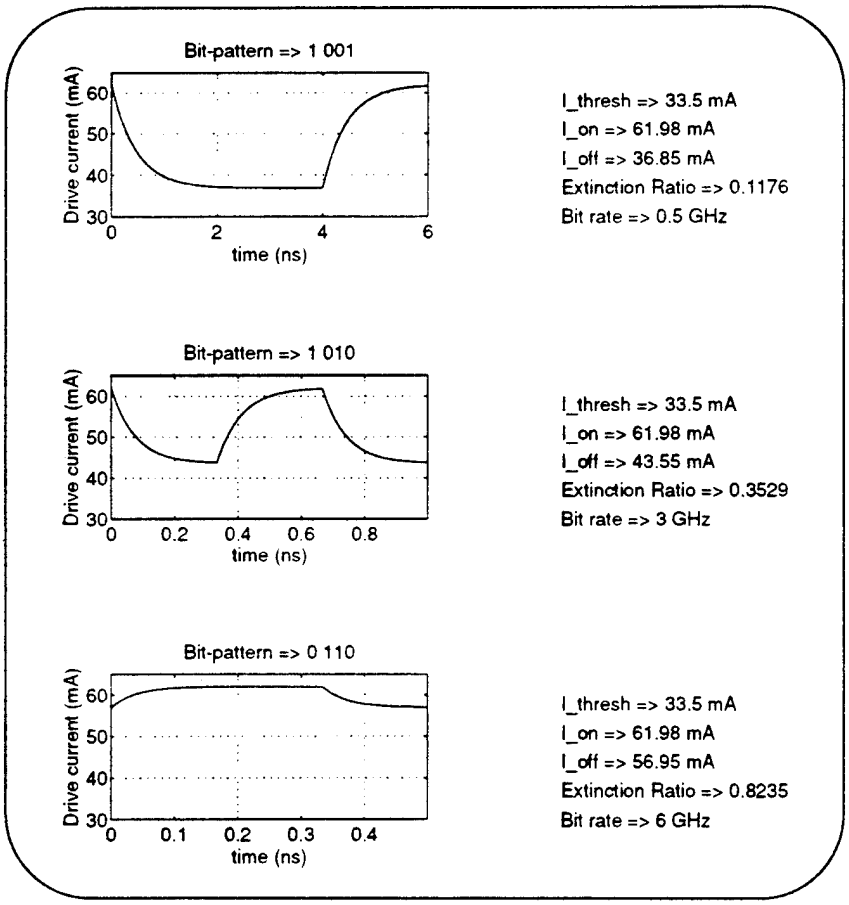

Figure 5. Examples of MATLAB generated laser drive currents.

After *I_p(t)* was created, *chrp_mn.m* passed the drive current data array, as well as the corresponding time data array, to the SIMULINK DFB laser model, *chirp.m*. The next section provides a brief overview of SIMULINK and outlines the creation of the laser model.

2. Single-mode DFB Laser SIMULINK Simulation

SIMULINK is a MATLAB tool, designed to transform a graphical representation of a mathematical model into a MATLAB m-file. The SIMULINK process has two steps. First, the model is graphically defined and, then, the model is simulated (analyzed).

Like other SIMULINK simulations, the DFB laser model was defined graphically by connecting "function blocks" together. Depicted in Figure 6, a "function block" performs a mathematical operation on its inputs, *a* and *b*, to produce an output, *f(a,b)*. Several function blocks were provided in SIMULINK. The ones most commonly used for this model were sum blocks, product blocks and inverting blocks. Sum blocks were used to perform addition or subtraction on their inputs. Product blocks multiplied their inputs together, and inverting blocks inverted their inputs. The inverting blocks and multiplication blocks were used to perform the division operation.

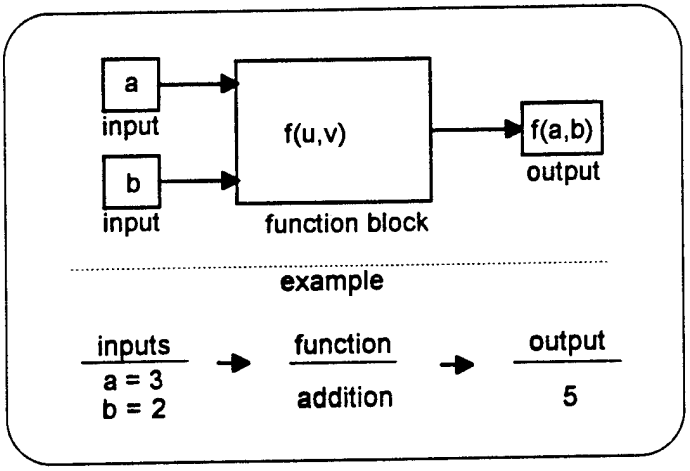

Figure 6. Example of a SIMULINK function block.

Other pre-defined blocks were also used in this model. Gain blocks, graphically represented by an op amp symbol, were used to multiply an input by a fixed amount. Blocks called "to workspace" and "from workspace" were used to pass data to and from a MATLAB workspace. Input blocks were used to provide constant values to the various function blocks. Finally, an integrator block, graphically depicted as a block with a "1/s" label, performed numerical integration.

Once the model was graphically defined, it could be simulated. However, in order to perform the required numerical integration, an integration type and initial values for the integration needed to be selected. Several integration types were provided in SIMULINK: Runge-Kutta third and fifth order methods, Gear's predictor-corrector method, Adam's predictor-corrector method, and Euler's method. The Runge-Kutta third order method was used.

The initial conditions used to integrate the derivative of the photon density and carrier density were also required. Two sets of values were necessary, corresponding to two initial bit conditions (*init* = 0 and *init* = 1). To find the initial values when *init* = 0, an all ZERO bit pattern was used. Since there is no change in the bit-pattern, the photon density and carrier density curves should remain at equilibrium. However, if the initial conditions for the photon density and carrier density were not set correctly, the signals would fluctuate until they reached equilibrium. In order to run the simulation, arbitrary initial conditions were provided for the photon and carrier density. After the simulation was completed, plots of the carrier and photon density signals were examined. Once it was determined that equilibrium levels for both photon density and carrier density had been reached, the equilibrium values were noted and used as the initial condition values (*p(0)* and *n(0)*). Likewise to find the initial conditions when *init* = 1, the model was simulated using an all ONE bit bit-pattern. When equilibrium levels had been reached, the last value of the photon density and carrier density were noted and used as the initial values, *p(1)* and *n(1)*. Table 2 shows the initial conditions that were determined and used in the simulations.

	init = 0	init = 1
photon density	p(0) = .271256e15	p(1) = 1.42154e15
carrier density	n(0) = 1.39315e18	n(1) = 1.39772e18

Table 2. Initial conditions used in simulation.

One of the features of SIMULINK was the ability to group blocks together to form "subsystems". Subsystems divide the model into small logical groups. Once a subsystem was defined, it was connected in the same manner as the pre-defined function blocks. Inside a subsystem block, were "inport" and "outport" blocks. These blocks connect inputs and outputs of the subsystem to the blocks within the subsystem.

Figure 7 shows the SIMULINK graphical model of the laser, which consisted of five major subsystems: the saturable gain coefficient (`G(t)`), the derivative of the photon density (`dn/dt`), the derivative of the carrier density (`dp/dt`), the instantaneous chirp frequency (`Chirp`), and the optical power emitted (`Power`).

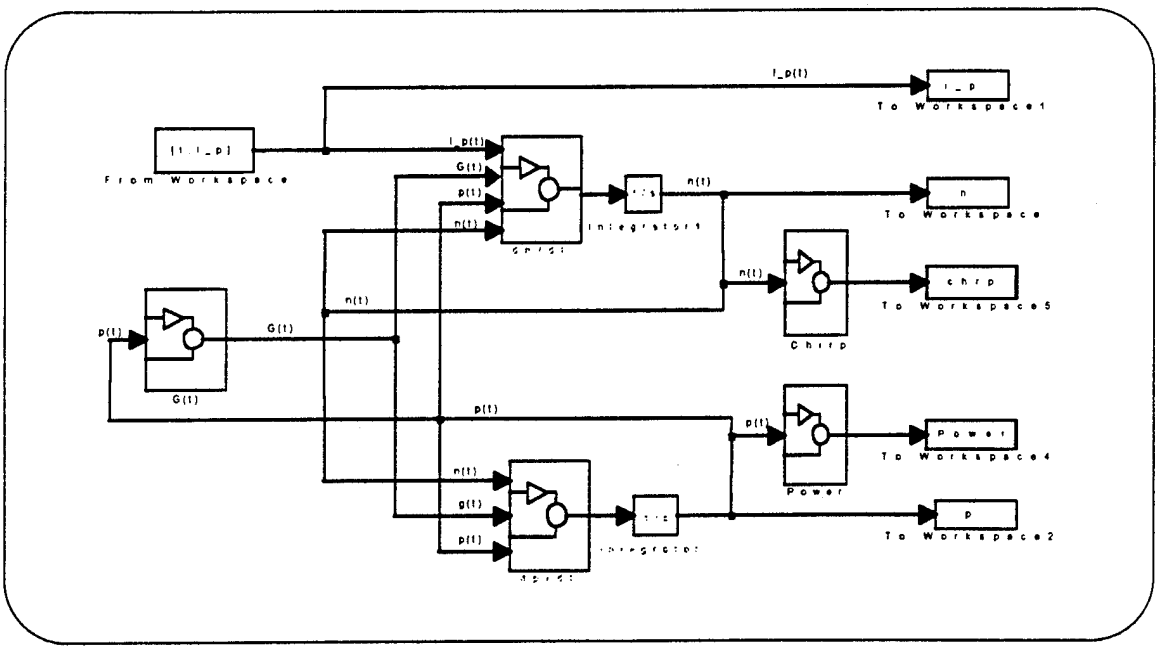

Figure 7. Major sections of simulation model.

In reviewing the block diagrams, the arrows indicate the direction of data flow. For clarity, all the inputs to a subsystem, or a function block, are shown on the left and the outputs on the right. Constants used in the simulation, found in Table 1, are indicated by their respective values inside an input block and are further distinguished by a shadow effect.

In order to help follow the SIMULINK diagrams, a detailed description of the saturable gain coefficient subsystem (Figure 8) is given. The other major subsystems are created similarly and are shown in Figures 9-12.

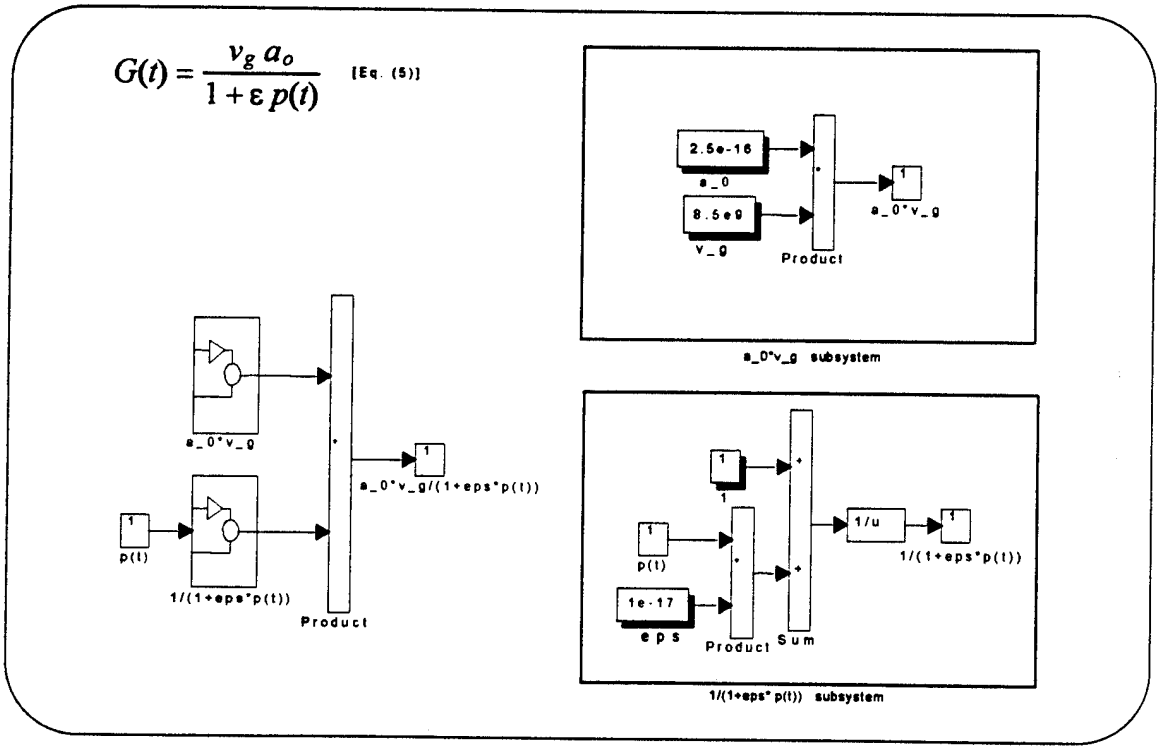

Figure 8. Saturable gain coefficient subsystem.

a. Saturable Gain Coefficient, G(t)

Figure 8 shows the breakdown of the saturable gain coefficient defined by Equation (5). This equation is repeated in the upper left corner of the figure. The diagram

at the bottom left of the figure represents the overall subsystem `G(t)`. This diagram shows how the overall subsystem is further separated into two "sub subsystems" and a product block. From Equation (5), *G(t)* was found by taking the product of a_0 and v_g, and multiplying by the inverse of $1 + \varepsilon p(t)$. The two multiplicands are produced in the two "sub subsystems", shown at the right side of Figure 8.

The subsystems for `G(t)` are labeled `a_0*v_g` and `1/(1+eps*p(t)`. The formation of the two subsystems are now considered.

1. The top right subsystem, `a_0*v_g`, calculates the product of two constants `a_0` and `v_g`, and the result is fed into the product block of the overall diagram.
2. The bottom right figure is similarly broken up:
   a) The constant `eps` and the input variable `p(t)` are multiplied together by a product block.
   b) The result, `eps*p(t)`, is then added to a constant, 1, in a sum block.
   c) The result of the addition is then passed through an inverting block, yielding `1/(1+eps*p(t))`.
   d) Finally, `1/(1+eps*p(t))` is fed into the product block of the overall diagram.

b. Derivative of Carrier Density, dn(t)/dt

Similarly, Figure 9 shows the connections that created the derivative of the carrier density. The overall subsystem, displayed at the left side of Figure (9), shows three subsystems and a product block feeding into a sum block. From Figure 7, four input variables are supplied to the `dn/dt` overall subsystem: `G(t)`, `p(t)`, `n(t)` and

I_p(t). These input variables are further distributed to the subsystems within the dn/dt subsystem.

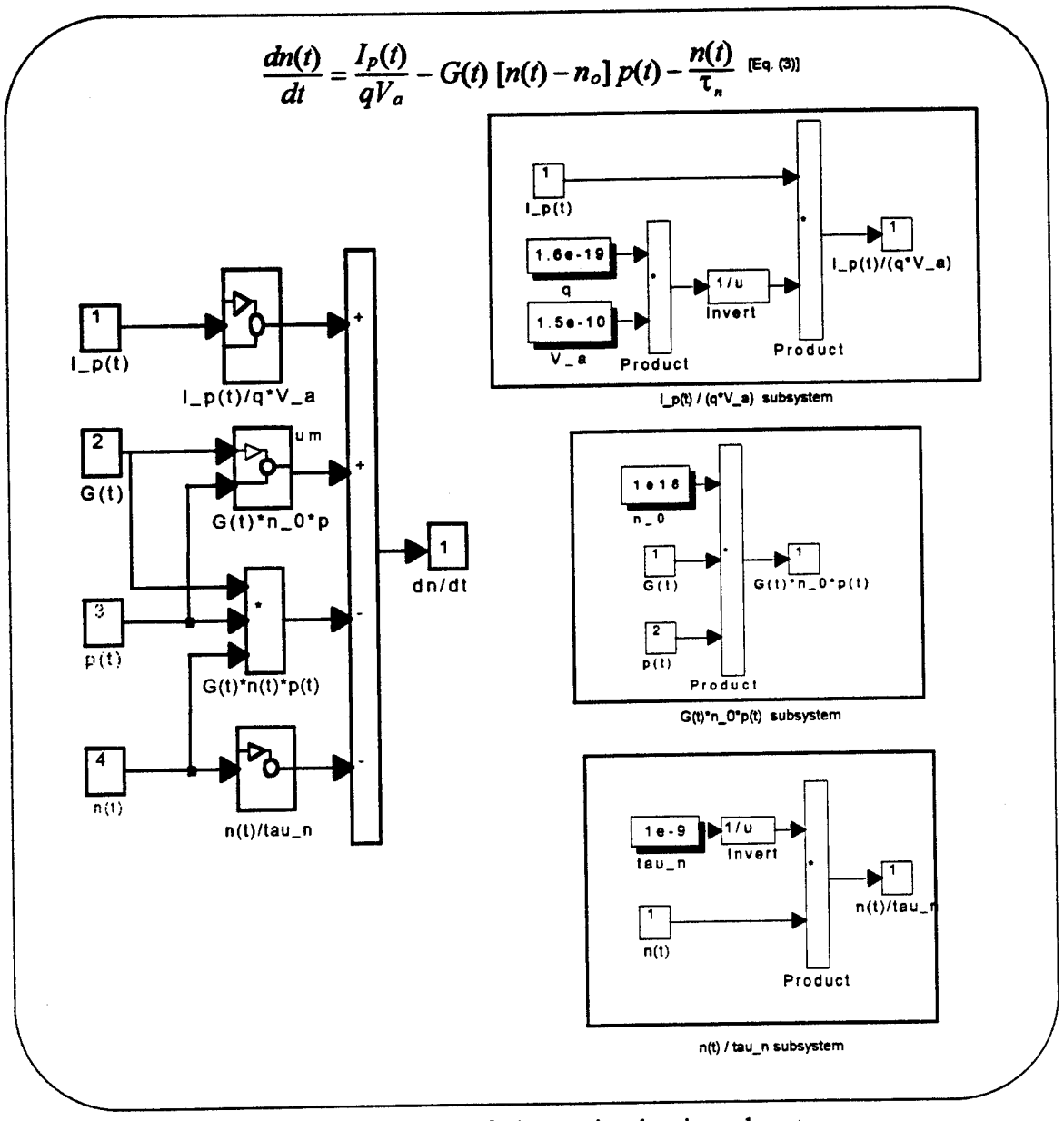

Figure 9. Derivative of the carrier density subsystem.

Equation (3), repeated at the top of Figure 9, was used to create the dn/dt subsystem. The first term on the right side of Equation (3) was calculated in the

top right subsystem diagram. This subsystem takes the input variable `I_p(t)` from an inport block and multiplies its value with the inverted product of `q` and `V_a`. The middle term on the right side Equation (3) was split into two parts. The first part was calculated by the subsystem depicted in the middle right of Figure 9. Here, the input variables `G(t)` and `p(t)` are multiplied with the constant `n_0` in a product block. The second part of the middle term was calculated with the product block found in the overall `dn/dt` subsystem diagram. The product block multiplied the input variables `G(t)`, `n(t)` and `p(t)`, and fed the result directly into the sum block of the `dn/dt` subsystem. The last subsystem, shown at the bottom right of Figure (9), calculated the last term of Equation (3). It took the product of the input variable `n(t)` and multiplied it by the inverted value of `tau_n`. The output of this subsystem, as with the other subsystems shown on the right side of Figure (9), were fed into the sum block in the overall `dn/dt` subsystem diagram. (Note that addition and subtraction was indicated by a "+" or "-" sign on the sum block.) The mathematical operation performed in the sum block reflected the same operation required in Equation (3).

c. Derivative of Photon Density, dp(t)/dt

Figure 10 shows the composition of the derivative of the photon density. Similar to the `dn/dt` subsystem, this subsystem, however, used only three input variables: `G(t)`, `p(t)`, and `n(t)`. Using Equation (2) (repeated at the top of the Figure 10), the `dp/dt` subsystem was further broken into three subsystems and a product block. The diagram on the left side of Figure 10 shows the overall `dp/dt` subsystem.

The first term on the right side of Equation (2) was split into two parts. The first part was calculated by a product block, located in the overall `dp/dt` subsystem. This product block multiplied `Gamma` with the input variables `G(t)`, `n(t)` and `p(t)`. The result of the product block fed directly into the sum block of the overall `dp/dt` subsystem. The second part of the first term was calculated in the top right subsystem.

$$\frac{dp(t)}{dt} = \Gamma G(t)\,[n(t) - n_o]\,p(t) - \frac{p(t)}{\tau_p} + \frac{\beta\Gamma n(t)}{\tau_n} \quad \text{[Eq. (2)]}$$

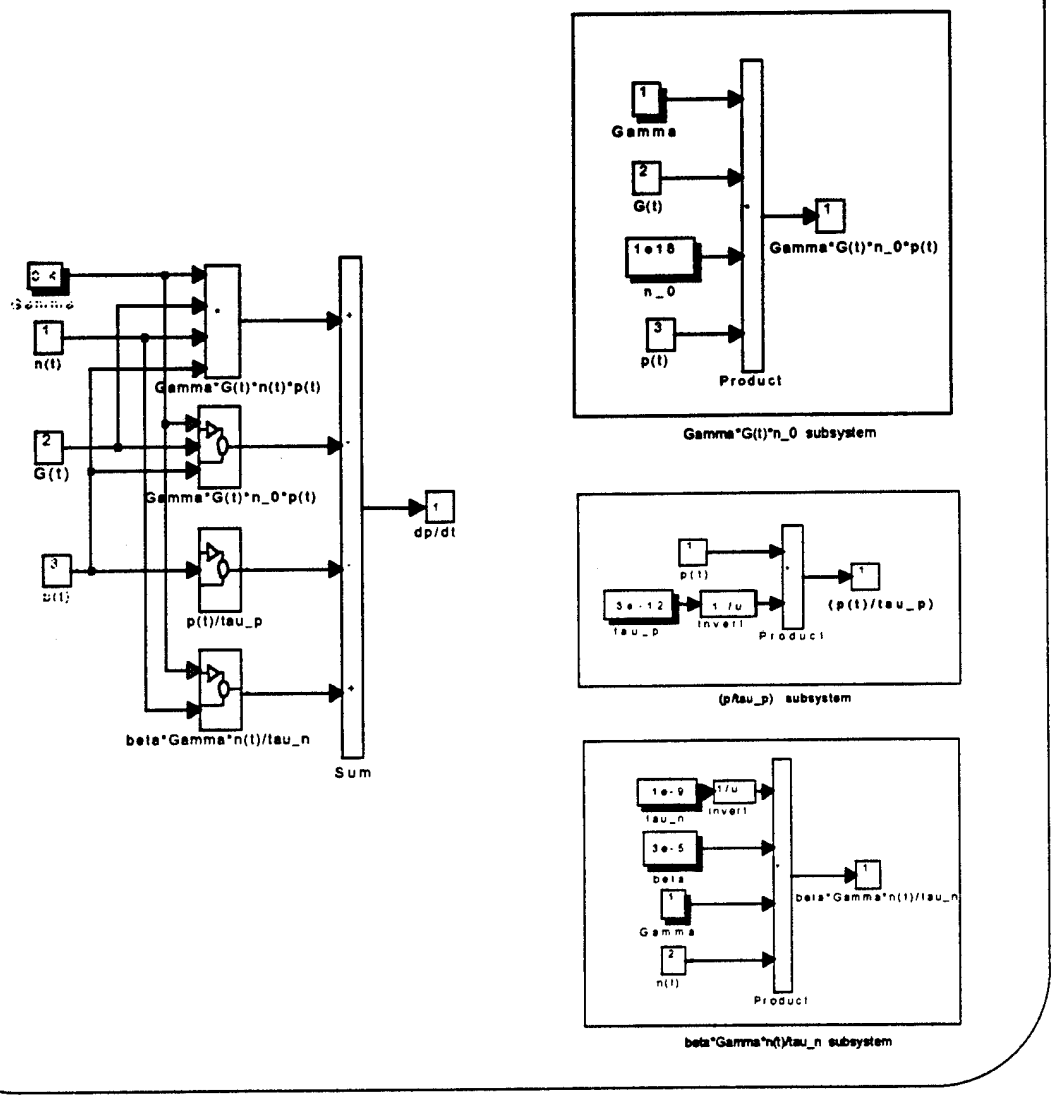

Figure 10. Derivative of the photon density subsystem.

Here, the input variables `G(t)` and `n(t)` are multiplied with the constants `Gamma` and `n_0`. The secondterm on the right side of Equation (2) was calculated in the middle right subsystem. The input variable `p(t)` was multiplied by the inverted value of `tau_p`. Finally, the third term of Equation (2) was calculated by the bottom right subsystem. Here, the input variable, `n(t)`, was multiplied by `beta`, `Gamma` and the inverted value of

tau_n. All three subsystems, shown at the right of Figure 10, were fed into the sum block of the overall dp/dt subsystem. As per Equation (2), the sum block indicates whether addition or subtraction was performed.

After the derivative of the photon density and carrier density were calculated, their outputs were fed into integrators. The integrators calculated n(t) and p(t). As shown in Figure 7, n(t) and p(t) are distributed and fed back into the system. The initial values used for the integration are given in Table 2, as discussed earlier.

d. Instantaneous Chirp Frequency, Δv(t)

The culmination of the SIMULINK model was the calculation of the instantaneous chirp frequency, shown in Figure 11. Here Equations (7) and (10) were combined to form

$$\Delta v(t) = \frac{1}{2\pi}\left(\frac{\alpha}{2}\right)\left(\Gamma v_g a_o[n(t) - n_o] - \frac{1}{\tau_p}\right). \tag{15}$$

Equation (15) was used to create the instantaneous chirp frequency subsystem.

Starting at the left side of Figure 11, the constant n_0 was subtracted from the input variable n(t) in a sum block. The result of this first sum block was then multiplied with the constants v_g, a_0 and Gamma in a product block. The result of this first product block was fed into a second sum block. The second sum block took the difference between the result of the product block and the inverse value of the constant tau_p. The result of the second sum block was then multiplied in a second product block by a factor of $\alpha/2$ ($\alpha/2$ was calculated in a gain block). The result of the second product block was scaled by a second gain block. The scaling factor for this gain block was set at $1/(2\pi)$.

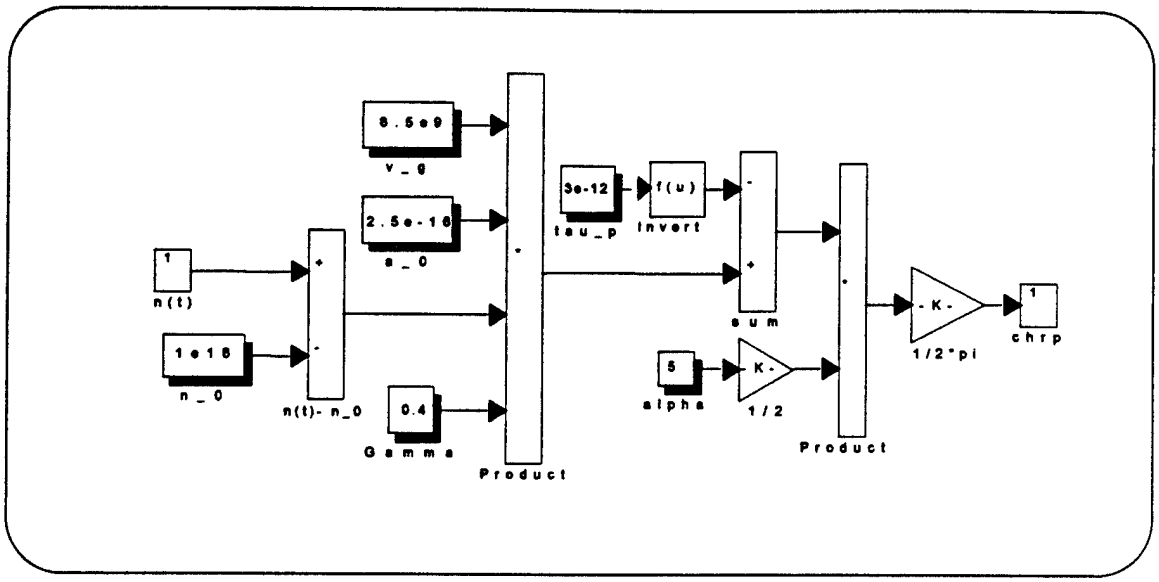

Figure 11. Instantaneous chirp frequency subsystem.

e. Optical Power Emitted P(t)

The optical power emitted was calculated as in Figure 12. By substituting the frequency, ν, for the speed of light divided by the wavelength, $\nu = c/\lambda$, Equation (6) becomes

$$P(t) = \frac{p(t)}{2}\frac{V_a \eta_o hc}{\Gamma \tau_p \lambda}. \tag{16}$$

Starting at the left side of Figure 12, the product of all the denominator terms (`lambda`, `2*tau_p`, and `Gamma`) of Equation (16) were calculated in a product block. The result of the product block was then inverted and multiplied with the numerator terms (input variable `p(t)`, `V_a`, `eta_0`, `h`, and `c`) in a second product block.

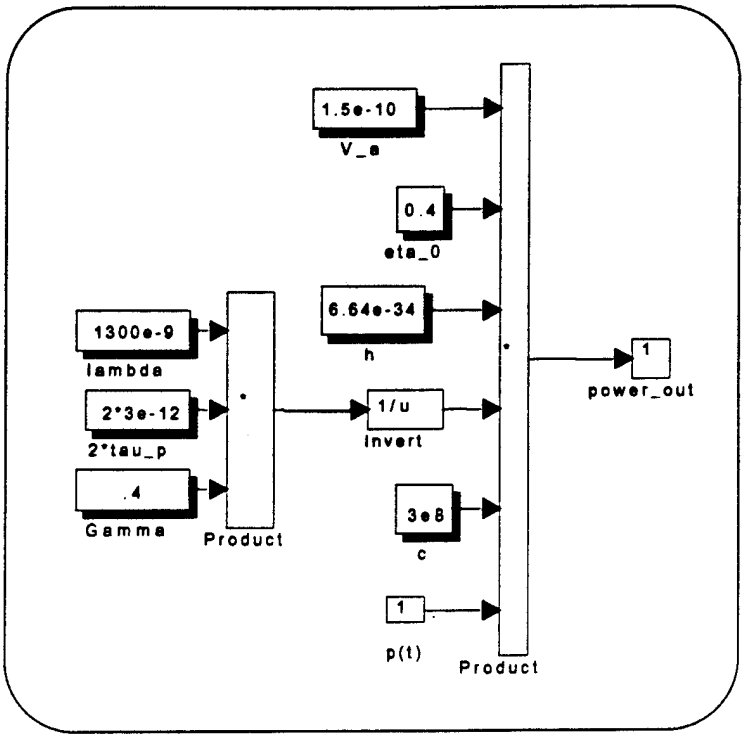

Figure 12. Optical power emitted subsystem.

The instantaneous chirp and the power emitted subsystems were connected to "to workspace" blocks. As mentioned earlier these blocks and the "from workspace" block pass data between the MATLAB workspace. Created as data arrays, the emitted power (`Power`), the instantaneous chirp frequency (`chrp`), the carrier density (`n`), the photon density (`p`), and a copy of the laser drive current (`i_p`) (shown in Figure 7) were all saved in a workspace.

In this chapter the mathematical expression for the laser drive current, as well as the laser rate equations, were modeled into MATLAB and SIMULINK. The next chapter describes the collection and storage of data, and how placing the data in separate workspaces automated the process.

III. DATA COLLECTION

The procedure for gathering data was to 1) create input parameters for the laser drive current, 2) create the drive current, 3) set the initial values for integration, 4) run a simulation of the DFB laser using the drive current as an input, and 5) collect and display the data produced by the simulations. As described in Chapter II, *chrp_mn.m* and *chirp.m* accomplished steps 2 and 4. The initial values in Step 3 are given in Table 2. However, to accomplish the other steps, a "workspace structure" was used. In a workspace, the simulation variables and/or output data arrays were maintained as individual data packages. After being assigned a name, the data packages were saved in memory and stored for future use. When needed, the data packages were reloaded into MATLAB and the information was extracted. This flexibility made it easier to retrieve and display simulation data.

A. DATA COLLECTION TO FIND CHARACTERISTICS OF CHIRP

The simulation was used in two ways: first, to find the general characteristics of frequency chirp and, second, to see how the extinction ratio value affects the model. In obtaining a generalization of chirp characteristics, the m-file *stage1.m* was created. *Stage1.m* set up simulations by combining different bit-patterns and data rates. A three bit bit-pattern with an initial condition (*init*) of 0 or 1 was used for the simulations. Table 3 shows the different initial conditions and bit-pattern combinations. Data rates of 0.5, 3, 6, and 9 gigabits per second (Gb/s) were used. These values reflect data rates associated with present LAN data rates and future designs using WDM. The sixteen bit-pattern combination and the four data rates resulted in sixty-four cases being simulated.

In the first set of simulations the extinction ratio, r, was maintained as a constant. An extinction ratio of 0.1882 was assumed. Since the extinction ratio remained the same, *I_off* was also constant. The resulting value for *I_off* was 38.36 mA. As mentioned earlier, *I_on* was held constant throughout all the simulations.

Initial Condition/Bit-patterns Combinations			
initial condition	drive current bits	initial condition	drive current bits
0	000	1	000
0	001	1	001
0	010	1	010
0	011	1	011
0	100	1	100
0	101	1	101
0	110	1	110
0	111	1	111

Table 3. Bit-patterns used in simulation.

For each of bit-pattern/data rate combinations, *stage1.m* simulated the MATLAB/SIMULINK DFB laser model. The model was initiated by a function call to *chrp_mn.m*. After *chrp_mn.m* completed the simulation run, all the parameters which defined the laser drive current (*r, I_off, I_on, I_thresh*, the bit rate, the bit-pattern, and *init*) were saved in a workspace along with the data arrays produced in the simulation (*i_p, n, p Power, chrp*). The workspace was then given a name (e.g., case1.mat, case2.mat, etc.) and saved to memory. (See Appendix A.)

The data arrays from the simulations were plotted and presented using *chrpdsp.m* (see Figure 13 for an example). In the figure, the laser power emitted, the frequency chirp, the drive current, the photon density and the carrier density were all plotted with respect to time. Additionally, case-specific information was included. The bit-pattern and bit rate are given above the plot of the power emitted and frequency chirp. The extinction ratio, *r*, along with the values for *I_thresh, I_on*, and *I_off* were provided in the text section (located right of the drive current plot). The maximum and minimum frequency chirp excursions were also calculated from the data and are provided in the text section. These values represent the most positive and most negative frequency excursions. The initial

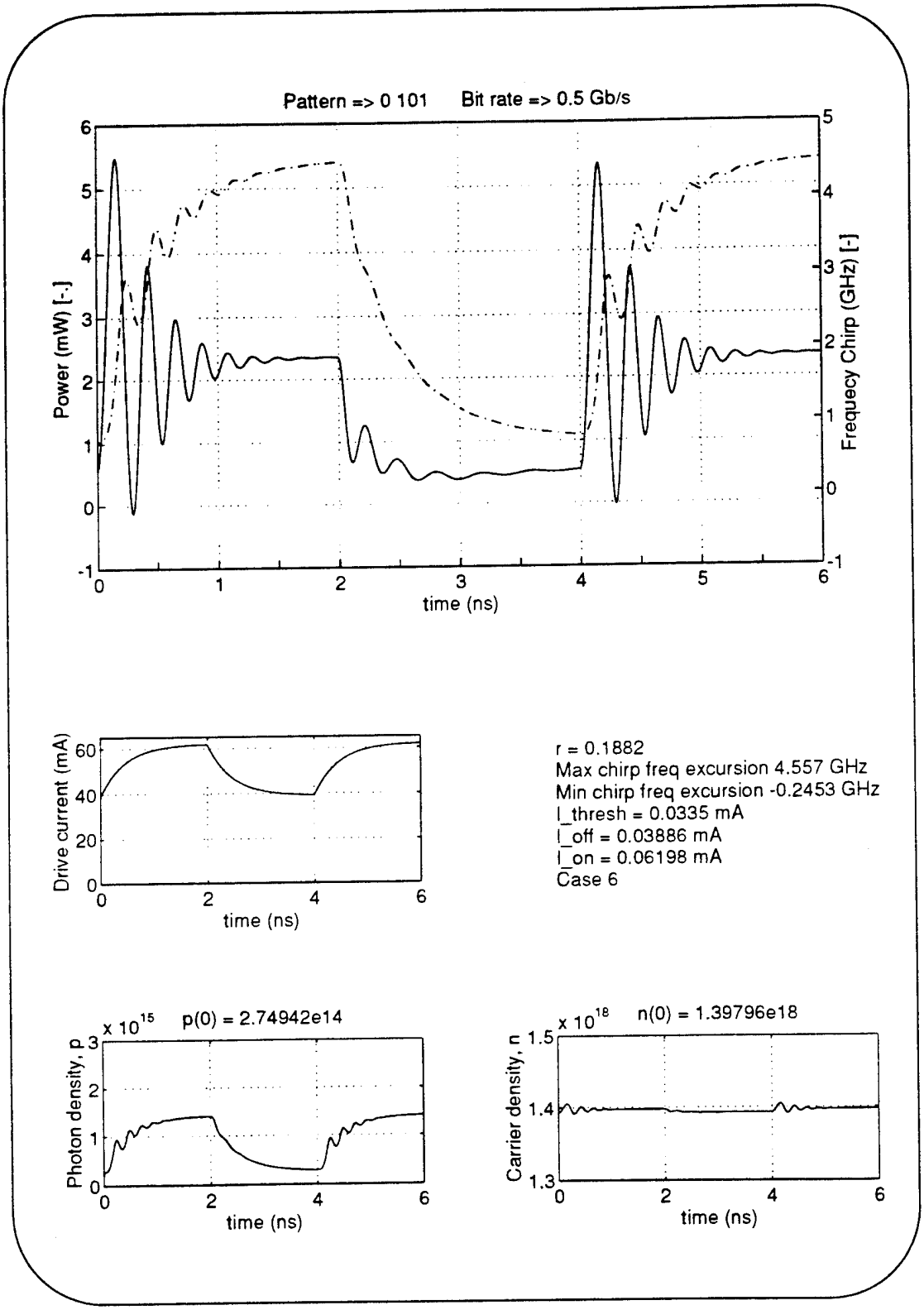

Figure 13. Display of simulation data.

condition for the photon density and carrier density were also provided in the title of their plots.

It was useful to display the laser output power and the frequency chirp on the same plot. This was accomplished with a MATLAB function obtained from Mathworks, *plotyy.m* (see Appendix A).

Another m-file, *stage4.m*, was also created to help display the data. *Stage4.m* allowed the user to call up a particular case, or a range of cases, and display the data from the respective simulations (see Appendix A).

Analysis of the plots will be provided later. However, as mentioned earlier, chirp can cause system degradation and limit the spacing in a multi-channel system. Therefore, the second area of research focused on the extinction ratio and how it affects the frequency excursions.

B. DATA COLLECTION FOR THE EXTINCTION RATIO EFFECTS

The extinction ratio was varied to examine its affect on the chirp. This was done by creating the m-file *extn_itr.m* (see Appendix A). Similar to *stage1.m, extn_itr.m* was used to set up the MATLAB/SIMULINK simulation. The different simulations involved varying the extinction ratio for a given bit-pattern and data rate. The bit-patterns were limited to 0 111, 0 101, 1 010 and 1 000. The four bit-patterns were combined with the four data rates previously used. The extinction ratio was varied between 0 and 1. The step size used to vary the extinction ratio was 0.01. This resulted in a total of 1,600 simulations.

Instead of putting each simulation in a separate case, the maximum frequency excursions from each of the simulations were stored along with their respective extinction ratio value. These values were grouped together based on the bit-pattern and data rate. Each data array held values for simulations having the same data rate and bit-pattern. A total of 16 extinction ratio data arrays were produced.

The data from the second group of simulations was used to plot the maximum frequency excursion versus extinction ratio curves. Figure 14 shows a typical plot of the maximum frequency chirp versus extinction ratio. In this particular case, the plot shows that the maximum frequency excursions curve had a minimum value. This minimum value will be discussed later in more detail.

To plot the extinction ratio curves, a second plotting routine, *plt_vec.m*, was created. *Plt_vec.m* used basic MATLAB plotting features to manipulate and display the data from the extinction ratio data arrays (see Appendix A).

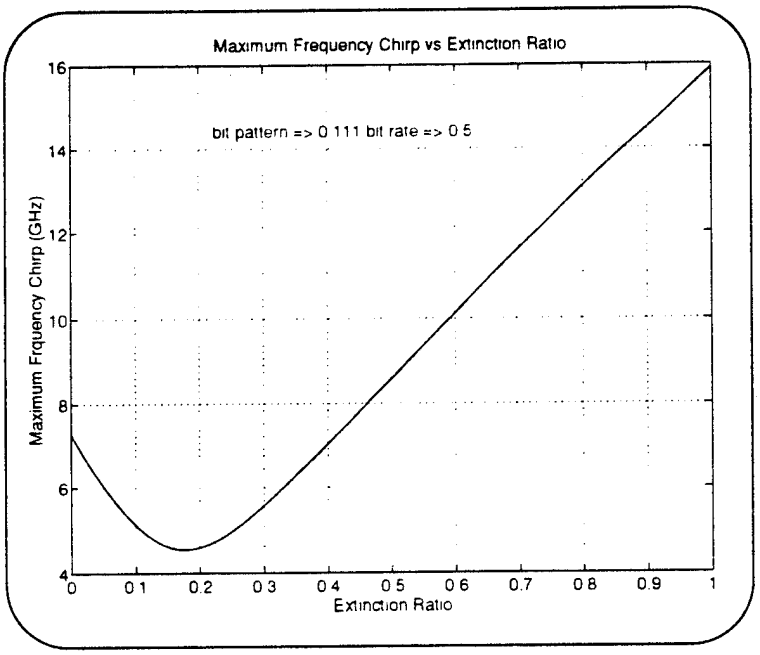

Figure 14. Typical frequency versus extinction ratio curve.

In this chapter two MATLAB m-files were described. *stage1.m* and *extn_itr.m*. These m-files set up simulations of the MATLAB/SIMULINK model. The data that was collected from the model were best analyzed in their graphical formats. The next chapter analyzes these plots in order to make general observations of the chirp effect.

IV. ANALYSIS OF DATA

The next two sections discuss the conclusions reached by analyzing the plots produced by the simulations. The first set of simulations was analyzed in an attempt to find general characteristics of chirp. These simulations focused on the trends in the frequency excursions caused by different bit-patterns and data rates. The second set of simulations was designed to evaluate the effects of the extinction ratio. Specifically, the effects of the extinction ratio on the maximum frequency excursions were explored.

A. BIT-PATTERN/DATA RATE ANALYSIS

The plots produced (provided in Appendix B) and the largest frequency excursion for each case (listed in Table 4) were examined to find trends in the laser chirp. Although some findings were not consistent throughout all of the simulations, some general observations could be made on the characteristics of the chirp.

1. General Characteristics of the Chirp

The differences in the maximum frequency excursions caused by a ZERO to ONE transition and a ONE to ZERO transition was first noted. The plots revealed that the transition from ZERO to ONE caused a greater frequency excursion than the transition from ONE to ZERO. In Figure 15, the frequency chirp curve is plotted for a bit-pattern of 1 010 with a data rate of 0.5 Gb/s. In this bit-pattern, both the transitions from ZERO to ONE and ONE to ZERO occur. Here, the maximum frequency excursion occurs when the second bit is processed, or more specifically, during the ZERO to ONE transition. Also note that the transient chirp related to the ZERO to ONE transition spans between -1 GHz to 5 GHz. The transient chirp for the ONE to ZERO transition was much smaller and spanned less than 2 GHz.

Pattern	Data Rate Gb/s			
	0.5	3	6	9
0 000	0.34	0.34	0.34	0.34
0 001	4.55	11.01	13.42	14.45
0 010	4.54	11.01	13.42	14.45
0 011	4.54	11.01	13.42	14.45
0 100	4.56	11.01	13.42	14.45
0 101	4.56	11.26	21.95	>19.87
0 110	4.56	11.01	13.42	14.45
0 111	4.56	11.01	13.42	14.45
1 000	1.88	-4.55	-7.26	-8.44
1 001	4.54	12.73	18.93	25.1
1 010	4.43	11.55	20.5	18.78
1 011	4.43	11.55	20.5	18.96
1 100	1.88	-4.54	-7.26	-8.44
1 101	4.43	11.55	20.49	18.57
1 110	1.88	-4.54	-7.26	-8.44
1 111	1.88	1.88	1.88	1.88

Table 4. Largest frequency excursion in GHz for each case. Negative values indicate that the frequency excursion had the largest value in the negative direction.

From the laser rate equations, the transient chirp and, therefore, the maximum frequency excursion, was a function of the model parameters (listed in Table 1). Later studies can apply different parameters to simulate the various laser sources available. By doing so, the transient chirp and its effects on the maximum frequency excursion can be predicted for specific optical systems.

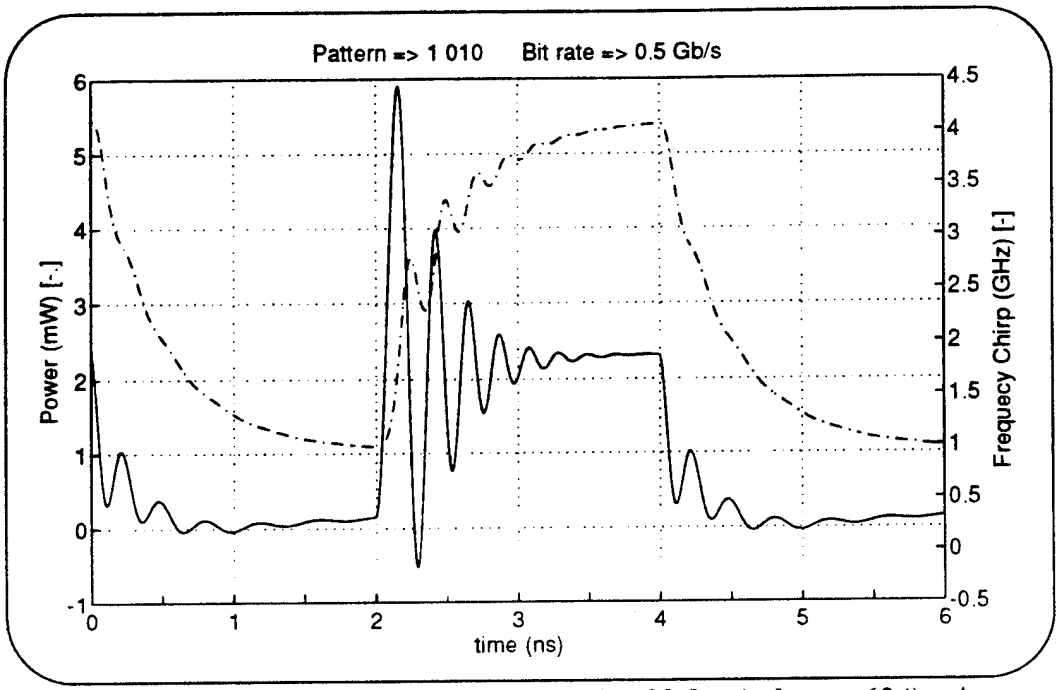

Figure 15. Example of bit transitions. *I_thresh* = 33.5 mA, *I_on* = 62.0 mA, *I_off* = 38.9 mA with an extinction ratio of 0.188.

2. Effects of Increased Data Rates on Chirp

The most significant finding from the first set of simulations was the increased maximum frequency excursion caused by an increase in the data rate. In general this observation held true; however, for the 1 010 and 1 011 bit-patterns, the maximum frequency excursion for the 9 Gb/s cases were lower than the 6 Gb/s cases.

Additionally, in the higher data rate cases, the bit would change well before the chirp oscillations had time to settle. As an example, Figure 16 shows the same bit-pattern, but with different data rates. Keeping in mind that the bit pattern is 1 010, notice that in the 0.5 Gb/s data rate case, the chirp settles before a new bit is processed and the power curve maintains the general shape of the drive current. However, in the higher data rate cases, the transient chirp does not settle within the bit period causing the power curves to

fluctuate throughout the bit period. Later efforts will determine the signal degradation caused when the duration of transient chirp exceeds the bit period.

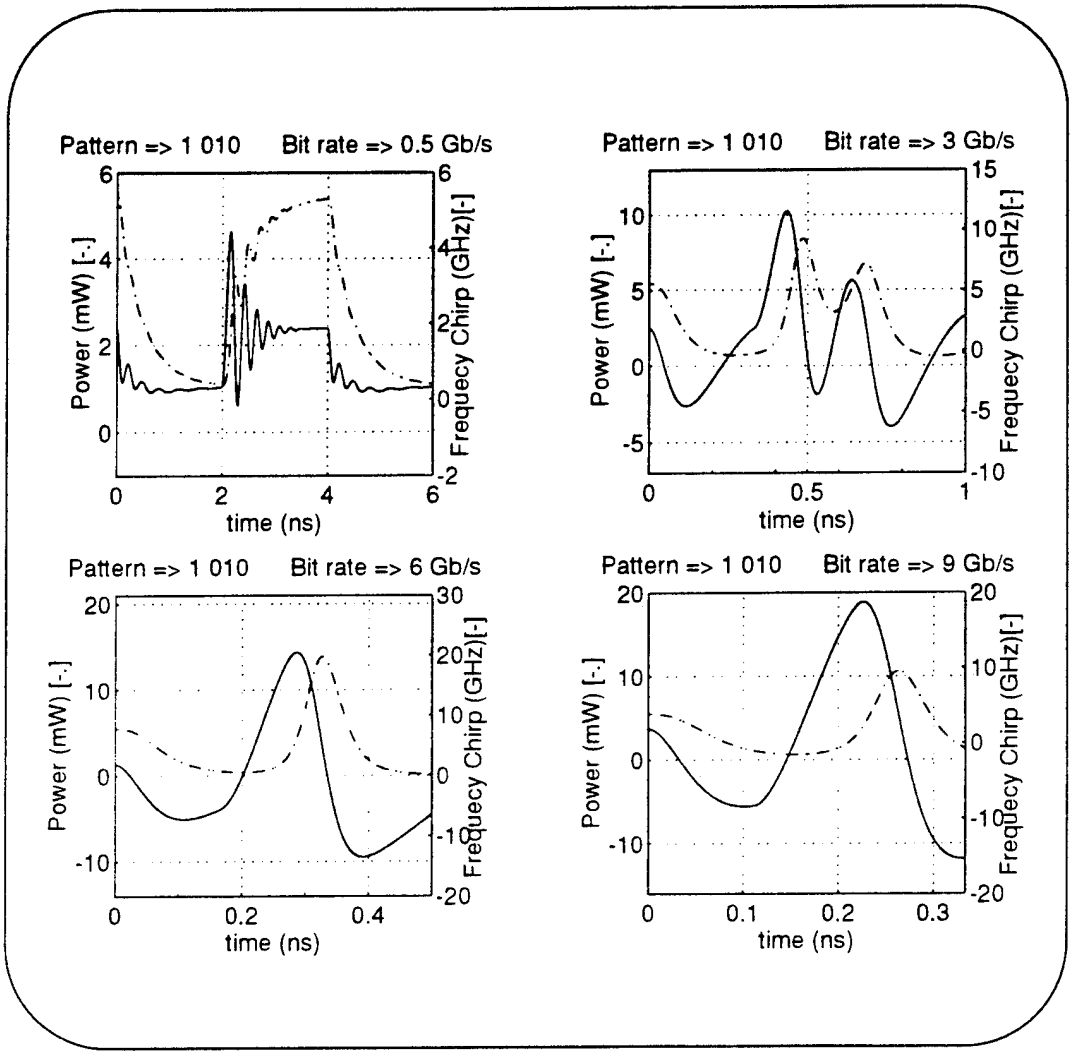
Pattern => 1 010 Bit rate => 0.5 Gb/s
Power (mW) [-]
Frequecy Chirp (GHz)[-]
time (ns)
Pattern => 1 010 Bit rate => 3 Gb/s
Power (mW) [-]
Frequecy Chirp (GHz)[-]
time (ns)
Pattern => 1 010 Bit rate => 6 Gb/s
Power (mW) [-]
Frequecy Chirp (GHz)[-]
time (ns)
Pattern => 1 010 Bit rate => 9 Gb/s
Power (mW) [-]
Frequecy Chirp (GHz)[-]
time (ns)

Figure 16. Chirp effects at different data rates. *I_thresh* = 33.5 mA, *I_on* = 62.0 mA, *I_off* = 38.9 mA with an extinction ratio of 0.188.

3. Predictability of the Effects of Chirp

The chirp was more predictable in the lower data rate cases than in the higher data rate cases. For example, in the 0.5 Gb/s cases, in all instances where a ZERO to ONE transition occurred, the maximum frequency excursion was approximately 4.5 GHz

(± 1 GHz). However, as the data rate increased, the deviation in the value of the maximum frequency excursion also increased. In the 3 Gb/s cases, the maximum frequency excursion deviated more than 1 GHz in some cases and, in the 9 Gb/s cases, the maximum frequency excursion deviated as much as 5 GHz.

Additionally, as the bit pattern became more complex (i.e., more bit transitions), the maximum frequency excursion became less predictable. This is best seen in the cases for the 1 010 and 0 101 bit-patterns. Notice that the values for these cases (listed in Table 4) are markedly different than the other values within the same data rate column.

B. EFFECTS OF EXTINCTION RATIO

It became evident that the chirp settling time was dependent on the maximum frequency excursions. Therefore, by minimizing the largest frequency excursions, the chirp relaxation oscillations would settle more rapidly. In the second set of simulations, the dependency of the chirp on the extinction ratio was explored.

As mentioned earlier only four bit-patterns were considered for this portion of the thesis. Plotting the maximum frequency excursion versus extinction ratio resulted in a variety of curves. In Figure 17, the data for 0 111 bit-pattern was plotted. This diagram shows that a minimum occurred on each curve for each of the data rates considered. This minimum was significant since it provides a value for the extinction ratio that minimizes the maximum frequency excursions. The minimum occurred around the extinction ratio value of 0.2. Figure 17 also shows, the maximum frequency excursions increase as the bit rate increases. This observation was consistent with the results found in the first set of simulations.

In the remaining extinction ratio bit-pattern cases, the plots (provided in Appendix C) did not follow any specific trend. Other than reaffirming the characteristics observed from the first set of simulations, the plots did not show any predictable behaviors.

However, it was noted that the length of the bit-patterns does not reflect a realistic digital system. Future study will have to examine the extinction ratio using longer pseudorandom patterns. A pseudorandom bit-pattern simulates a more realistic drive current and may lead to a better estimate of optimal extinction ratio values.

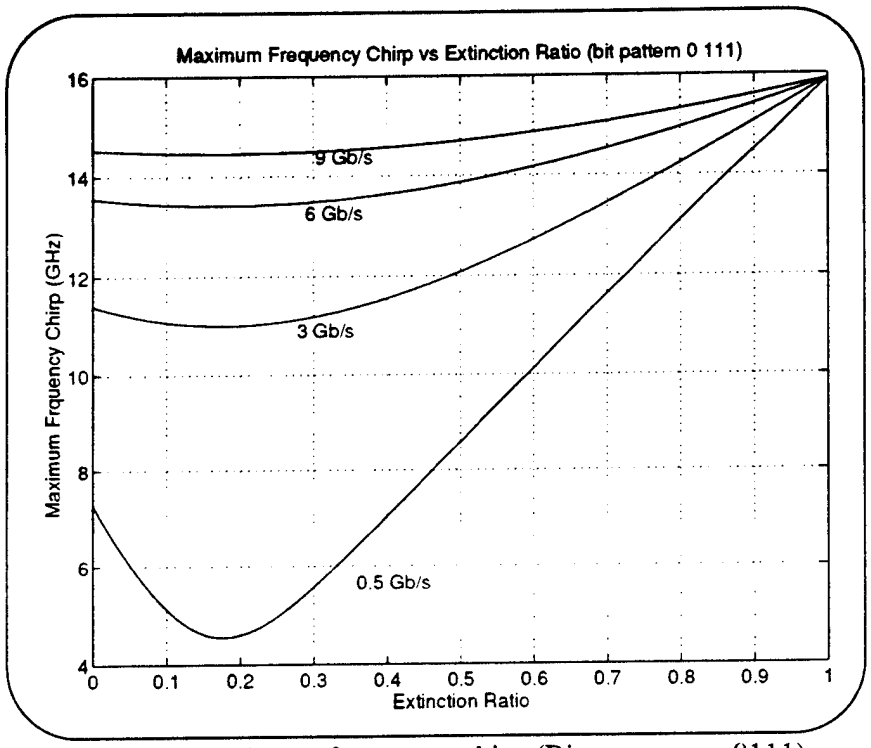

Figure 17. Maximum frequency chirp (Bit-pattern => 0111).

In analyzing the data generated by the simulations, it became apparent that an infinite number of cases could be considered. However, the trends and observations provided from the plots gave a general representation of laser chirp. The next chapter reviews the creation of the MATLAB/SIMULINK model and summarizes the findings in this chapter.

V. SUMMARY

This thesis implemented a model of a distributed feedback laser in order to predict the effects of chirp. The model, which was based on expression for a laser drive current and the laser rate equations, was implemented using MATLAB and SIMULINK. The laser drive current, which represented a signal using an OOK format, was modeled in MATLAB. Coded in an m-file, the drive current was shaped depending on the bit-pattern, the data rate and the current parameters (*I_on, I_off, I_thresh, init* and the extinction ratio). The drive current was created as a data array. Once the drive current data array was produced, it was passed into the DFB laser SIMULINK model. Using the drive current, the model simulated the dynamics of the DFB laser producing data arrays for the laser power emitted, the instantaneous chirp frequency, photon density and carrier density. These data arrays, the drive current data array and parameters that shaped the drive current were all saved in a workspace. Using workspaces allowed the data collection to be automated. By setting up the simulation in a workspace and saving the data produced from the simulation in the same workspace, information was logically grouped in data packages. After the simulations were completed, specific data packages could be recalled and the information produced could be extracted and analyzed.

Two simulation sets were conducted. The first simulation set was performed to find general characteristics of chirp. These simulations focused on the bit pattern and the data rates. It was found that the ZERO to ONE transitions caused the greatest frequency excursions. This excursion, caused by the transient chirp, was a function of the laser parameters used (listed in Table 1). Later studies can apply different parameters to model the various laser sources available. By doing so, the transient chirp and its effects on the maximum frequency excursion can be predicted better.

The most significant finding, however, was the effect of increased data rates. As the data rate increased, the duration of the relaxation oscillation in the transient chirp did not settle out before a new bit was processed. Later efforts will need to determine the signal degradation caused when the duration of transient chirp exceeds the bit period.

Finally, in the first set of simulations, it was determined that the predictability of chirp decreases as the bit rate increases and as the bit-pattern becomes more complex. This observation tends to emphasis the need to reduce the chirp, in order to increase the data rate of a channel.

The second set of simulations provided some insight into the effects of varying the extinction ratio. The plots of the maximum frequency excursions versus extinction ratio had varying results. For the 0 111 bit-pattern cases, a minimum value near $r = 0.2$ occurred in each curve. This minimum represents a value of the extinction ratio where the maximum frequency excursion would be minimized. The other plots, however, did not exhibit any predictable behavior. Future study should incorporate the use of longer pseudorandom bit-patterns to simulate a more realistic drive current. These simulation may lead to a general setting for the extinction ratio that would minimize the maximum frequency excursion for a digitally modulated signal.

The MATLAB simulation of DFB laser provided insight into the behavior of chirp. The importance of predicting the effects of frequency chirp is evident in the design of WDM/WDMA systems. In a dense WDM/WDMA system, the combined crosstalk and chirp effect limit the spacing between channels and degrades the transmitted signal. By characterizing and finding ways to limit the chirp, denser systems can be constructed. Combined with other advances in optical technology, such as improved Fabry-Perot filters and laser source enhancements, the high-capacity, high-data rate systems envisioned can be realized and made useful for mass data transfer applications.

APPENDIX A. MATLAB CODE

This appendix contains MATLAB codes used in this thesis. The order of presentation is given below:

A-1	*chrp_mn.m*	main simulation program
A-2	*stage1.m*	input parameter generator (different bit-patterns)
A-3	*extn_itr.m*	input parameter generator (different extinction ratios)
A-4	*stage4.m*	display m-file, selects specific cases
A-5	*chrp_dsp.m*	function call to produce display graphic
A-6	*vec_plt.m*	display extinction ratio plots
A-7	*plotyy.m*	special plot feature, provided by Mathworks

A-1. *Chrp_mn.m*

This is the main m-file function that initiates the simulation. It creates the laser drive current and makes a function call to the SIMULINK model.

```
%chrp_mn.m  This function take input parameters from either
%           stage1.m or extn_itr.m, and creates a laser driving
%           current. It then makes a function call to chirp.m to
%           execute a simulation run.

function [ ] = chrp_mn( );
global B ns N a I_thresh I_on I_off r I_p Power chrp p ...    n i_p t
init case_no;

% Calculate driving current input current parameters
 T_B = 1/B;                              %% Bit period
 tau_rise =0.5*T_B;                      %% Rise-time
 tau_fall = tau_rise;                    %% Fall time
 N = length(a);

% Setup arrays
 ns = 1000;
 t = zeros(ns,1);       % Initialize time array
 t(:) = linspace(0,N*T_B,ns);       % Divide N bit periods
                                         %  into n pieces.
 I_p = zeros(ns,1);                 % Intialize I_p array.

%% Start of I_p iteration routine

% Initial bit
 if init == 1
   I_start = I_on;
  else
   I_start = I_off;
 end

% Bit Pattern
 incr_beg = 1;

 for j = [1:N];
  incr = j*ns/N;

 if a(1,j) == 1
   I_aim = I_on;
   tau = tau_rise;
  else
   I_aim = I_off;
   tau = tau_fall;
 end

 I_p(incr_beg:floor(incr)) = I_aim - (I_aim-I_start).* ...
   exp(-2.2*(t(incr_beg:floor(incr))-t(incr_beg))/tau);

 I_start = I_p(floor(incr));   %save last value of I_p
```

```
 incr_beg = ceil(incr);        %save position of last I_p

end

%%% End of I_p Creation


%%% Start SIMULINK Simulation

% Initial values for SIMULINK Chirp Model
 start = N/B/1000;
 min_inc = N/B/1000;
 max_inc = N/B/1000;
 tol = 1e-5;
 stop = N/B;

 ss = [start stop];
 incr = [tol min_inc max_inc];

% SYNTAX NOTE: x0 must be column array
 if init == 1
   x0 = [1.39772*1e18
         1.42154*1e15];
   else

   x0 = [1.39315*1e18
         2.71256*1e14];
 end

% Simulation
[t,x,y] = rk23('chirp', ss, x0, incr);

%%% End SIMULINK Simulation
```

A-2. *Stage1.m*.

This m-file creates input variable for chrp_mn.m, iterating bit-patterns and bit rates.

```
%stage1.m  This m-file produces the input parameters for chrp_mn.m and
%          creates a workspace to store input and output values.

clear

 global B ns N a I_thresh I_on I_off r I_p Power chrp p n i_p2 t ...
init case_no;

%Calculate necessary input values.

 I_thresh = 33.5e-3;                        %% I_thresh is 33.5 mA
 I_on = 1.85*I_thresh;                      %% I_on is 1.85x threshold
 x = 1.16; I_off = x*I_thresh;                    %% Set I_off
 r=(I_off-I_thresh)/(I_on-I_thresh);              %% Extinction ratio.

A = [ 0 0 0                              %Matrix with 8 different patterns
      0 0 1
      0 1 0
      0 1 1
      1 0 0
      1 0 1
      1 1 0
      1 1 1];

b = [.5e9 3e9 6e9 9e9];                  %Four different bit rates

count = 0;
 for i = [1:4]                     %iterate for 4 Bit rates
  for init = [0:1]                 %iterate for 2 initial conditions
   for     j = [1:8]               %iterate for 8 possible Bit-patterns

     count = count + 1;
       a = A(j,:);
       B = b(1,i);

   chrp_mn                         %functional call to execute simulation

%SETUP WORKSPACE AND STORE DATA
   case_no = count;
   savcase = [ 'save case' num2str(count) ' t Power chrp p n i_p2 B ...
a I_thresh I_on I_off r init case_no' ];

   eval ([savcase]);     %save values in a workspace


    end
  end
end
```

A-3. *Extn_itr.m*

This m-file sets up the second set of simulation. It iterates the extinction ratio for specific bit-patterns and bit rates.

```
%extn_itr.m  This m-file sets up the second set of simulation.
%            It iterates the extinction ratio for specific
%            bit-patterns and bit rates.


global B ns N a I_thresh I_on I_off r I_p Power chrp p n i_p2 t ...
 init plot_no;

%This routine iterates the value of x that varies the extinction ratio

b = [.5 3 6 9];                          %Bit rates of interest
aA = [0 1 1 1                            %Bit patterns of interest
      1 0 0 0
      0 1 0 1
      1 0 1 0];

lst_plot = 0;

for j = [1:4];
 a = aA(j,2:4);

  init = aA(j,1);

  for i = [1:4]
   B = b(1,i)*1e9;

   arr_count = 0;

   for x = [1:.01:1.85]
    I_thresh= 33.5e-3;
    I_on = 1.85*I_thresh; I_off = x*I_thresh;
    r=(I_off-I_thresh)/(I_on-I_thresh);
    chrp_mn

    arr_count = arr_count + 1;
    temp_max_chrp = max(abs(chrp));
    temp_r = r;

    vec(arr_count,2) = temp_max_chrp;    %create data arrays with
    vec(arr_count,1) = temp_r;           %maximum excursion values

   end

  lst_plot = lst_plot + 1;               %save arrays in a workspace
  savplot = [ 'save plot' num2str(lst_plot)  ' vec a B init' ];
  eval ([savplot]);
```

```
    clear vec a B init;
  end
end
```

A-4. *Stage4.m*

Stage4.m is a menu-driven display program, that allows the user to specify specific cases or a range of cases to display.

```
%stage4.m This program allows the users to call up specific simulation
%         cases, and view or print the associcated figure.

case_in = 0;
 while 1
 if case_in == 4, break,end
 clear;
 clg;

case_in = menu('Which case to Display', 'Specific', 'Range', ...
'Print All', 'Done');

%PRINT ALL THE GRAPHICS
 if case_in == 3
 k = 59;
 while 1

 k= k+1;
 filek = ['case' int2str(k)];
 filename = [filek '.mat'];
   if ~exist(filename),break,end
   eval(['load ' filename])
   pause off
 chrpdsp(t,Power,chrp,p,n,i_p2,B,a,I_thresh,I_on,I_off,r,init,case_no);

 print  all  -append -dps
 pause
 clg
end
end

%PRINT A SET OF GRAPHIC IN A SPECIFIED RANGE WITH THE OPTION OF PRINTING
if case_in == 2
 start = input('Starting Case #');
 stop = input('End Case #');

 for k = (start:stop);
  filek = ['case' int2str(k)];
  filename = [filek '.mat'];
  eval(['load ' filename])

 chrpdsp(t,Power,chrp,p,n,i_p2,B,a,I_thresh,I_on,I_off,r,init,case_no);
  prnt = menu('Print Out', 'Yes', 'No');
  orient tall;
  if prnt == 1,print -dps,end;
 pause
 end
end
```

```
%DISPLAY A SPECIFIC CASE WITH THE OPTION OF PRINTING

if case_in == 1
k = input('Case #');
filek = ['case' int2str(k)];
 filename = [filek '.mat']
 eval(['load ' filename])
 chrpdsp(t,Power,chrp,p,n,i_p2,B,a,I_thresh,I_on,I_off,r,init,case_no);
 prnt = menu('Print Out', 'Yes', 'No');
 orient tall;
 if prnt == 1,print -dps,end;
 pause
end

end
```

A-5. *Chrp_dsp.m*

This m-file function plots the data produced in chirp.m.

```
%chrp_dsp.m  This function produces the graphic of a specified case,
%            ploting the data from simulation runs.

function [ ] =chrpdsp(t,Power,chrp,p,n,i_p2,B,a,I_thresh, ...
 I_on,I_off,r,init,case_no);

orient tall
subplot(211)

y_max = max(Power)*1e3;
y_min = min(Power)*1e3;

if max(chrp)*1e-9 > y_max,y_max=max(chrp*1e-9);,end;
if min(chrp)*1e-9 < y_min,y_min=min(chrp*1e-9);,end;

y_max = round(y_max)+1;
y_min = round(y_min)-1;

b=B*1e-9;

plotyy(1e9*t,1e3*Power,1e9*t,1e-9*chrp,'Frequecy Chirp (GHz)');
xlabel('time (ns)');ylabel('Power (mW)');
title(['Pattern => 'num2str(init)' ' num2str(a) '    Bit rate => ' ...
num2str(b) ' Gb/s']);
axis([0 max(1e9*t) y_min y_max]);grid;

subplot(427)
plot(1e9*t,p,'b'); ylabel('Photon density, p'); xlabel('time (ns)');
title('p(0) = 1.4217e15');axis([0 1e9*max(t) 0 3e15]);grid;

subplot(428)
plot(1e9*t,n,'b'); ylabel('Carrier density, n'); xlabel('time (ns)');
title('n(0) = 1.3978e18');axis([0 max(1e9*t) 1.3e18 1.5e18]);grid;

subplot(425)
plot(1e9*t,1e3*i_p2,'b');ylabel('Drive current (mA)'); xlabel('time ...
(ns)');
axis([0 max(1e9*t) 0 65]);grid;

subplot(426)
axis('off')
text(0,.45,['I_thresh = ' num2str(I_thresh)]);
text(0,.3,['I_off = ' num2str(I_off)]);
text(0,.15,['I_on = ' num2str(I_on)]);
text(0,.9,['r = ' num2str(r)]);
text(0,0,['Case ' num2str(case_no)]);
text(0,.75,['Max chirp freq excursion ' num2str(1e-9*max(chrp)) 'GHz']);
text(0,.6,['Min chirp freq excursion ' num2str(1e-9*min(chrp)) ' GHz']);
```

A-6. *Plt_vec.m*

This program extracts data from the data arrays produced in the second simulation set. First, it loads all the data arrays into a matrix and, then, plots the extinction ratio versus maximum frequency excursion curves.

```
%plt_vec.m  This program extracts data from the data obtained
%           in the second simulation set. First, it loads all
%           the data arrays into a matrix and, then, plots the
%           extinction ratio versus maximum frequency
%           excursion curves.

clear
!rm ext_gr.ps



for i = [0:3];

for j = [1:4];
 eval ( ['load plot' num2str(i*4+j)] );
  pltmatx(:,j) = vec(:,1);
  pltmaty(:,j) = vec(:,2)*1e-9;
end

plot(pltmatx(:,1),pltmaty(:,1),pltmatx(:,2),pltmaty(:,2), ...
pltmatx(:,3),pltmaty(:,3),pltmatx(:,4),pltmaty(:,4));
 xlabel('Extinction Ratio');
 ylabel('Maximum Frquency Chirp (GHz)');

 gtext('0.5 Gb/s');
 gtext('3 Gb/s');
 gtext('6 Gb/s');
 gtext('9 Gb/s');
 title(['Maximum Frequency Chirp vs Extinction Ratio (bit pattern ' ...
num2str(init) ' ' num2str(a) ')']);
 print ext_gr -append
clg

end
```

A-7. *Plotyy.m*

This m-file is a plotting function that allows both vertical sides of a plot to have separate labels and scales. This function was provided from Mathworks technical support division.

```
function [ax,pl,ylab]=plotyy(x1,y1,x2,y2,y2label,options)
% PLOTYY  Plot graphs with Y tick labels on left and right side.
%       PLOTYY(x1,y1,x2,y2) plots y1 vs. x1 with y-axis labeling
%       on left, and plots y2 vs. x2 with y-axis labeling on right.
%
%       PLOTYY(x1,y1,x2,y2,y2label) places an optional y-label on
%       the right side of the plot, since MATLAB doesn't normally
%       support right-hand side y-labels.
%
%       [ax,pl] = PLOTYY(x1,y1,x2,y2) returns the handles of the two
%       axes created by plotyy in ax and the handles of the lines
%       created by plotyy in pl.
%
%       [ax,pl,ylab] = PLOTYY(x1,y1,x2,y2,y2label) also returns the
%       handle of the text object used for y2label in ylab.
%
%       PLOTYY(x1,y1,x2,y2,y2label,options) allows for an options
%         vector as follows:
%%          OPTIONS(1) : 0 for linear x-axis, 1 for log x-axis
%           OPTIONS(2) : 0 for linear y1-axis, 1 for log y1-axis
%           OPTIONS(3) : 0 for linear y2-axis, 1 for log y2-axis
%           OPTIONS(4:5) : x-axis limits, in form [xmin xmax]
%           OPTIONS(6:7) : y1-axis limits, in form [y1min y1max]
%           OPTIONS(8:9) : y2-axis limits, in form [y2min y2max]
%
%           Specify NaN for any option to use default value.
%
%       For example,
%
%           plotyy(x1,y1,x2,y2,'',[0 1 0 1.5 3 nan nan 0 10])
%
%       plots y1 vs. x1, y2 vs. x2, with log y1-axis scaling an x-axis
%       range of 1.5 to 3, the default y1-axis range, and a y2-axis
%         range of 0 to 10.


%Known bugs:
% Due to a bug in 4.0a on Sun and SGI (and perhaps others)
% setting the ylabels units to normalized (so they stick with the
% axis as the figure is resized) does not work correctly.  In
% this case, the ylabel is still drawn, but it won't follow the axis
% around on the screen if the figure is resized.


% constants:
NUMOPTS  = 9;  % Maximum number of arguments in OPTIONS vector
OI_XLOG      = 1;  % Index of Options vector for x-axis scaling
OI_Y1LOG = 2;  % Index of Options vector for y1-axis scaling
```

```
OI_Y2LOG = 3;  % Index of Options vector for y2-axis scaling
OI_XMIN  = 4;  % Index of Options vector for x-axis min limit
OI_XMAX      = 5;  % Index of Options vector for x-axis max limit
OI_Y1MIN = 6;  % Index of Options vector for y1-axis min limit
OI_Y1MAX = 7;  % Index of Options vector for y1-axis max limit
OI_Y2MIN = 8;  % Index of Options vector for y2-axis min limit
OI_Y2MAX = 9;  % Index of Options vector for y2-axis max limit


% error checking:
if nargin<4,
 error('PLOTYY requires at least 4 input arguments.');
elseif nargin>6,
 error('PLOTYY accepts no more than 6 input arguments.');
elseif nargout>3,
 error('PLOTYY returns a maximum of 3 output arguments.');
end


% check for options vector:
if nargin==6,
 options(length(options)+1:NUMOPTS)=nan*ones(NUMOPTS-length(options),1);
else
 options=nan*ones(NUMOPTS,1);  % use all default values
end


% first calculate overall x-axis range:
x1min=min(x1(~isnan(x1)));
x2min=min(x2(~isnan(x2)));
x1max=max(x1(~isnan(x1)));
x2max=max(x2(~isnan(x2)));
xrange=[min(x1min,x2min) max(x1max,x2max)];


if ~isnan(options(OI_XMIN)),
 xrange=[options(OI_XMIN) xrange(2)];
end
if ~isnan(options(OI_XMAX)),
 xrange=[xrange(1) options(OI_XMAX)];
end


% Set up (x2,y2) plot first:
axes2=gca;
p2=plot(x2,y2);
set(gca,'YDir','rev');  % This line and the next are the guts of plotyy.
view(360-200*eps,-90);  % They allow the function to display y tick
                        % labels on the right hand side of the plot.


% set up (x1,y1) plot now:

% create a new axis in same location as the old axis:
axes1=axes('Position',get(axes2,'Pos'));
```

```
p1=plot(x1,y1);


% set both axes to have same x range:
set(axes1,'XLim',xrange);
set(axes2,'XLim',xrange);

% handle OPTIONS vector:
if options(OI_XLOG)==0,
 set(axes1,'XScale','linear');
 set(axes2,'XScale','linear');
elseif options(OI_XLOG)==1,
 set(axes1,'XScale','log');
 set(axes2,'XScale','log');
end


if options(OI_Y1LOG)==0,
 set(axes1,'YScale','linear');
elseif options(OI_Y1LOG)==1,
 set(axes1,'YScale','log');
end


if options(OI_Y2LOG)==0,
 set(axes2,'YScale','linear');
elseif options(OI_Y2LOG)==1,
 set(axes2,'YScale','log');
end


if ~isnan(options(OI_Y1MIN));
 set(axes1,'YLim',get(axes1,'YLim').*[0 1]+[options(OI_Y1MIN) 0]);
end


if ~isnan(options(OI_Y1MAX));
 set(axes1,'YLim',get(axes1,'YLim').*[1 0]+[0 options(OI_Y1MAX)]);
end


if ~isnan(options(OI_Y2MIN));
 set(axes2,'YLim',get(axes2,'YLim').*[0 1]+[options(OI_Y2MIN) 0]);
end


if ~isnan(options(OI_Y2MAX));
 set(axes2,'YLim',get(axes2,'YLim').*[1 0]+[0 options(OI_Y2MAX)]);
end


% now tidy the plot up a bit:
ticklen=get(axes1,'TickLength');
set(axes2,'TickLength',[ticklen(1) ticklen(1)]);
set(axes2,'TickDir',get(axes1,'TickDir'));
```

```
set(axes2,'XTickLabels','');
set(axes1,'Box','off');


% If both y1 and y2 are vectors (not matrices) make
% the color of y2 be the second color in the ColorOrder.
% (This is to make the plot aesthetic.)

[m1,n1]=size(y1);
[m2,n2]=size(y2);



if (m1==1 | n1==1) & (m2==1 | n2==1),
 ColorOrd=get(axes1,'ColorOrder');
 if size(ColorOrd,1)~=1, % in case ColorOrder only has 1 color in it
  set(p2,'Color',ColorOrd(2,:));
 end
end



% create y2label if required:
if nargin > 4,
 if ~isempty(y2label),
  ylab=text(0,0,y2label);
  save_axes1_units=get(axes1,'Units');     % save current state
  set(ylab,'Units','pixels');              % convert everything to
  set(axes1,'Units','pixels');             % same units
  axes1pos=get(axes1,'Position');
% get "typical" ylabel offset from axes, add it to width of axes1
% to get y2label's x-coordinate:
  typical_ylabel_handle=get(axes1,'YLabel');
  typ_ylabel_pos=get(typical_ylabel_handle,'Position');
  ylaboffset=-1*typ_ylabel_pos(1);
  ylabxcoordinate=ylaboffset+axes1pos(3);
% y2label's y-coordinate is same as "typical" value:
  ylabycoordinate=typ_ylabel_pos(2);

  set(ylab,'Position',[ylabxcoordinate ylabycoordinate]);
  set(ylab,'HorizontalAlignment','center');
  set(ylab,'Rotation',90);

% Due to a bug in 4.0a on Sun and SGI (and perhaps others)
% setting the ylabels units to normalized (so they stick with the
% axis as the figure is resized) does not work correctly.  In
% this case, draw the ylabel, but set it so it won't stick to axis
% position:

if ~strcmp(version,'4.0a'),
  set(ylab,'Units','normalized');
end


% restore old 'units' settings:
  set(axes1,'Units',save_axes1_units);
```

```
% y2 label is usually clipped if using default axes position.
% Therefore shrink axes width by 5%
% to leave room for it:
  axespos=get(axes1,'Position');
  set([axes1,axes2],'Position',axespos-[0 0 .05 0]);
 end % ~isempty(y2label)
end % creation of y2label


% return handles to axes and lines:
if nargout>0,ax=[axes1;axes2];end
if nargout>1,pl=[p1;p2];end
```

APPENDIX B. BIT- PATTERN PLOTS

This appendix contains the sixty-four graphic produced in the first group of simulations. The sixteen bit-patterns are iterated against four different bit rates. The patterns for 0.5 Gb/s are found on pages 56-62. Likewise, the patterns for 3 Gb/s are found on pages 63-79; patterns for 6 Gb/s are found on pages 80-86; and patterns for 9 Gb/s are found on pages 87-103.

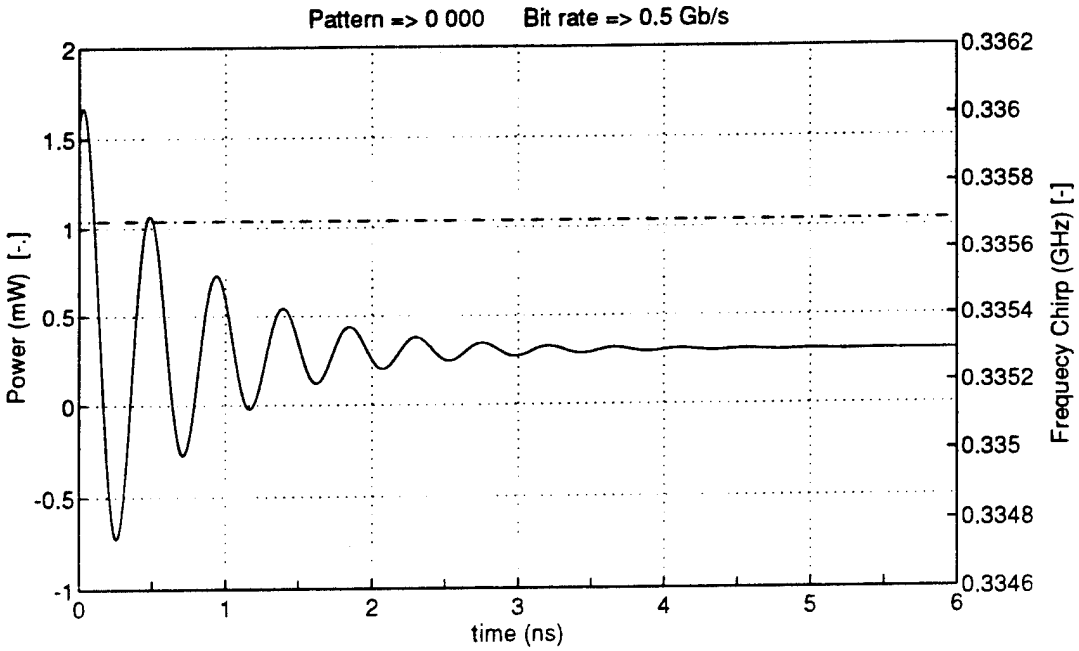

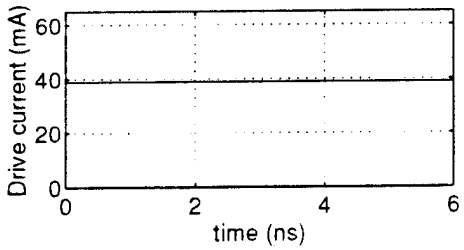

r = 0.1882
Max chirp freq excursion 0.336 GHz
Min chirp freq excursion 0.3347 GHz
I_thresh = 0.0335 mA
I_off = 38.86 mA
I_on = 61.98 mA
Case 1

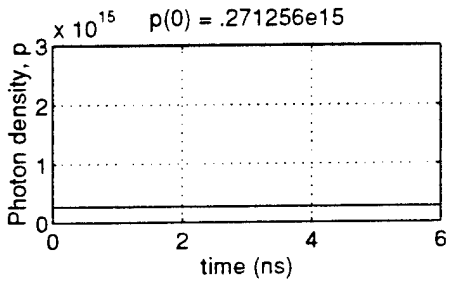

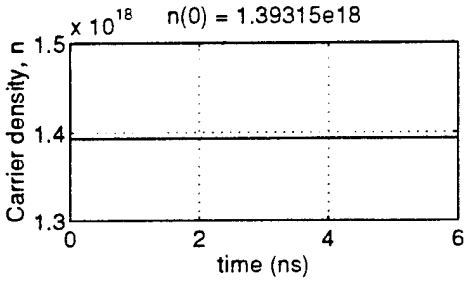

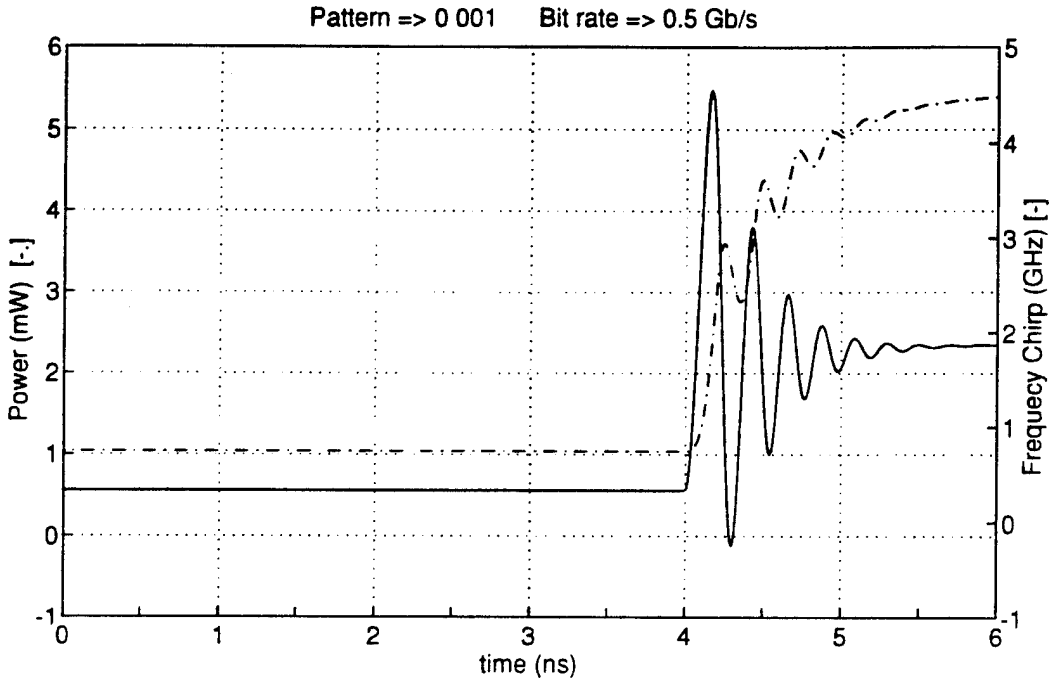

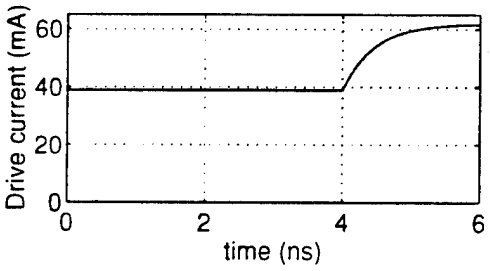

r = 0.1882
Max chirp freq excursion 4.546 GHz
Min chirp freq excursion -0.2391 GHz
I_thresh = 0.0335 mA
I_off = 38.86 mA
I_on = 61.98 mA
Case 2

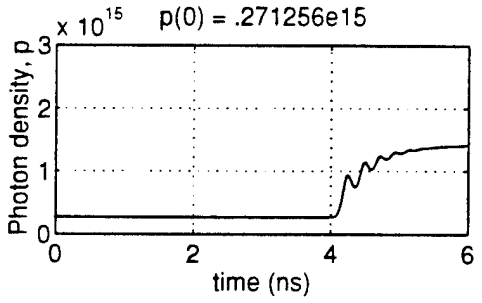

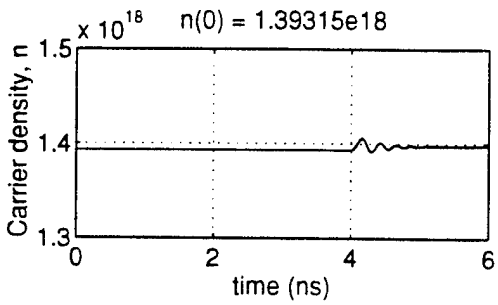

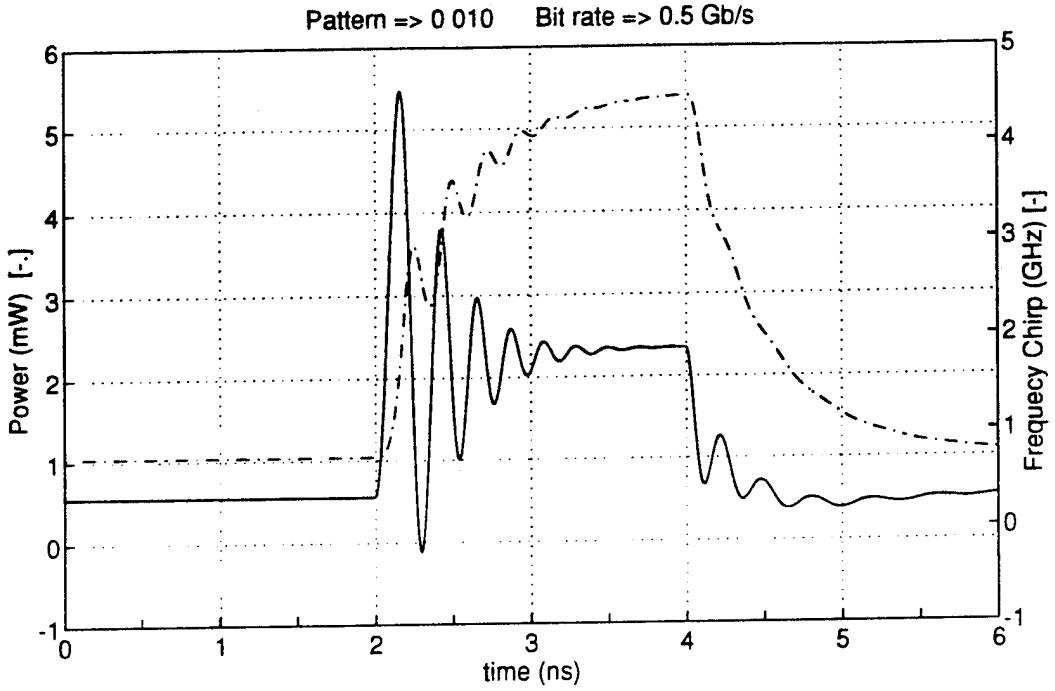

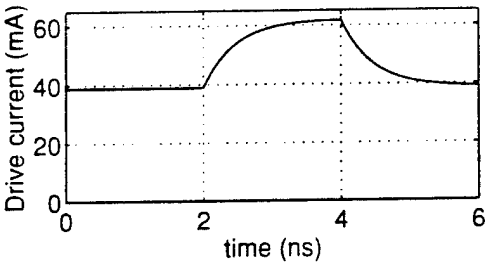

r = 0.1882
Max chirp freq excursion 4.542 GHz
Min chirp freq excursion -0.2405 GHz
I_thresh = 0.0335 mA
I_off = 38.86 mA
I_on = 61.98 mA
Case 3

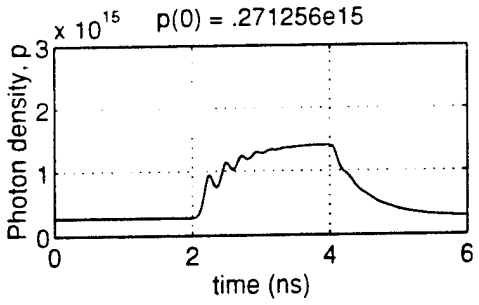

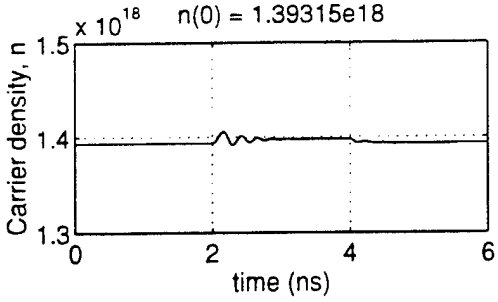

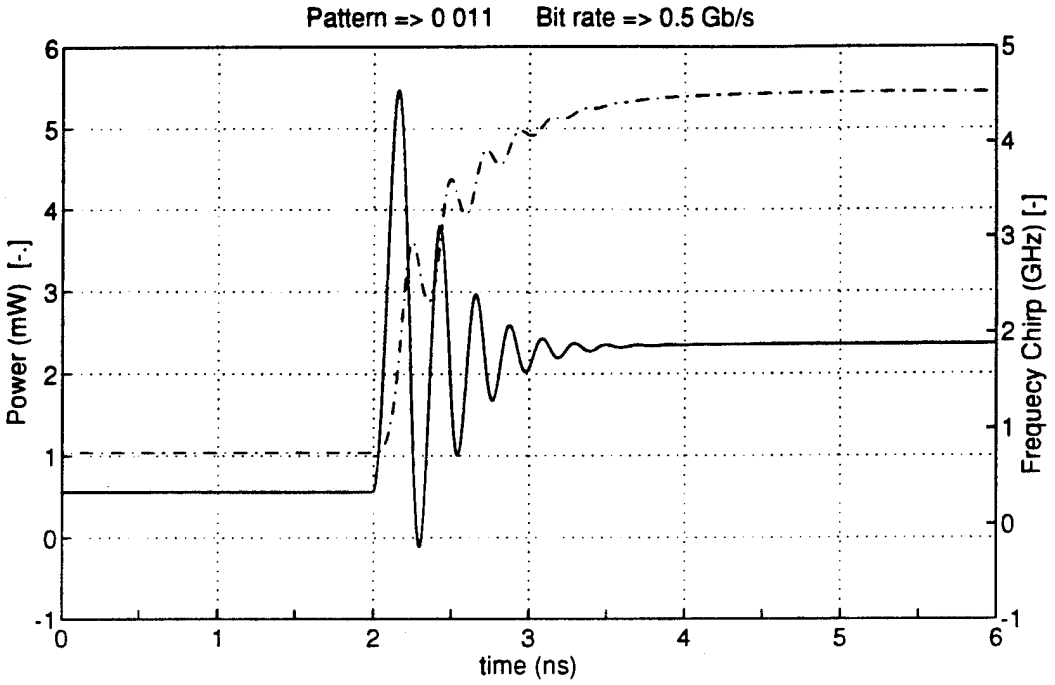

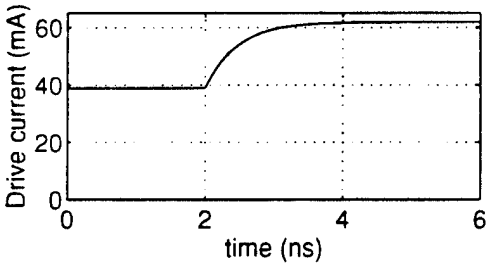

r = 0.1882
Max chirp freq excursion 4.542 GHz
Min chirp freq excursion -0.2405 GHz
I_thresh = 0.0335 mA
I_off = 38.86 mA
I_on = 61.98 mA
Case 4

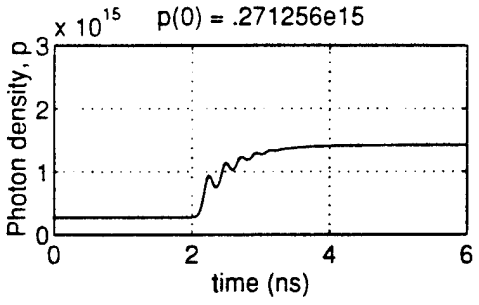

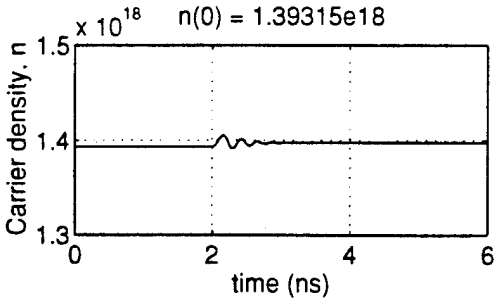

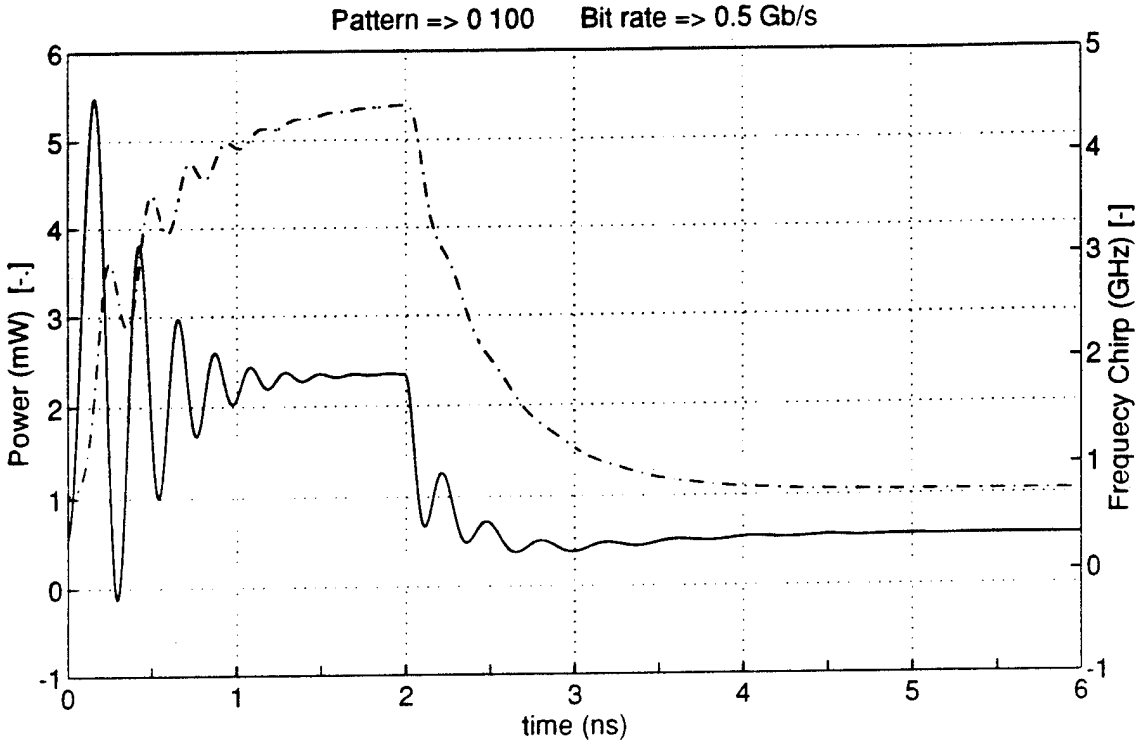

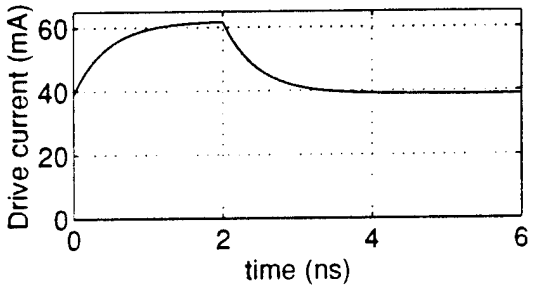

r = 0.1882
Max chirp freq excursion 4.557 GHz
Min chirp freq excursion -0.2453 GHz
I_thresh = 0.0335 mA
I_off = 38.86 mA
I_on = 61.98 mA
Case 5

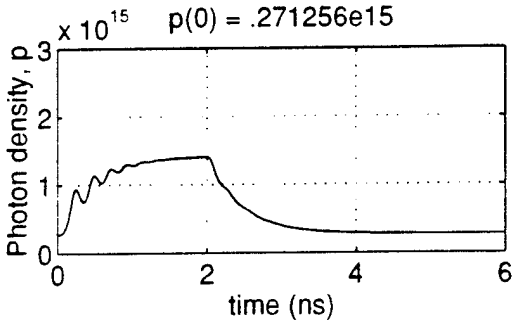

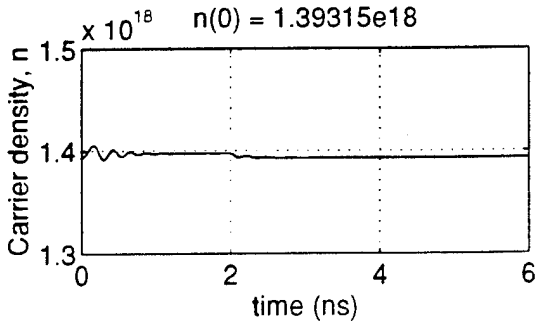

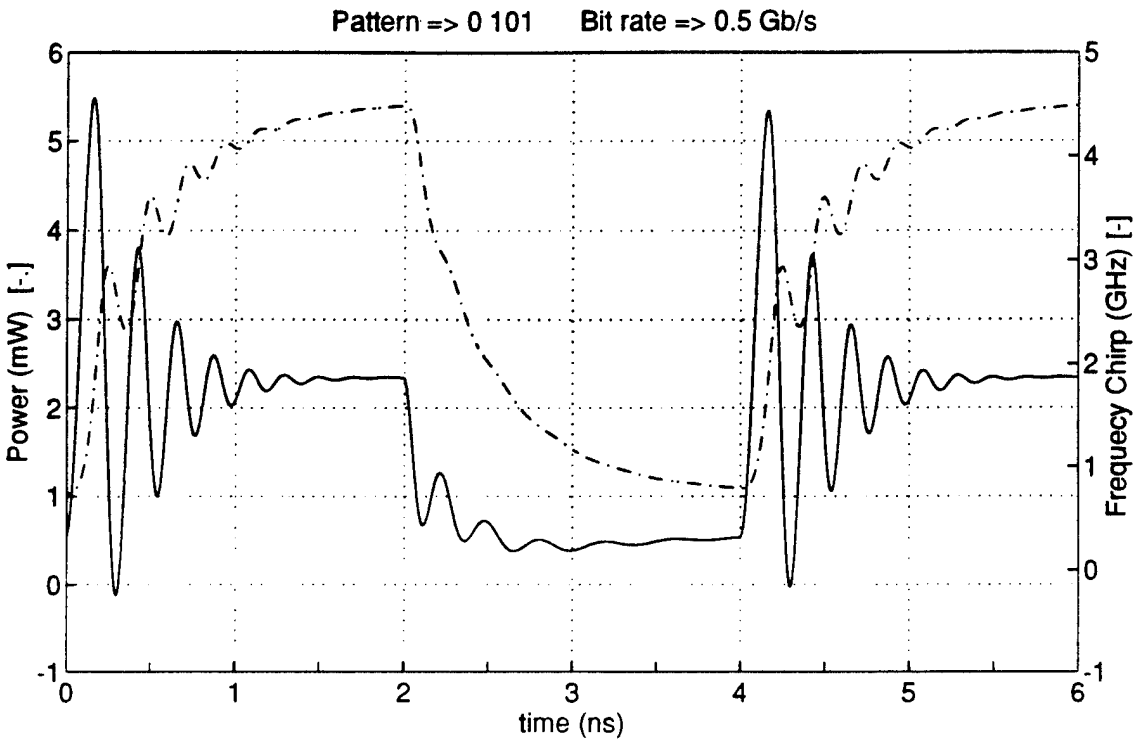

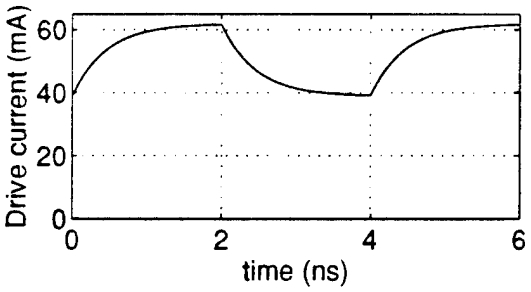

r = 0.1882
Max chirp freq excursion 4.557 GHz
Min chirp freq excursion -0.2453 GHz
I_thresh = 0.0335 mA
I_off = 38.86 mA
I_on = 61.98 mA
Case 6

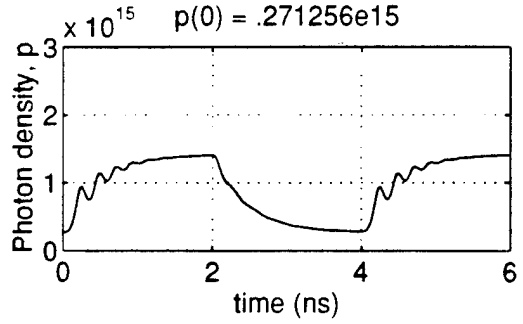

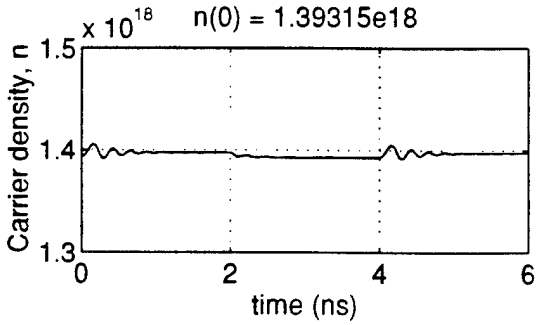

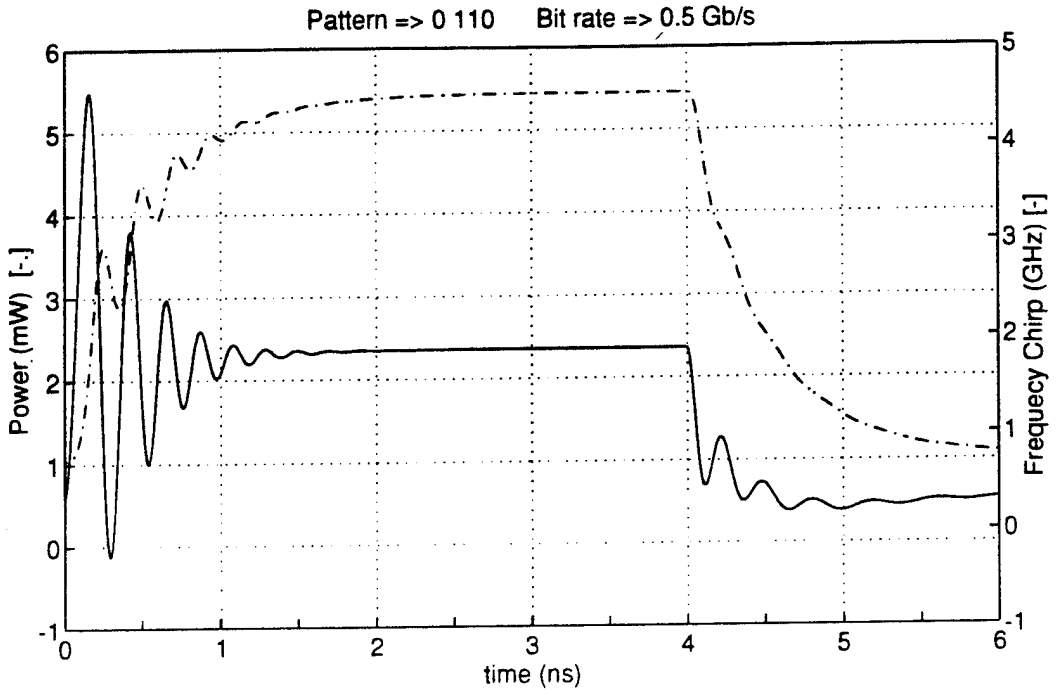

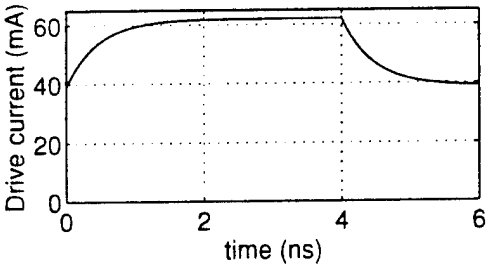

r = 0.1882
Max chirp freq excursion 4.557 GHz
Min chirp freq excursion -0.2453 GHz
I_thresh = 0.0335 mA
I_off = 38.86 mA
I_on = 61.98 mA
Case 7

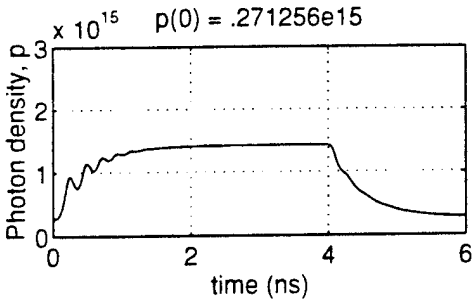

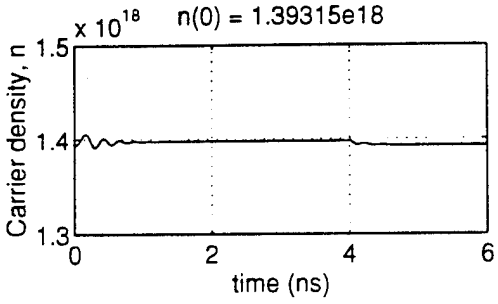

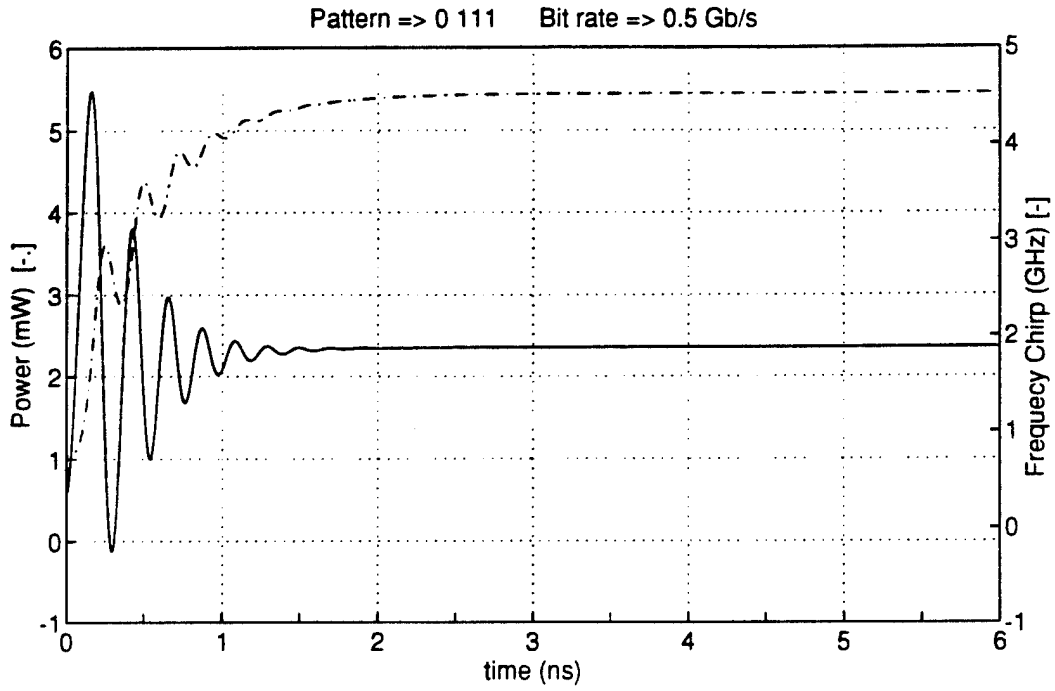

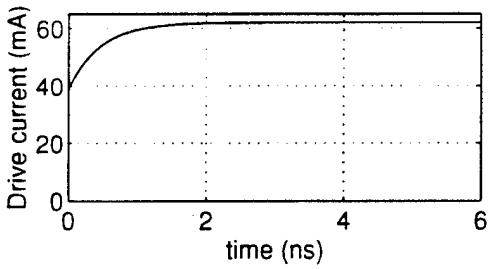

r = 0.1882
Max chirp freq excursion 4.557 GHz
Min chirp freq excursion -0.2453 GHz
I_thresh = 0.0335 mA
I_off = 38.86 mA
I_on = 61.98 mA
Case 8

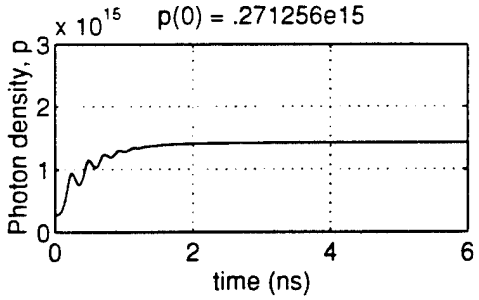

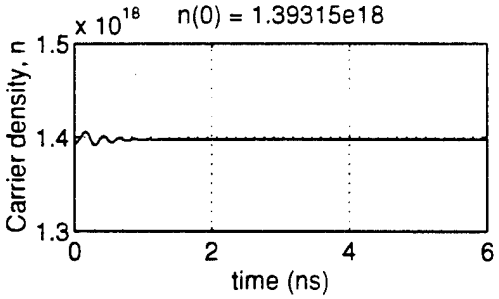

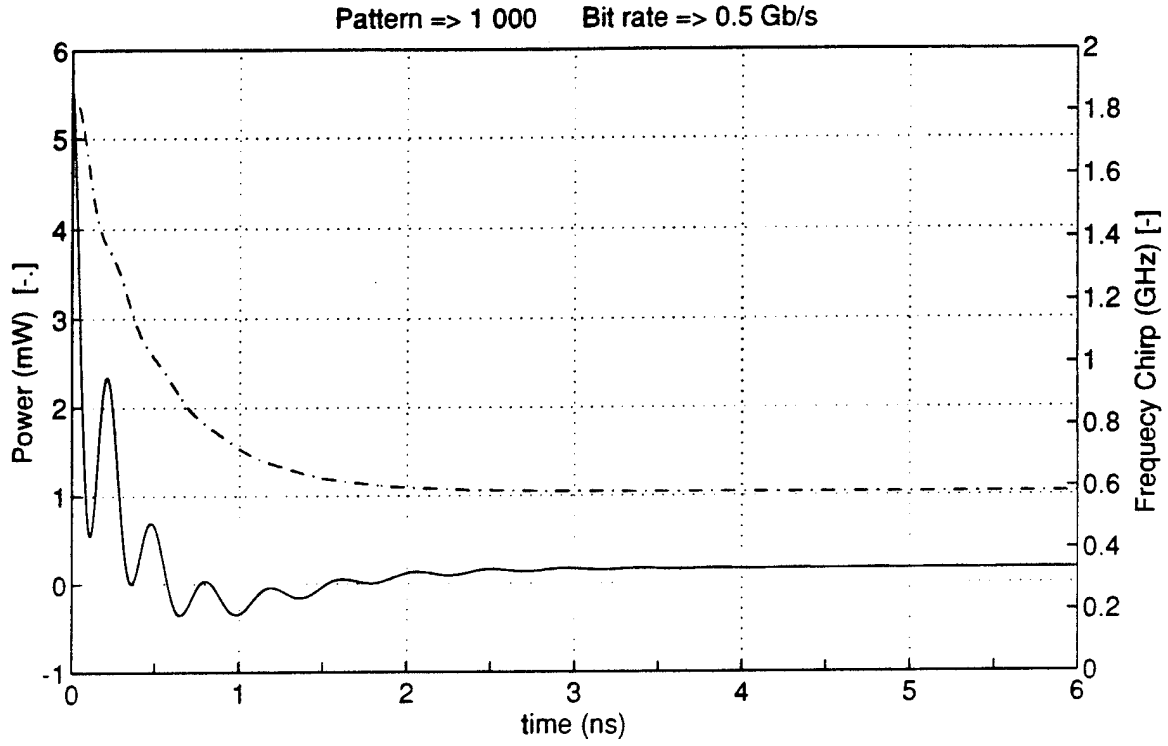

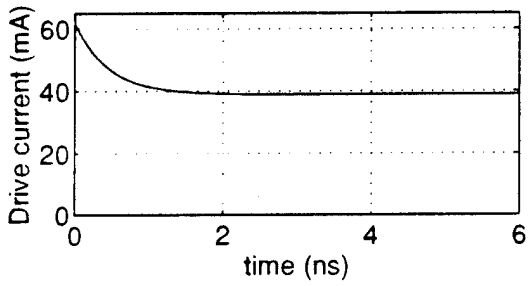

r = 0.1882
Max chirp freq excursion 1.882 GHz
Min chirp freq excursion 0.1845 GHz
I_thresh = 0.0335 mA
I_off = 38.86 mA
I_on = 61.98 mA
Case 9

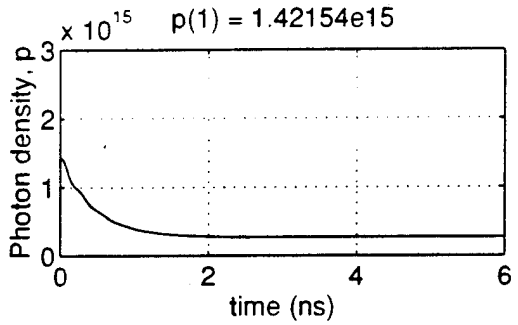

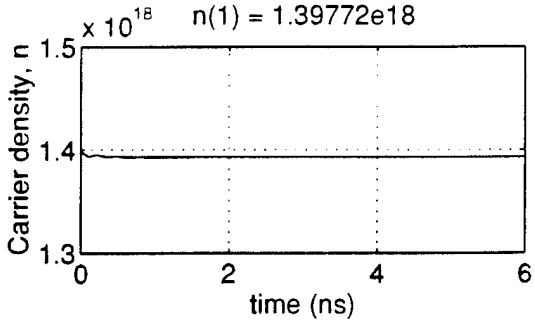

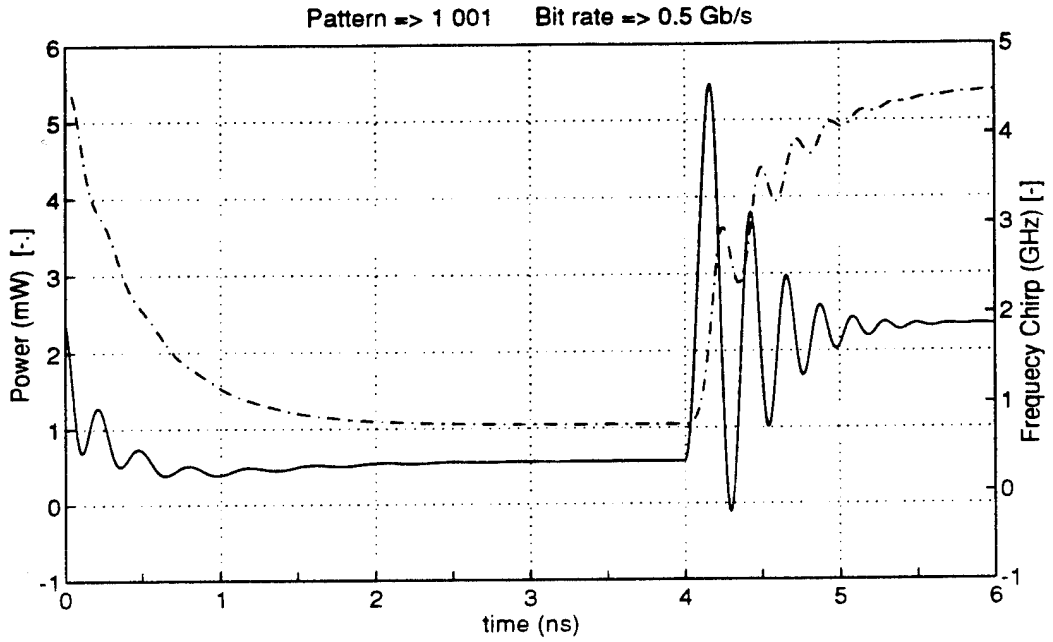

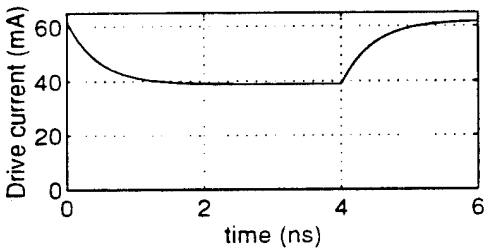

r = 0.1882
Max chirp freq excursion 4.544 GHz
Min chirp freq excursion -0.238 GHz
I_thresh = 0.0335 mA
I_off = 38.86 mA
I_on = 61.98 mA
Case 10

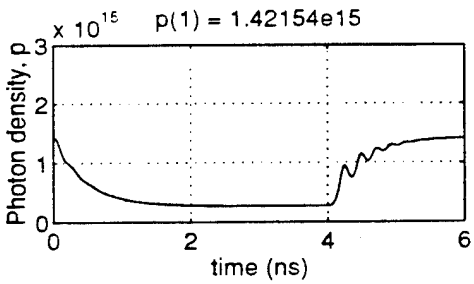

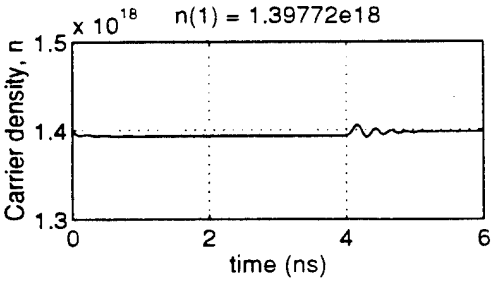

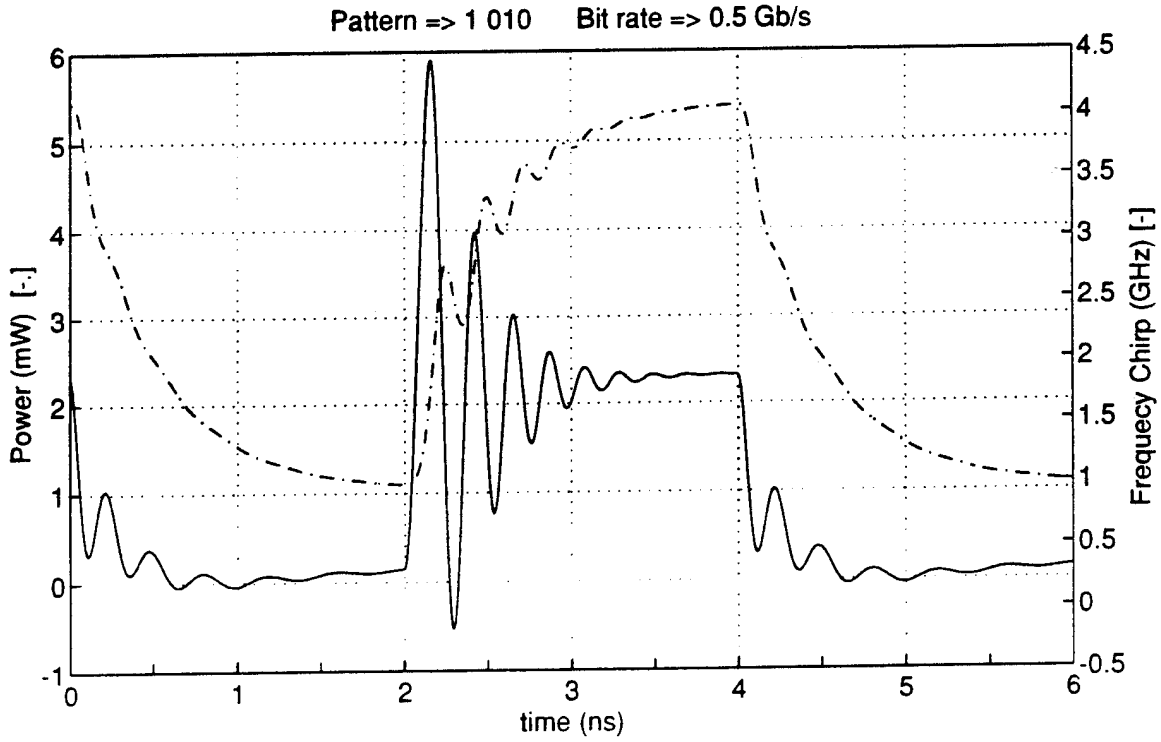

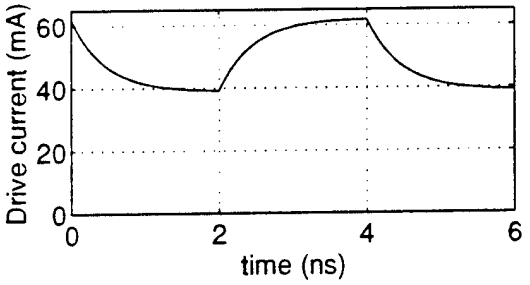

r = 0.1882
Max chirp freq excursion 4.43 GHz
Min chirp freq excursion -0.1606 GHz
I_thresh = 0.0335 mA
I_off = 38.86 mA
I_on = 61.98 mA
Case 11

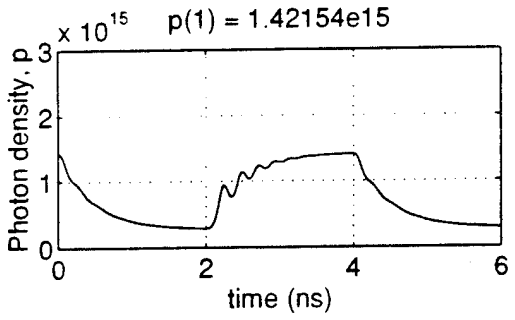

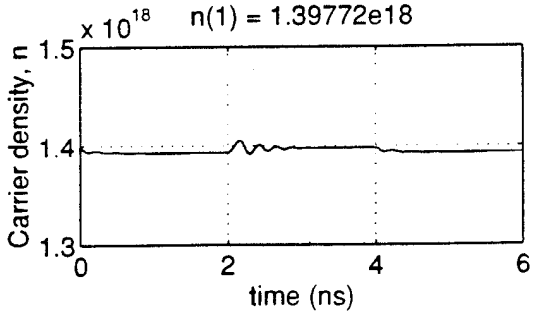

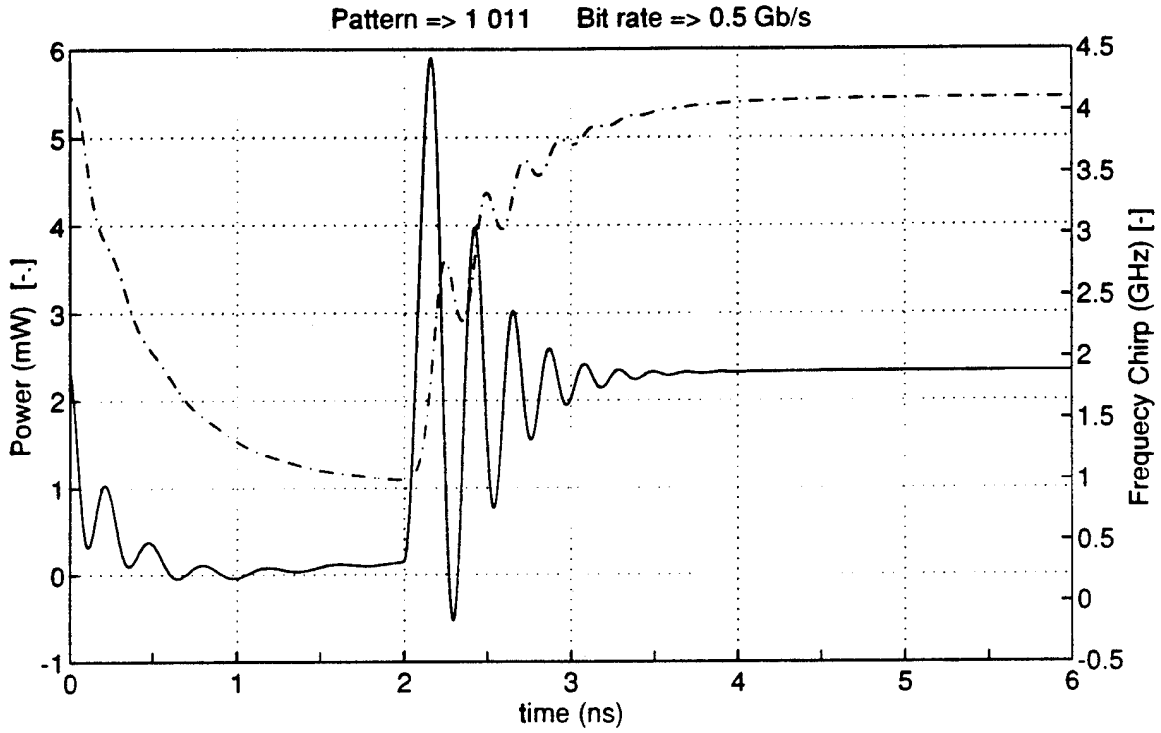

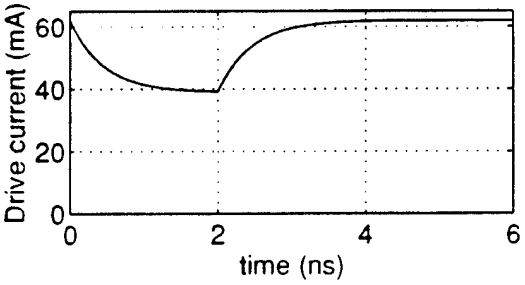

r = 0.1882
Max chirp freq excursion 4.43 GHz
Min chirp freq excursion -0.1606 GHz
I_thresh = 0.0335 mA
I_off = 38.86 mA
I_on = 61.98 mA
Case 12

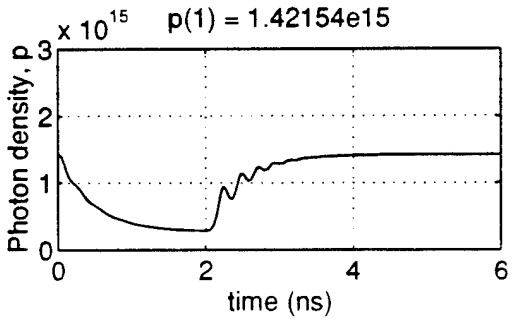

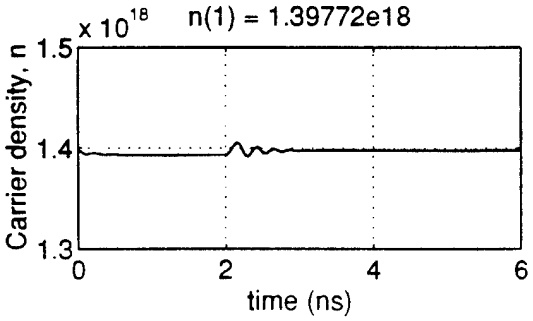

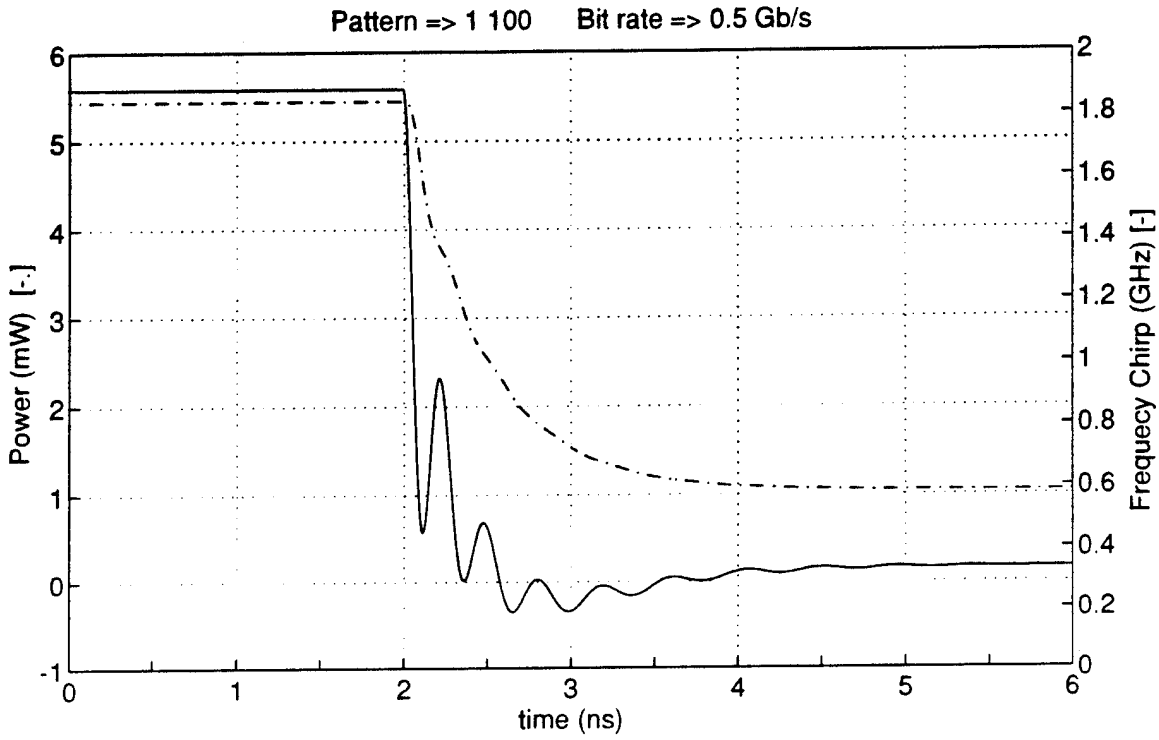

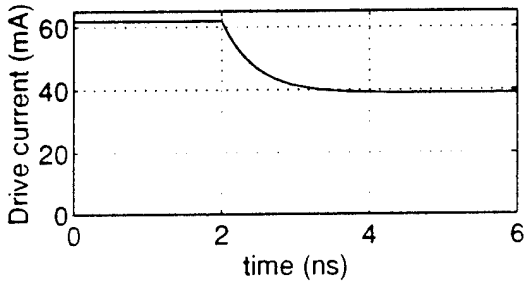

r = 0.1882
Max chirp freq excursion 1.882 GHz
Min chirp freq excursion 0.186 GHz
I_thresh = 0.0335 mA
I_off = 38.86 mA
I_on = 61.98 mA
Case 13

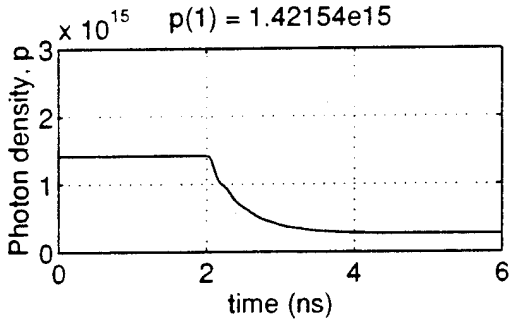

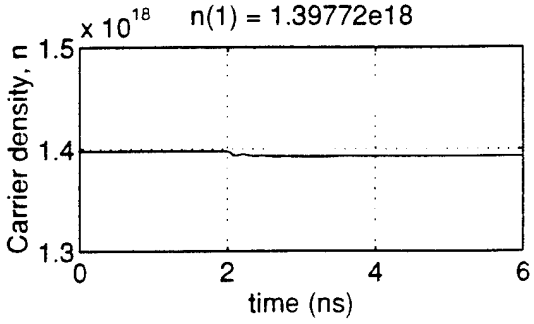

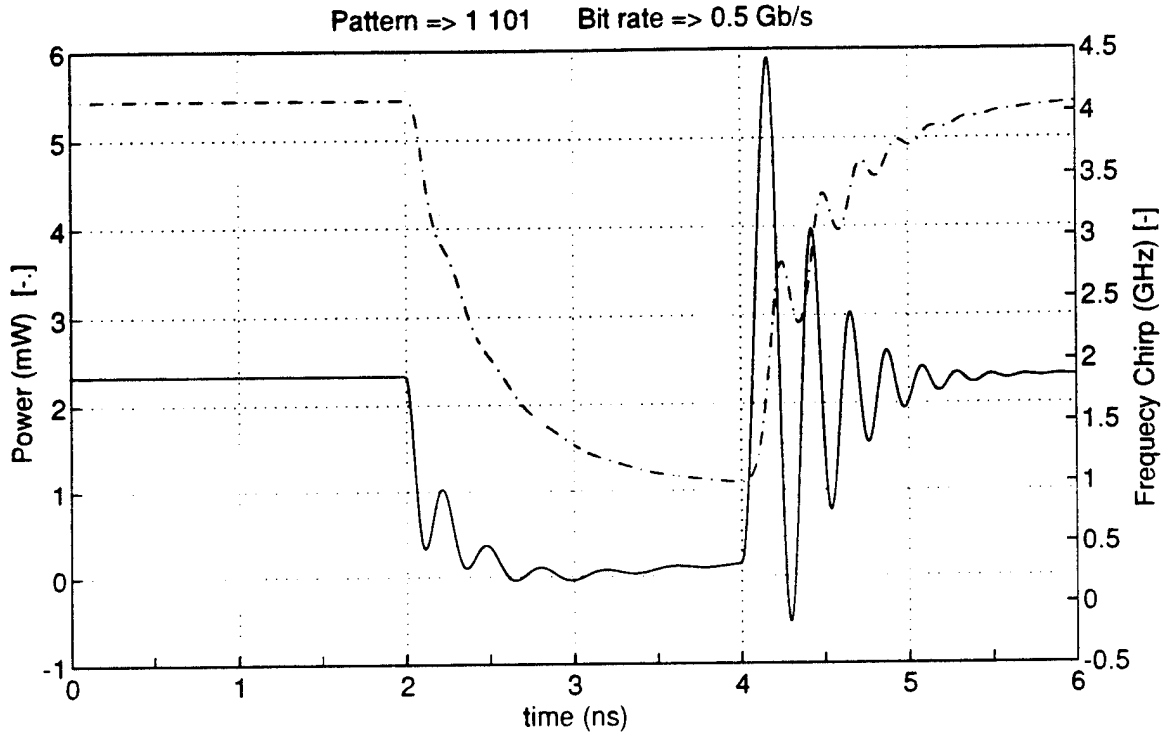

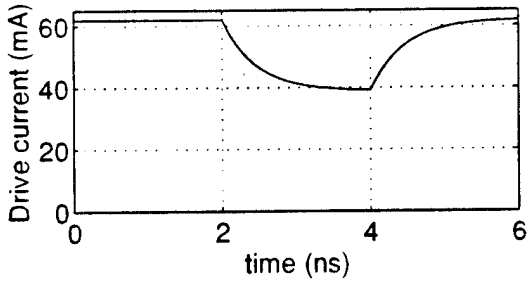

r = 0.1882
Max chirp freq excursion 4.427 GHz
Min chirp freq excursion -0.163 GHz
I_thresh = 0.0335 mA
I_off = 38.86 mA
I_on = 61.98 mA
Case 14

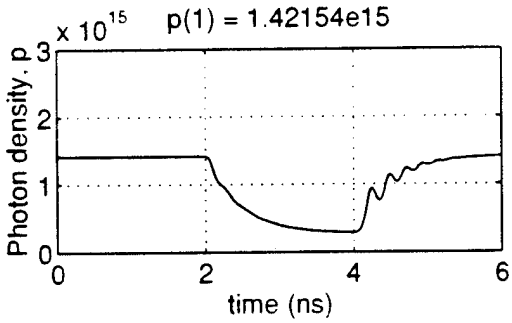

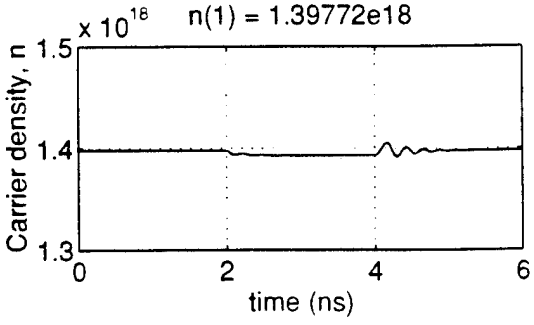

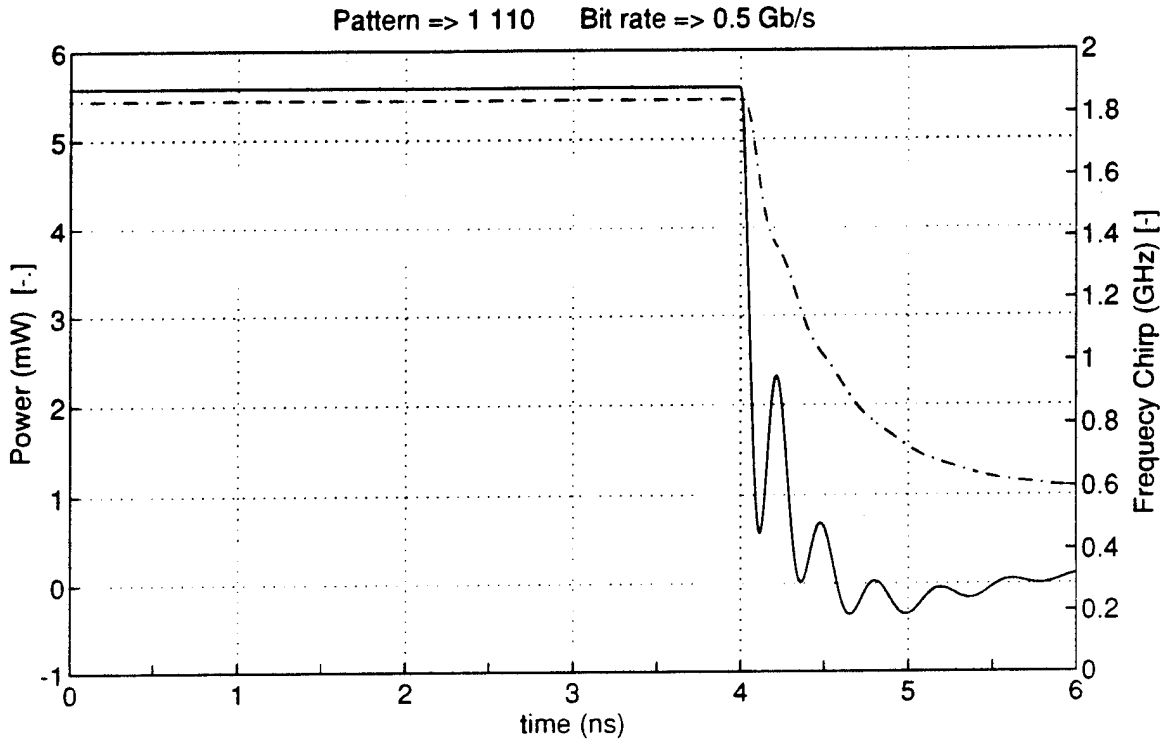

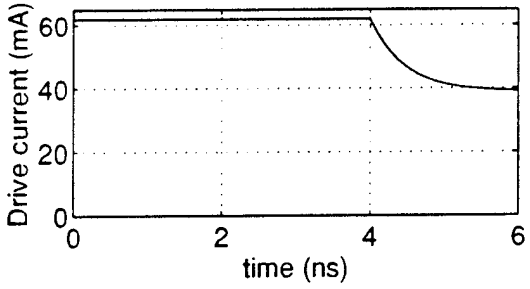

r = 0.1882
Max chirp freq excursion 1.882 GHz
Min chirp freq excursion 0.1861 GHz
I_thresh = 0.0335 mA
I_off = 38.86 mA
I_on = 61.98 mA
Case 15

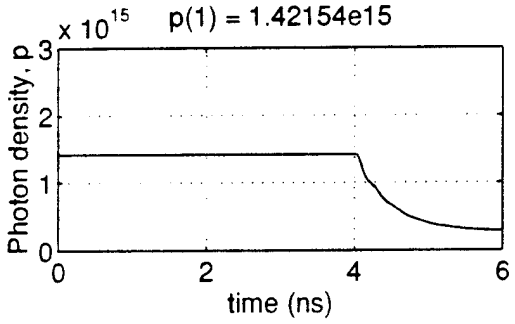

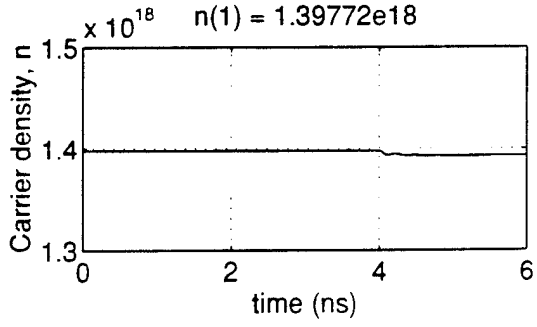

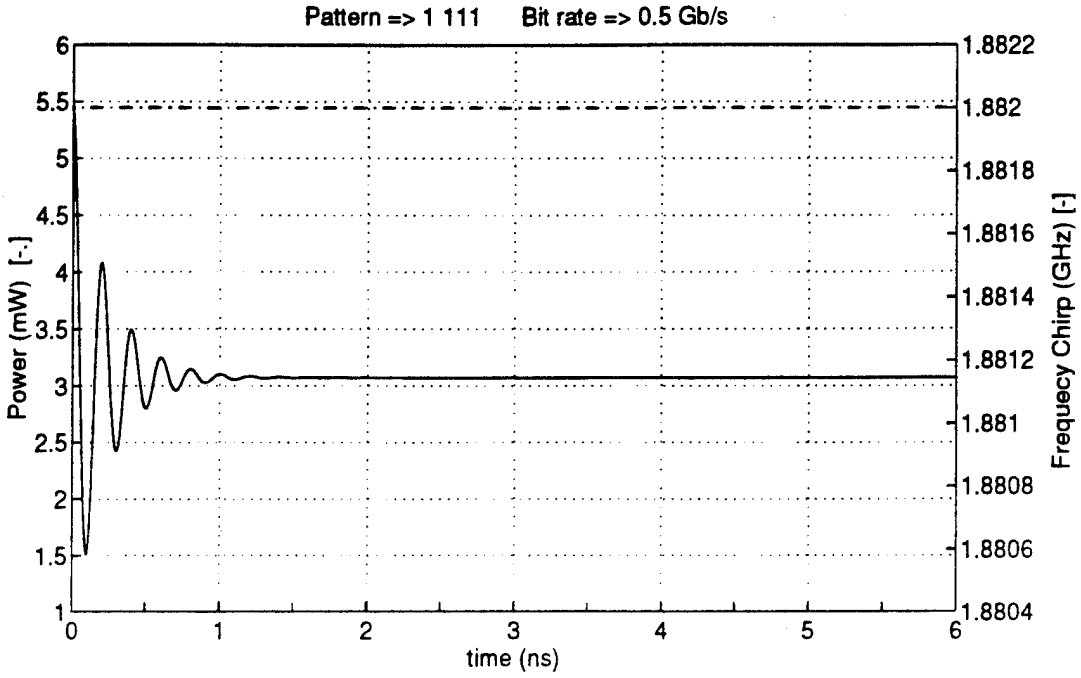

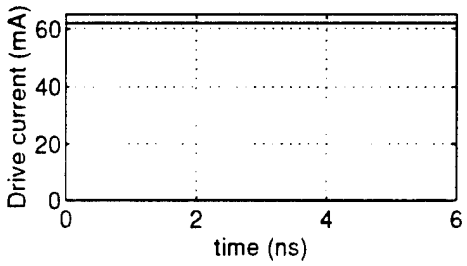

r = 0.1882
Max chirp freq excursion 1.882 GHz
Min chirp freq excursion 1.881 GHz
I_thresh = 0.0335 mA
I_off = 38.86 mA
I_on = 61.98 mA
Case 16

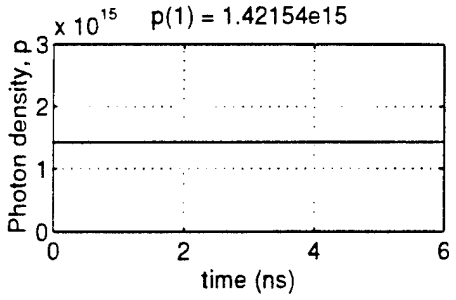

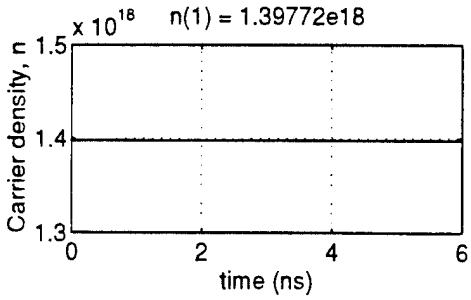

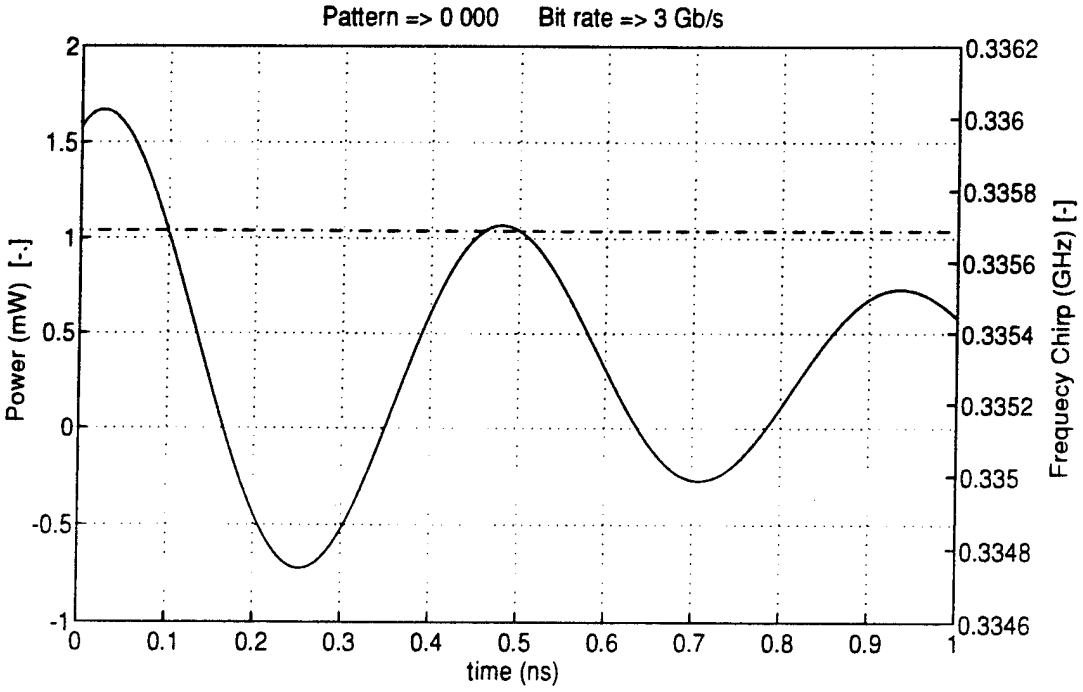

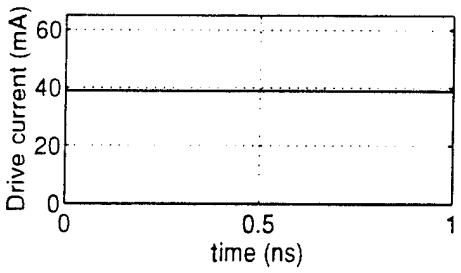

r = 0.1882
Max chirp freq excursion 0.336 GHz
Min chirp freq excursion 0.3347 GHz
I_thresh = 0.0335 mA
I_off = 38.86 mA
I_on = 61.98 mA
Case 17

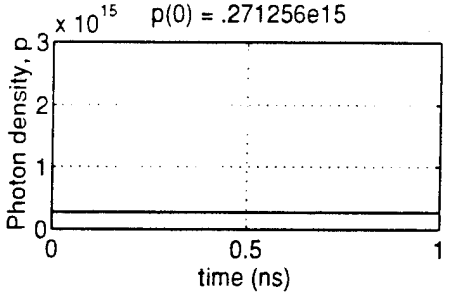

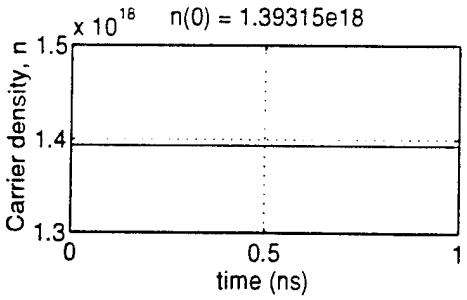

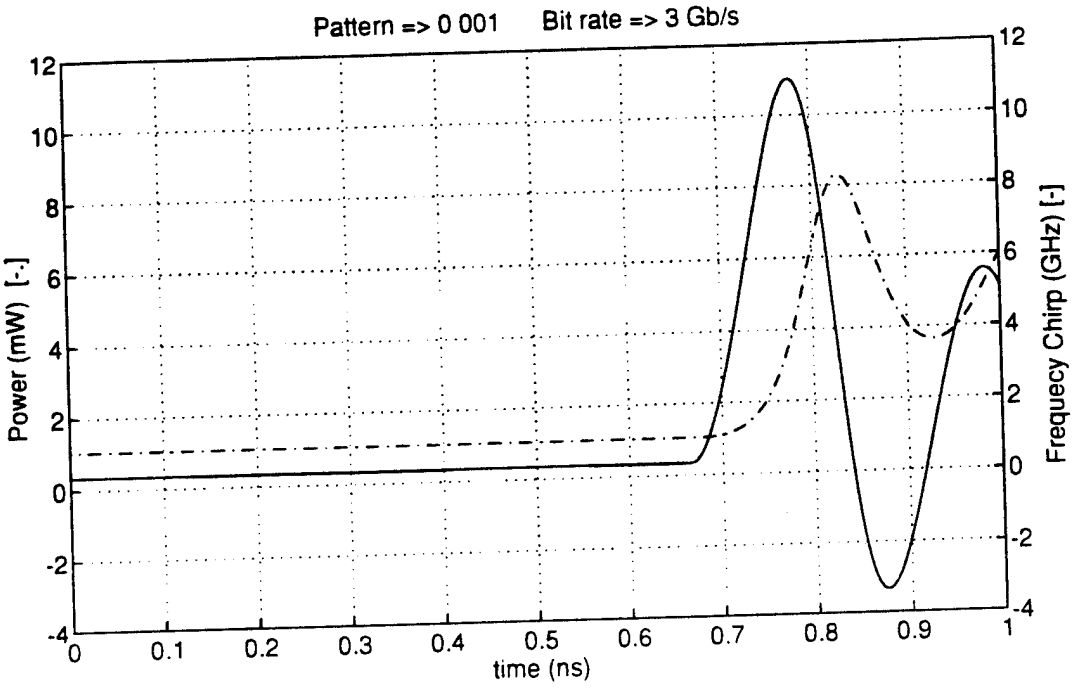

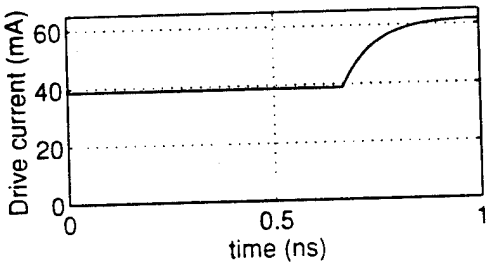

r = 0.1882
Max chirp freq excursion 11.01 GHz
Min chirp freq excursion -3.331 GHz
I_thresh = 0.0335 mA
I_off = 38.86 mA
I_on = 61.98 mA
Case 18

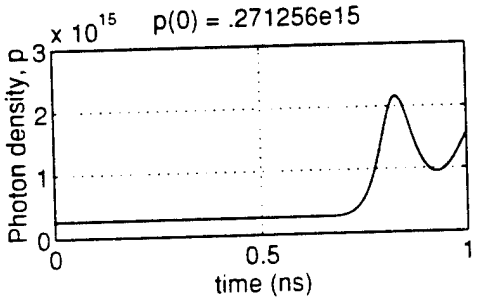

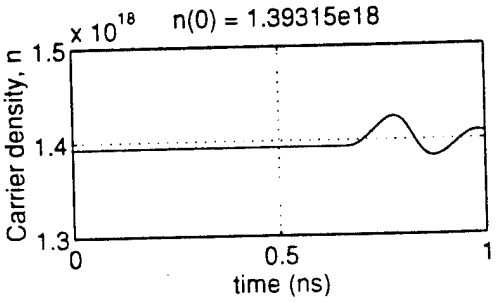

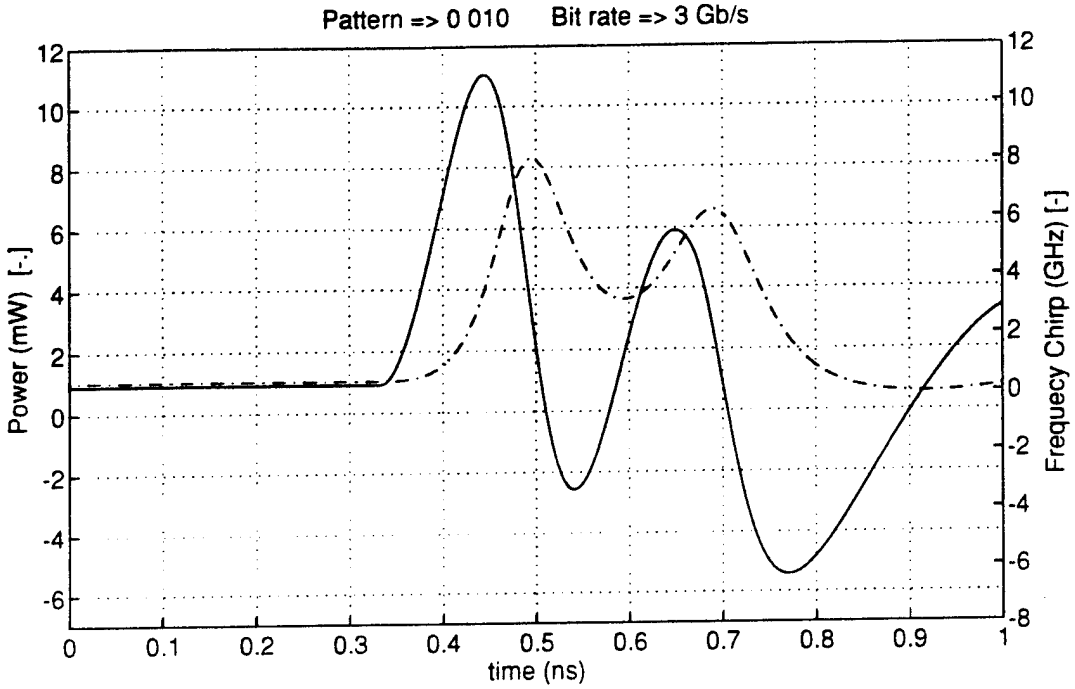

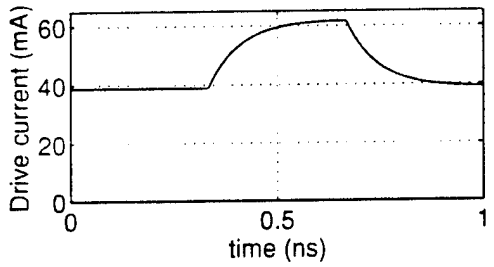

r = 0.1882
Max chirp freq excursion 11.01 GHz
Min chirp freq excursion -6.339 GHz
I_thresh = 0.0335 mA
I_off = 38.86 mA
I_on = 61.98 mA
Case 19

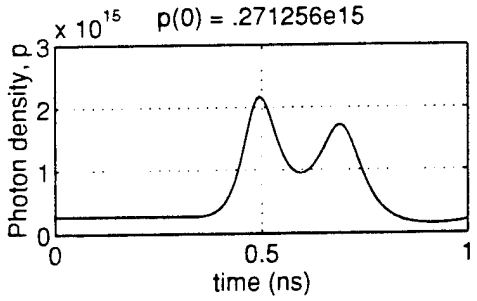

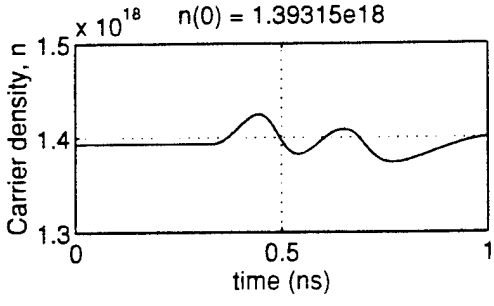

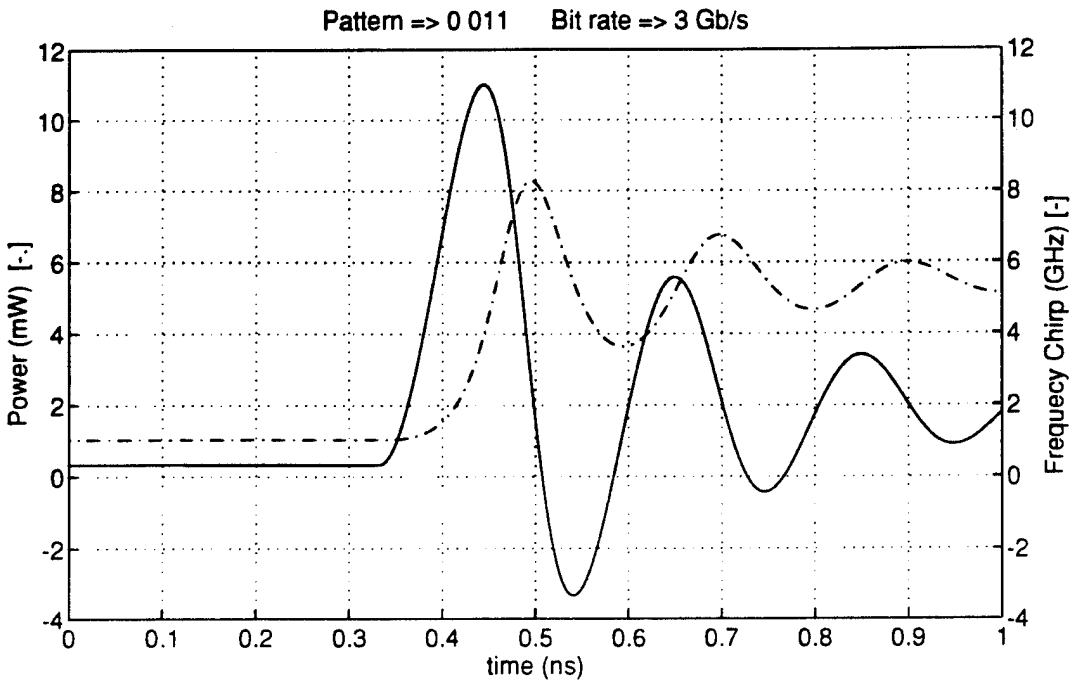

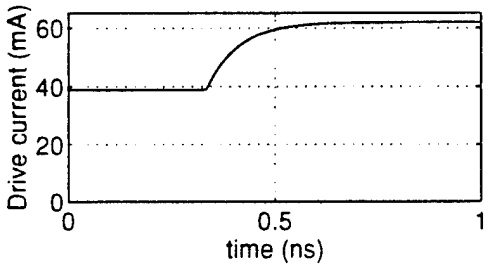

r = 0.1882
Max chirp freq excursion 11.01 GHz
Min chirp freq excursion -3.332 GHz
I_thresh = 0.0335 mA
I_off = 38.86 mA
I_on = 61.98 mA
Case 20

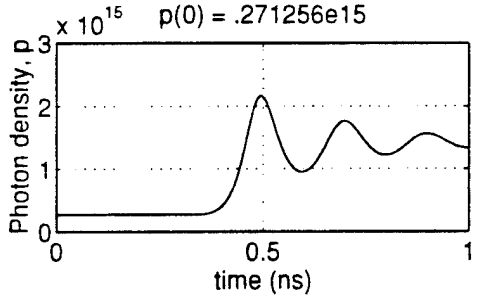

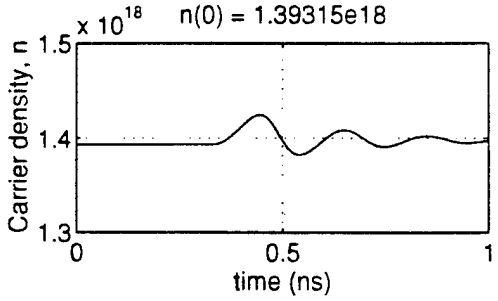

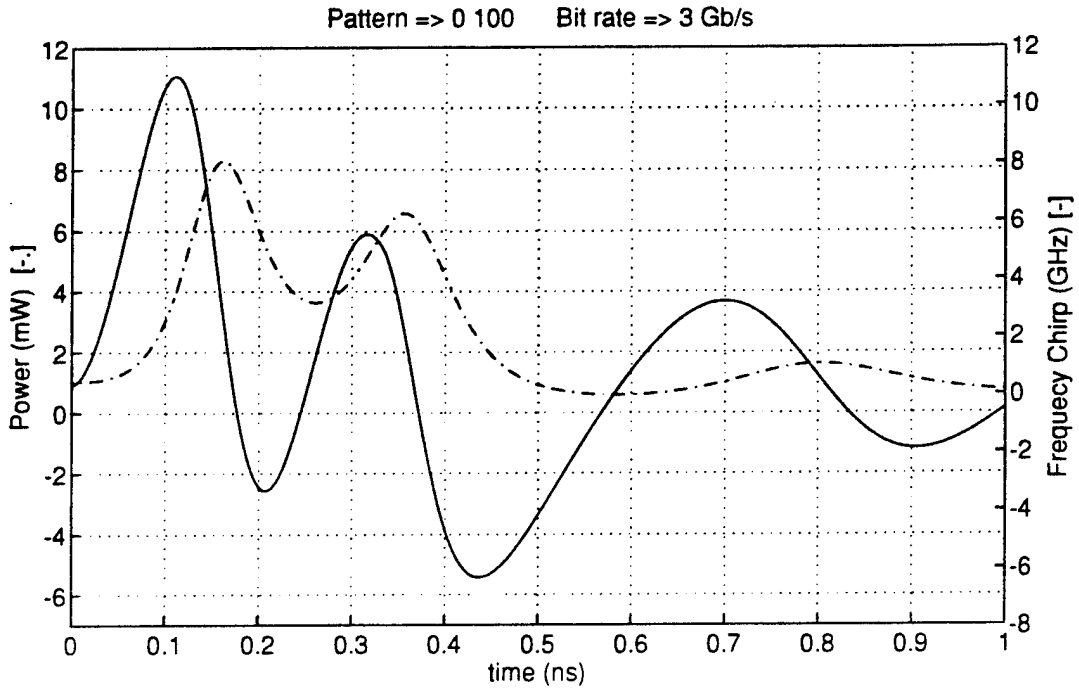

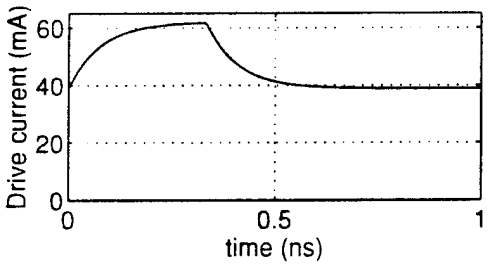

r = 0.1882
Max chirp freq excursion 11.01 GHz
Min chirp freq excursion -6.34 GHz
I_thresh = 0.0335 mA
I_off = 38.86 mA
I_on = 61.98 mA
Case 21

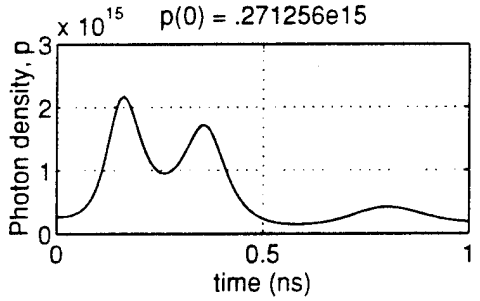

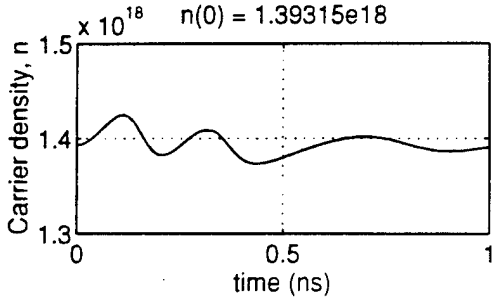

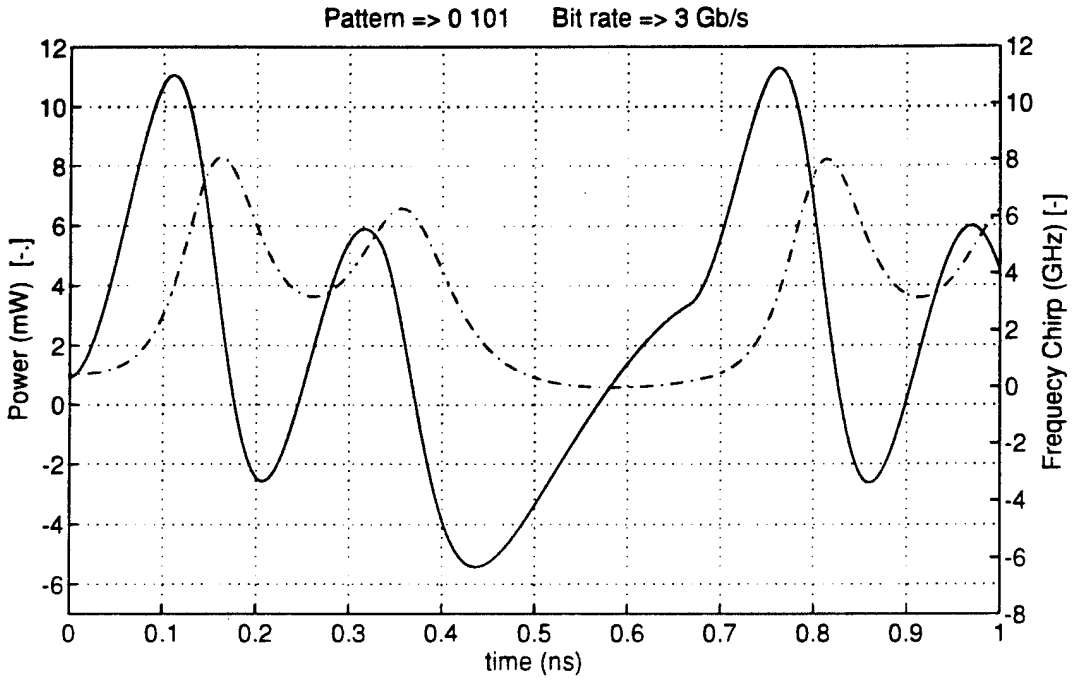

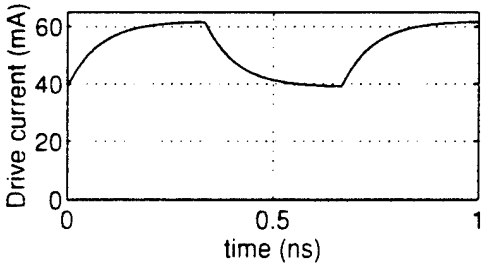

r = 0.1882
Max chirp freq excursion 11.26 GHz
Min chirp freq excursion -6.34 GHz
I_thresh = 0.0335 mA
I_off = 38.86 mA
I_on = 61.98 mA
Case 22

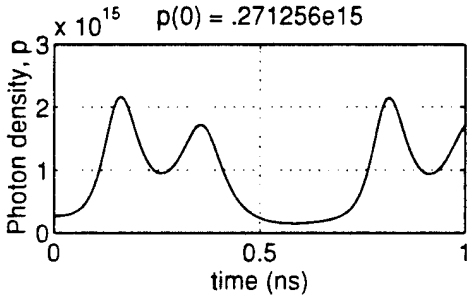

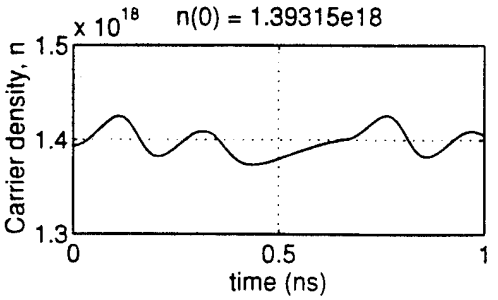

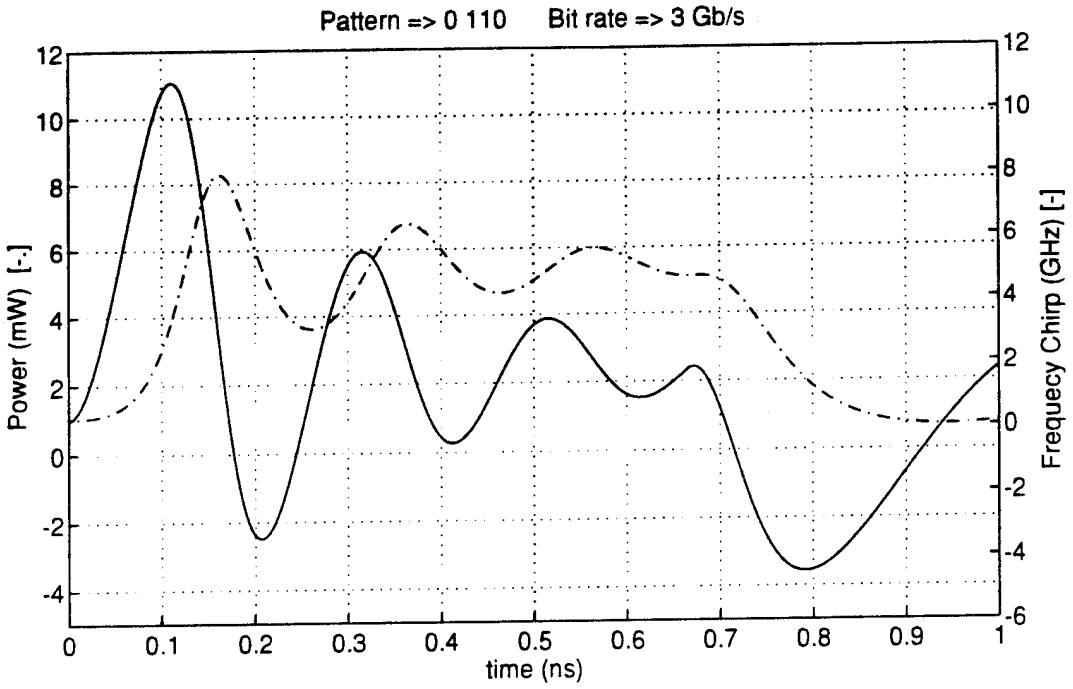

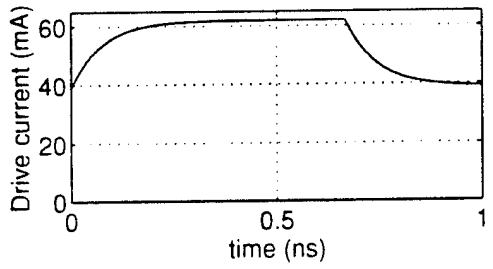

r = 0.1882
Max chirp freq excursion 11.01 GHz
Min chirp freq excursion -4.486 GHz
I_thresh = 0.0335 mA
I_off = 38.86 mA
I_on = 61.98 mA
Case 23

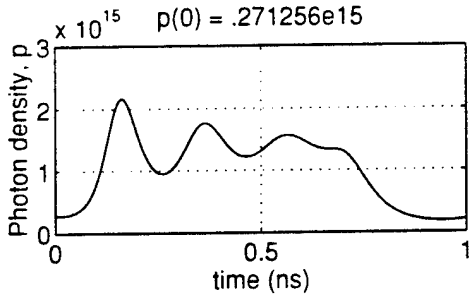

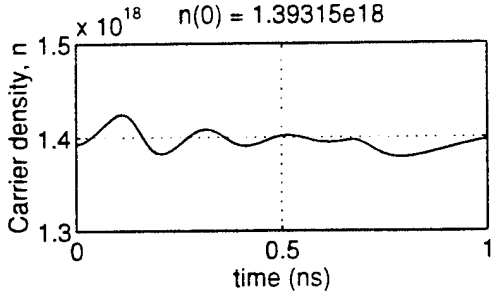

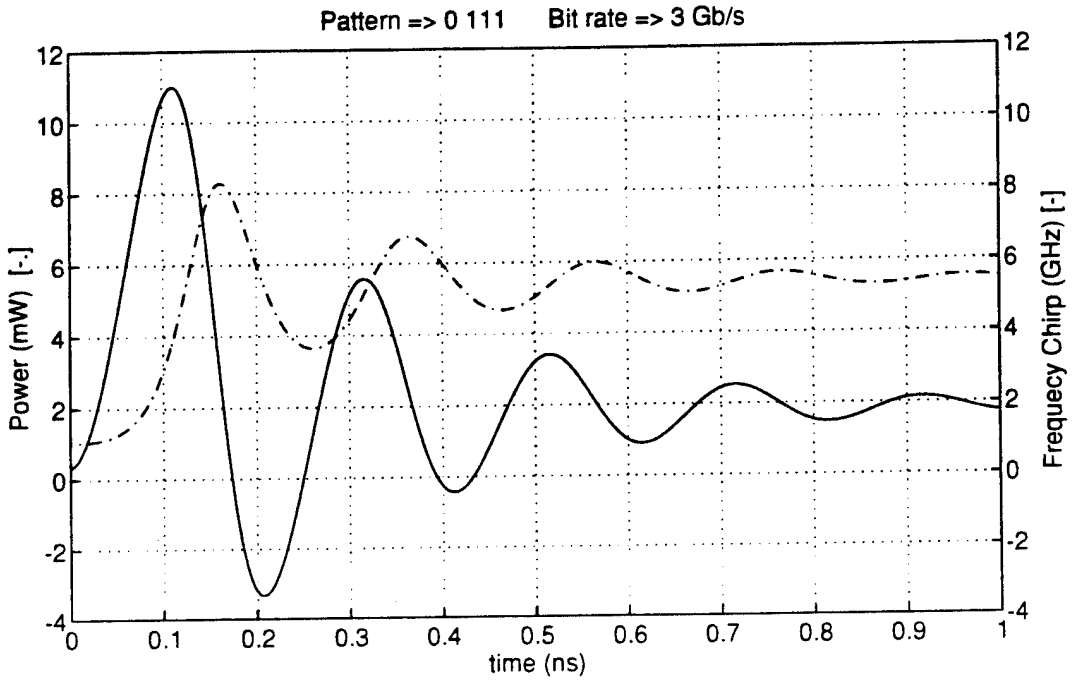

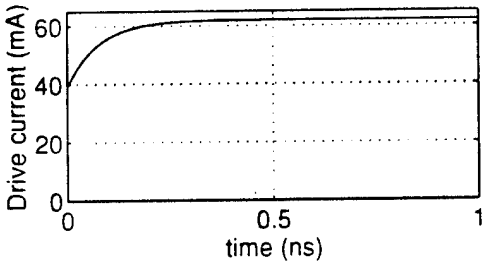

r = 0.1882
Max chirp freq excursion 11.01 GHz
Min chirp freq excursion -3.333 GHz
I_thresh = 0.0335 mA
I_off = 38.86 mA
I_on = 61.98 mA
Case 24

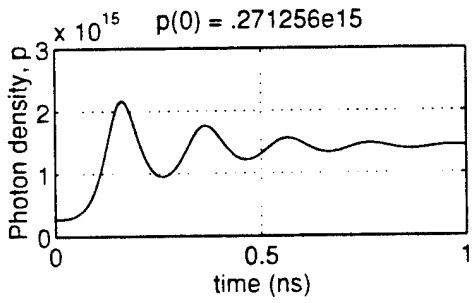

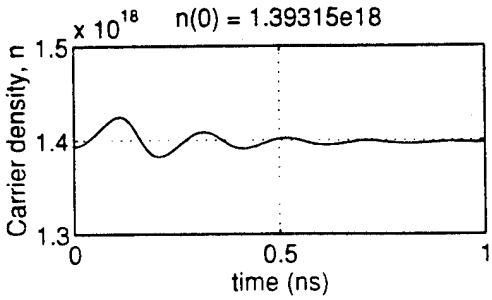

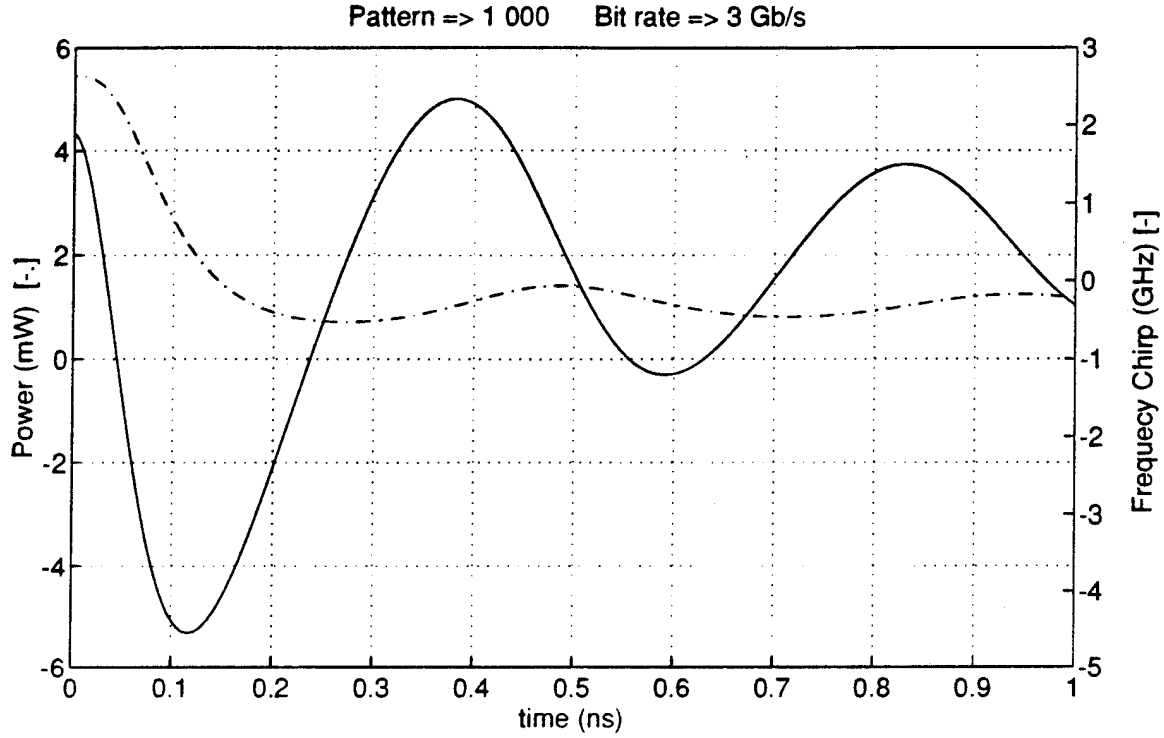

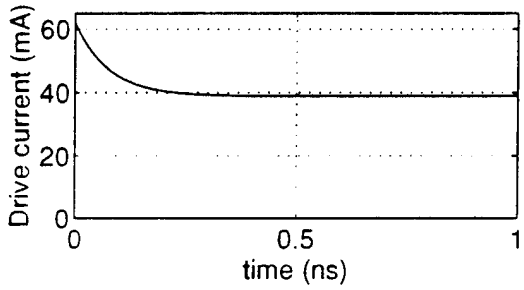

r = 0.1882
Max chirp freq excursion 2.331 GHz
Min chirp freq excursion -4.546 GHz
I_thresh = 0.0335 mA
I_off = 38.86 mA
I_on = 61.98 mA
Case 25

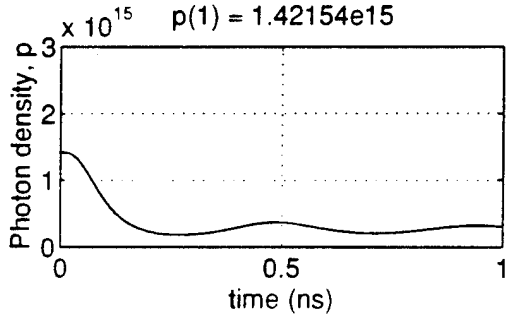

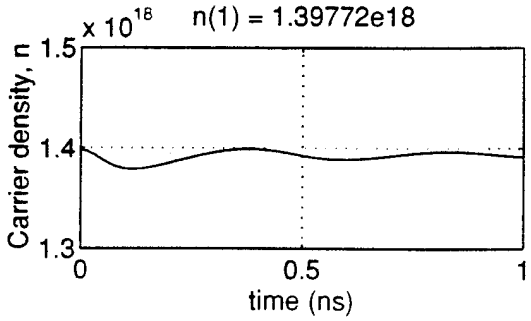

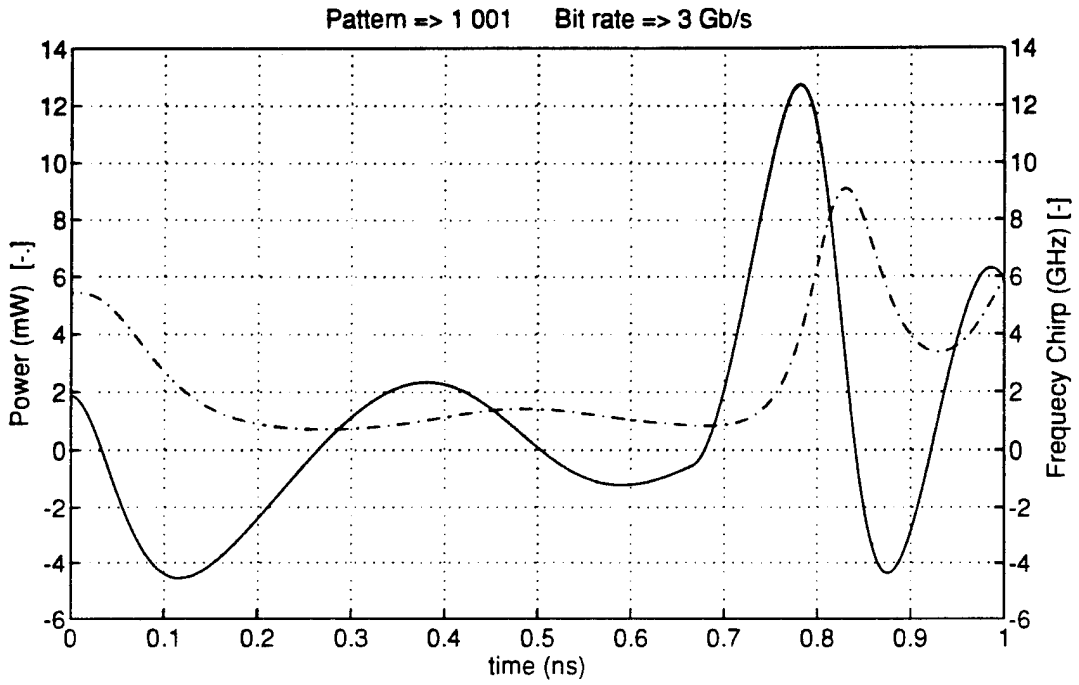

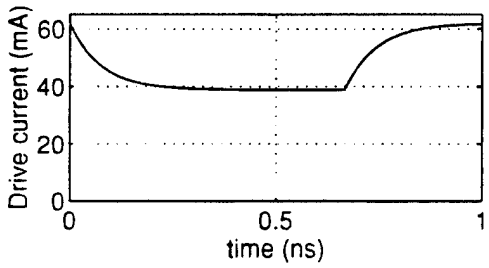

r = 0.1882
Max chirp freq excursion 12.73 GHz
Min chirp freq excursion -4.546 GHz
I_thresh = 0.0335 mA
I_off = 38.86 mA
I_on = 61.98 mA
Case 26

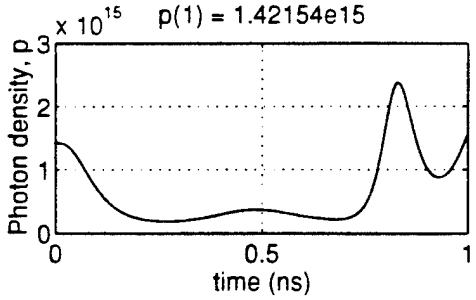

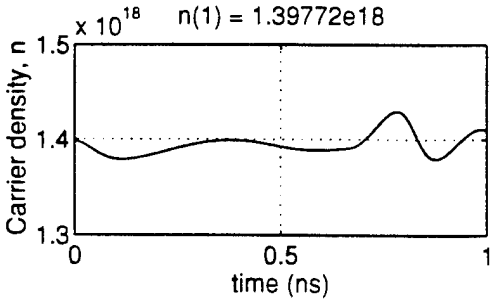

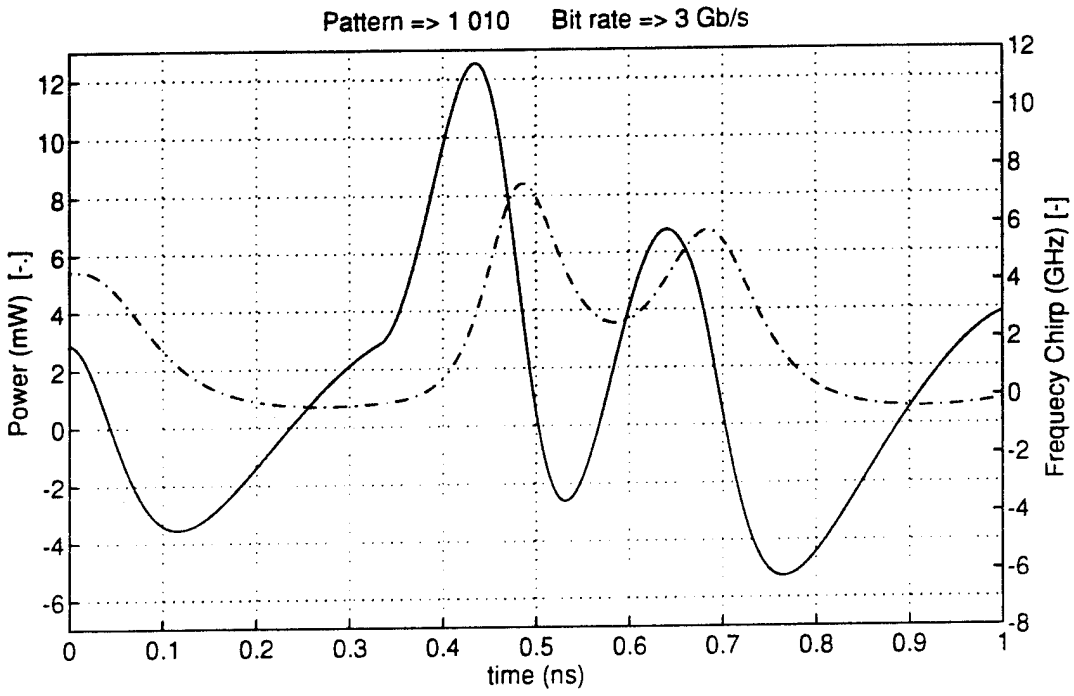

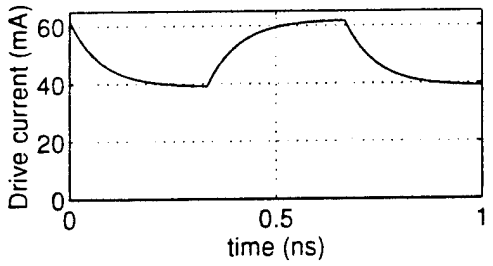

r = 0.1882
Max chirp freq excursion 11.55 GHz
Min chirp freq excursion -6.254 GHz
I_thresh = 0.0335 mA
I_off = 38.86 mA
I_on = 61.98 mA
Case 27

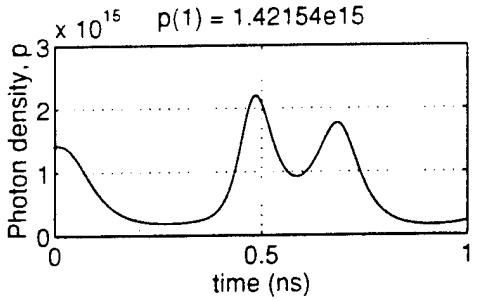

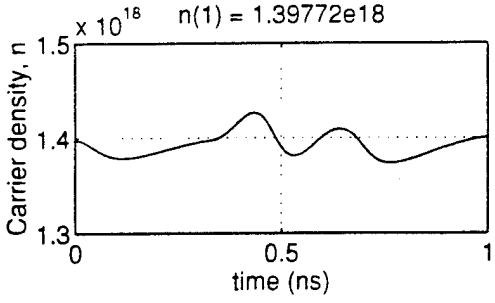

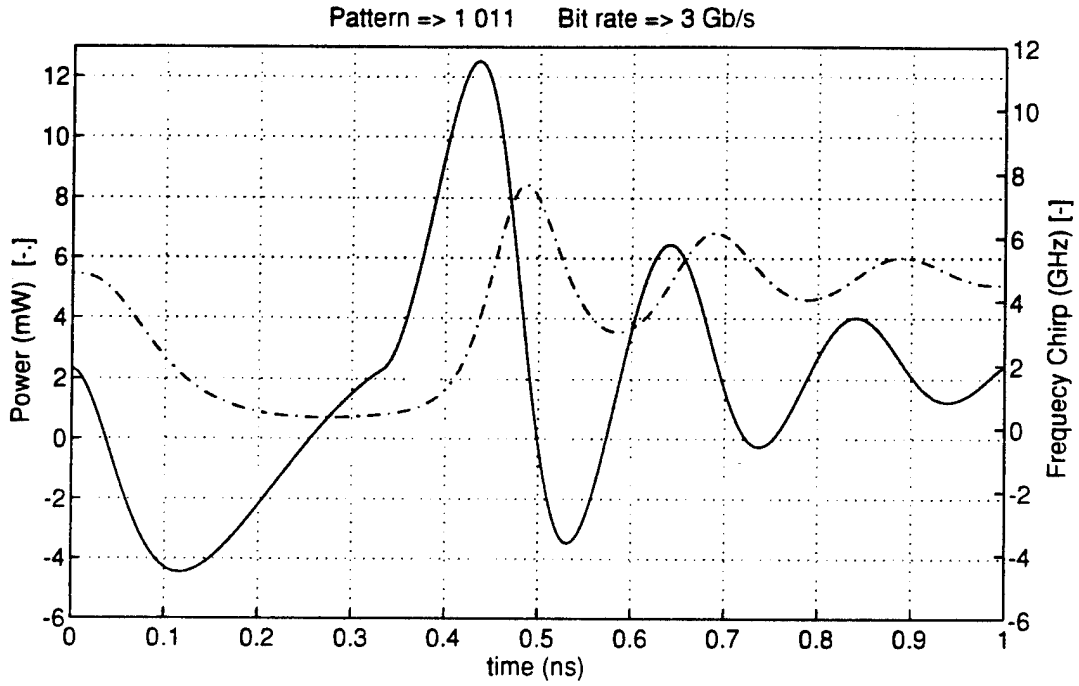

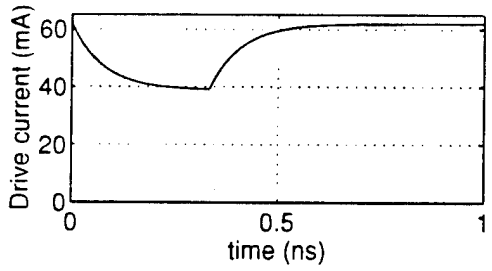

r = 0.1882
Max chirp freq excursion 11.55 GHz
Min chirp freq excursion -4.546 GHz
I_thresh = 0.0335 mA
I_off = 38.86 mA
I_on = 61.98 mA
Case 28

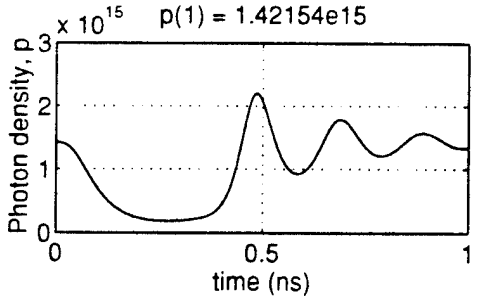

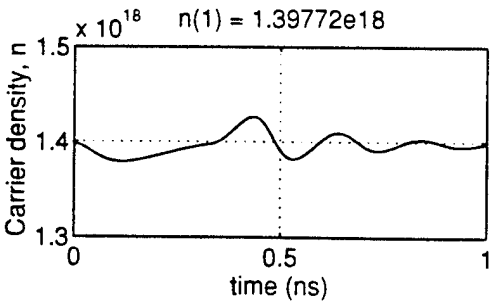

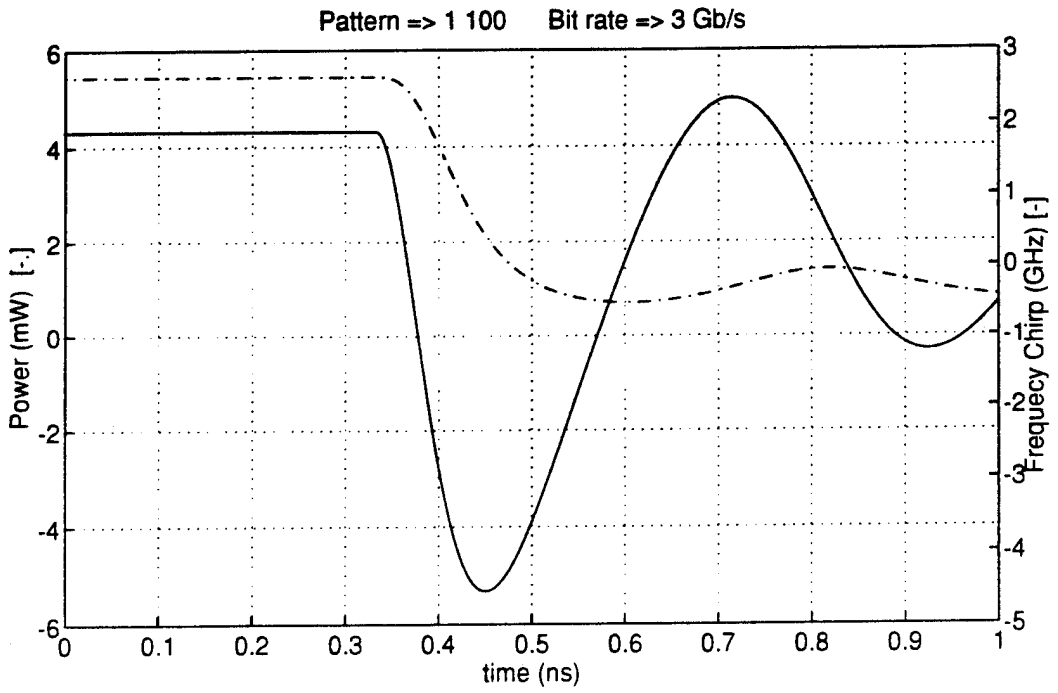

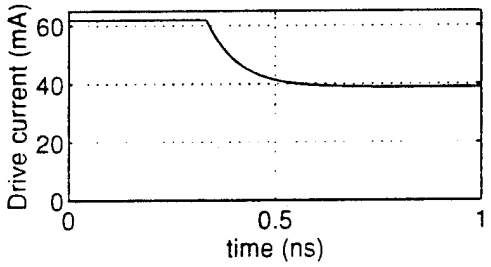

r = 0.1882
Max chirp freq excursion 2.33 GHz
Min chirp freq excursion -4.544 GHz
I_thresh = 0.0335 mA
I_off = 38.86 mA
I_on = 61.98 mA
Case 29

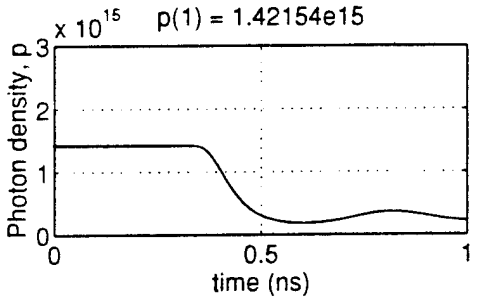

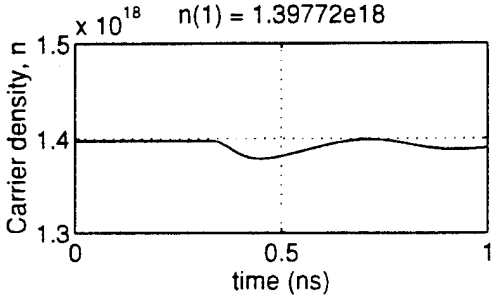

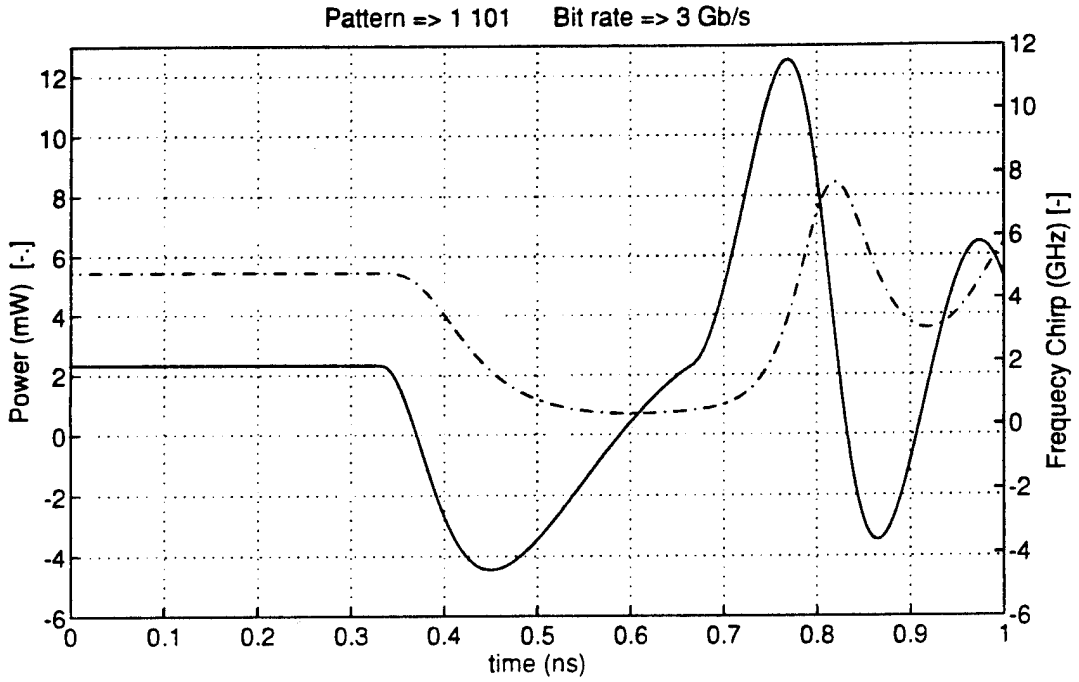

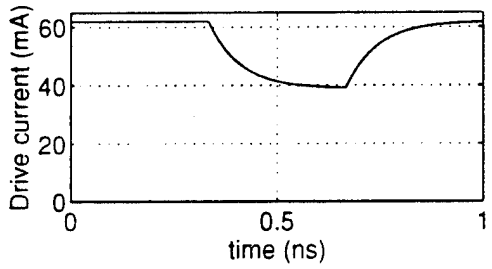

r = 0.1882
Max chirp freq excursion 11.55 GHz
Min chirp freq excursion -4.544 GHz
I_thresh = 0.0335 mA
I_off = 38.86 mA
I_on = 61.98 mA
Case 30

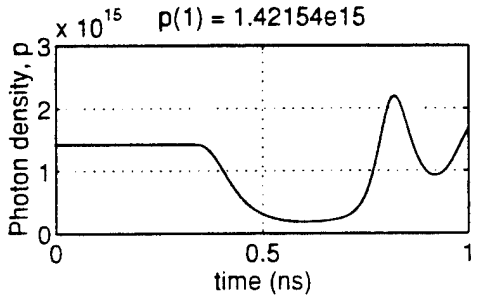

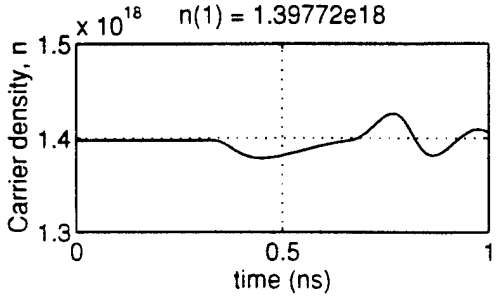

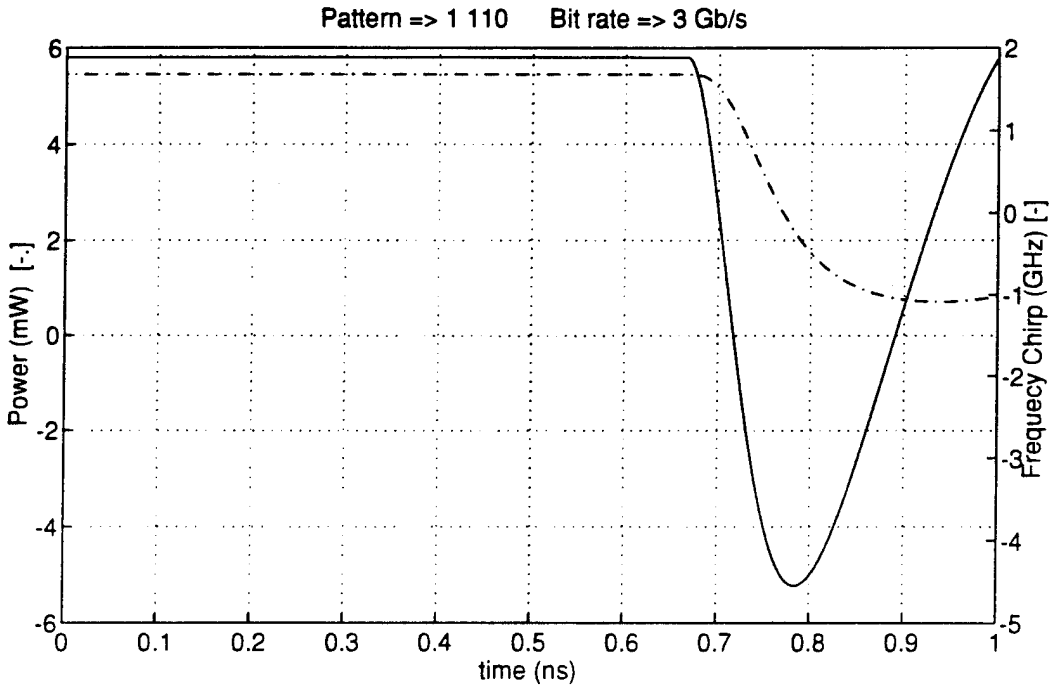

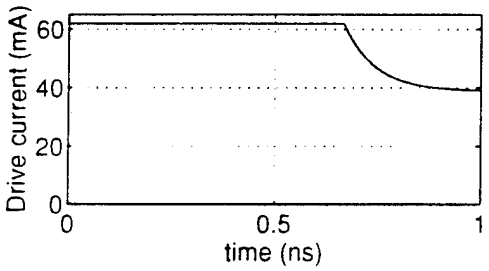

r = 0.1882
Max chirp freq excursion 1.882 GHz
Min chirp freq excursion -4.545 GHz
I_thresh = 0.0335 mA
I_off = 38.86 mA
I_on = 61.98 mA
Case 31

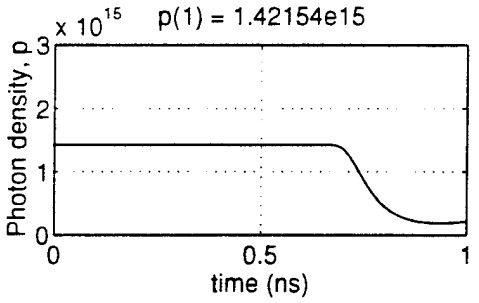

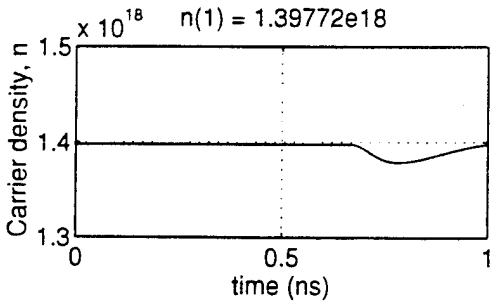

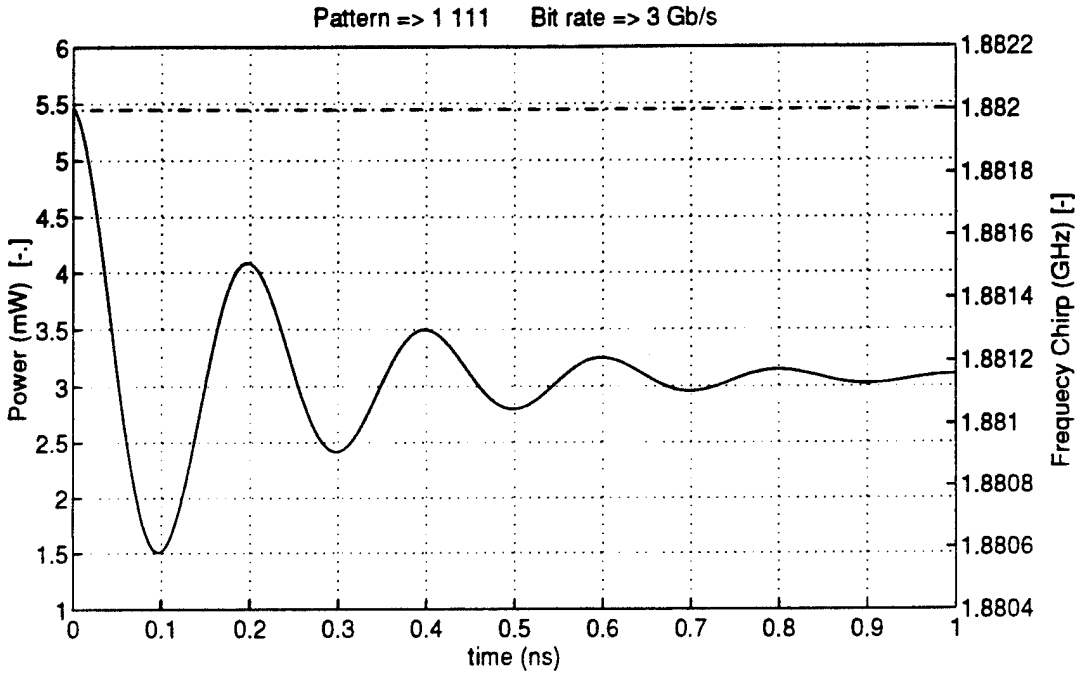

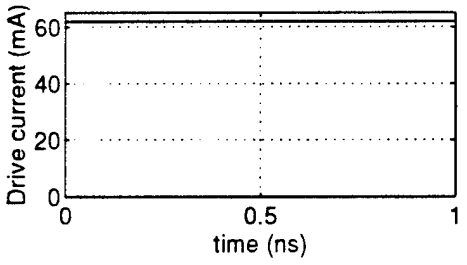

r = 0.1882
Max chirp freq excursion 1.882 GHz
Min chirp freq excursion 1.881 GHz
I_thresh = 0.0335 mA
I_off = 38.86 mA
I_on = 61.98 mA
Case 32

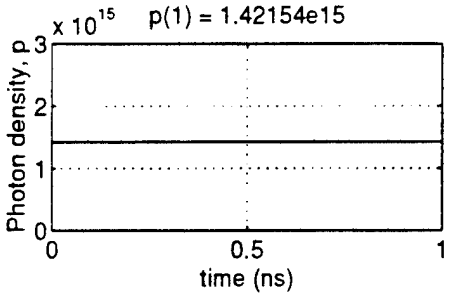

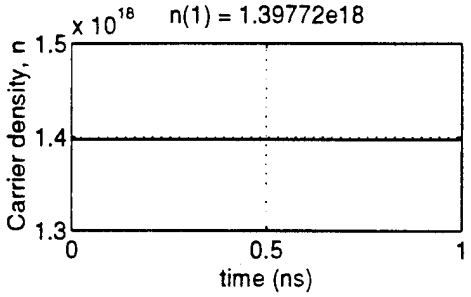

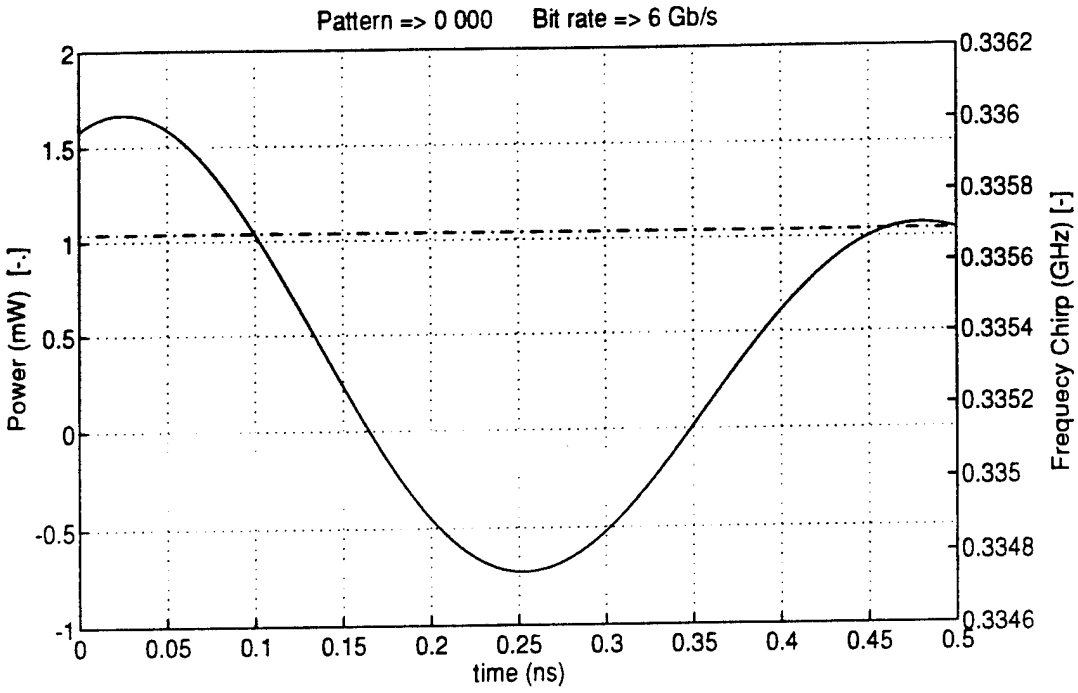

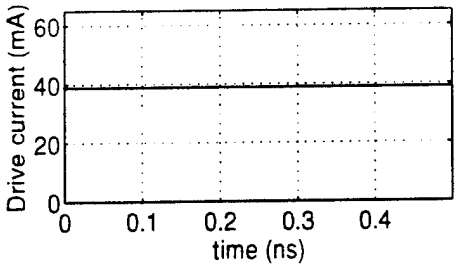

r = 0.1882
Max chirp freq excursion 0.336 GHz
Min chirp freq excursion 0.3347 GHz
I_thresh = 0.0335 mA
I_off = 38.86 mA
I_on = 61.98 mA
Case 33

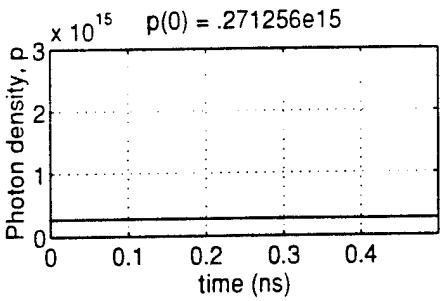

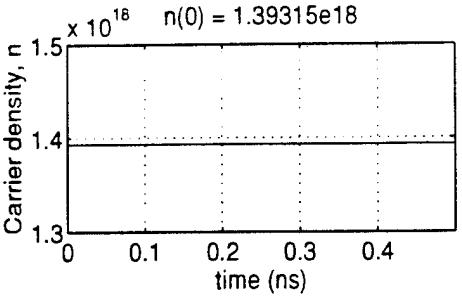

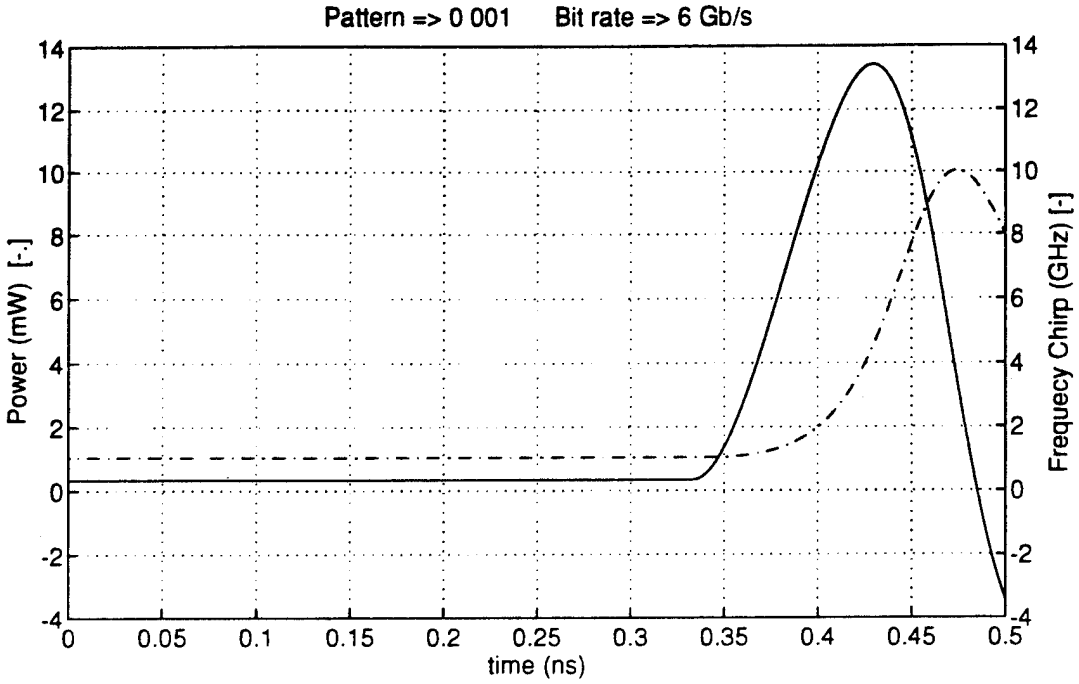

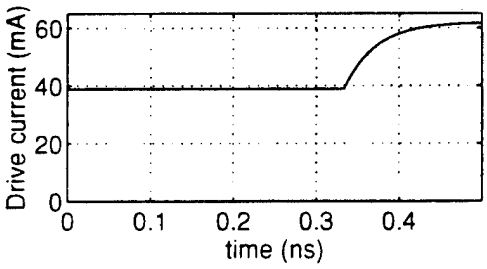

r = 0.1882
Max chirp freq excursion 13.42 GHz
Min chirp freq excursion -3.429 GHz
I_thresh = 0.0335 mA
I_off = 38.86 mA
I_on = 61.98 mA
Case 34

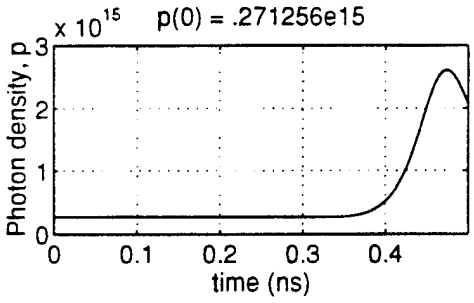

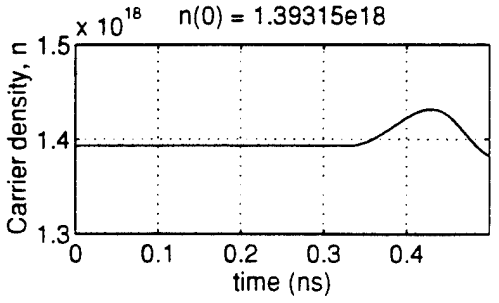

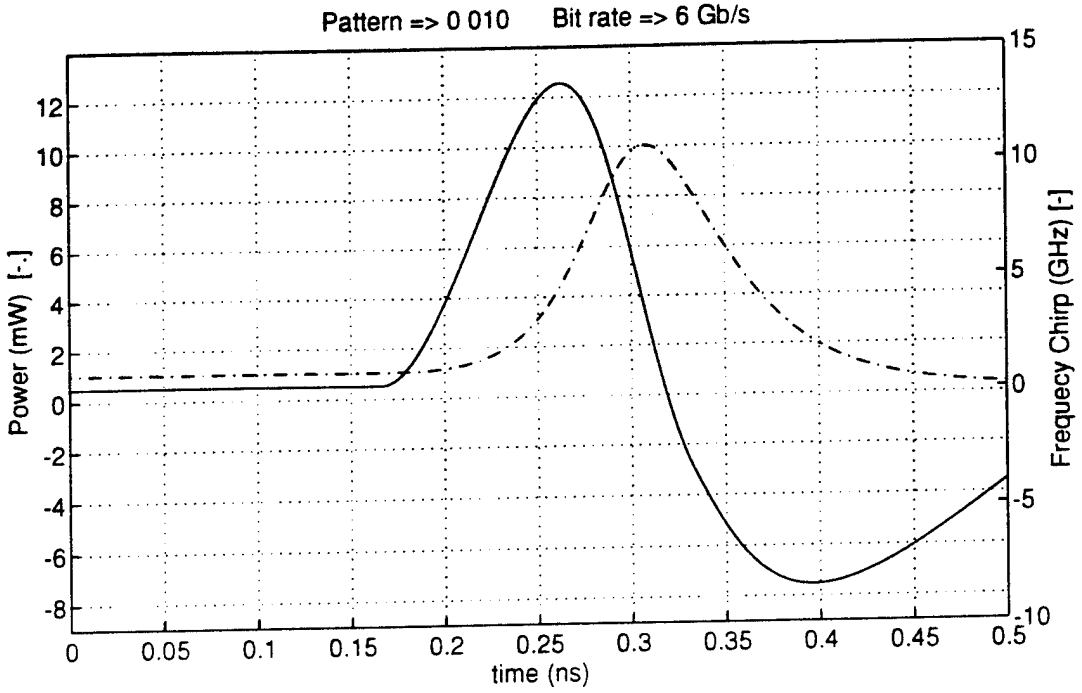

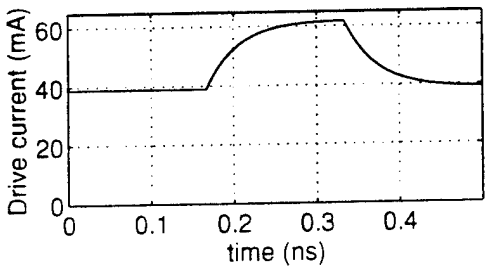

r = 0.1882
Max chirp freq excursion 13.42 GHz
Min chirp freq excursion -8.403 GHz
I_thresh = 0.0335 mA
I_off = 38.86 mA
I_on = 61.98 mA
Case 35

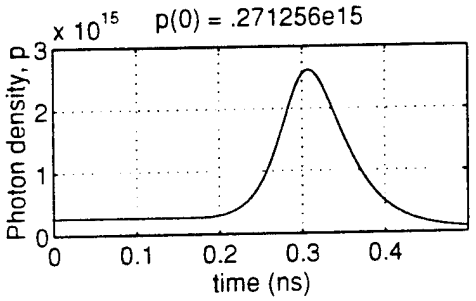

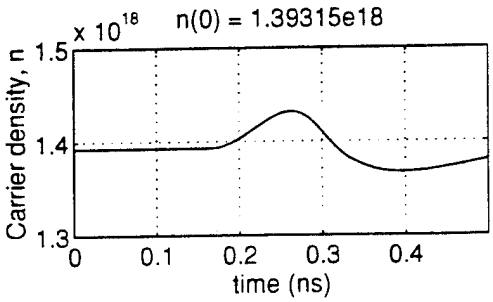

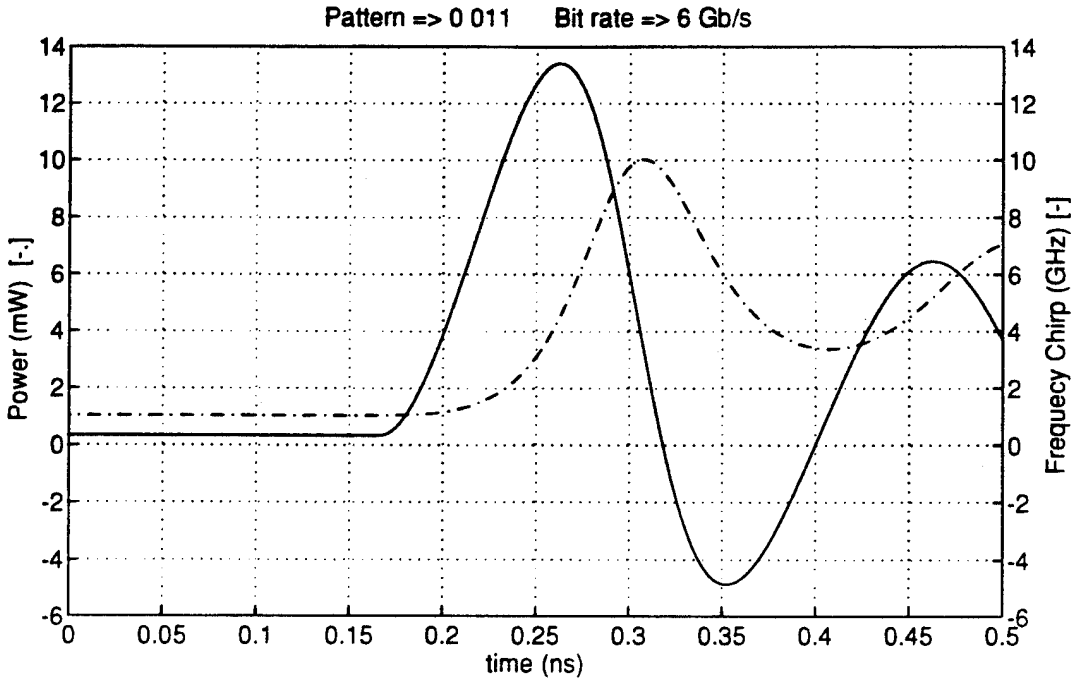

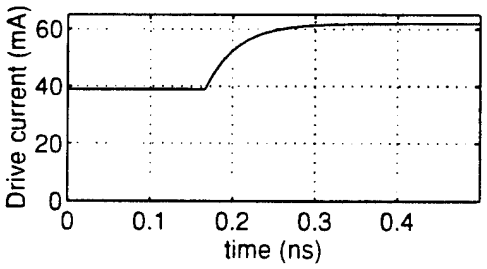

r = 0.1882
Max chirp freq excursion 13.42 GHz
Min chirp freq excursion -4.861 GHz
I_thresh = 0.0335 mA
I_off = 38.86 mA
I_on = 61.98 mA
Case 36

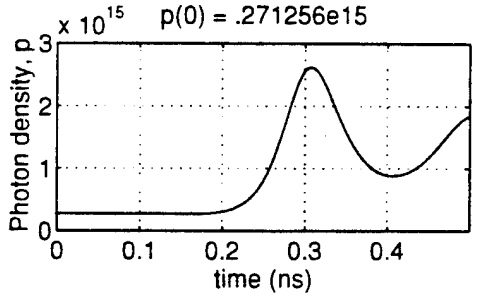

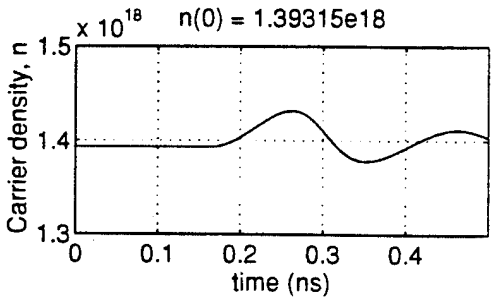

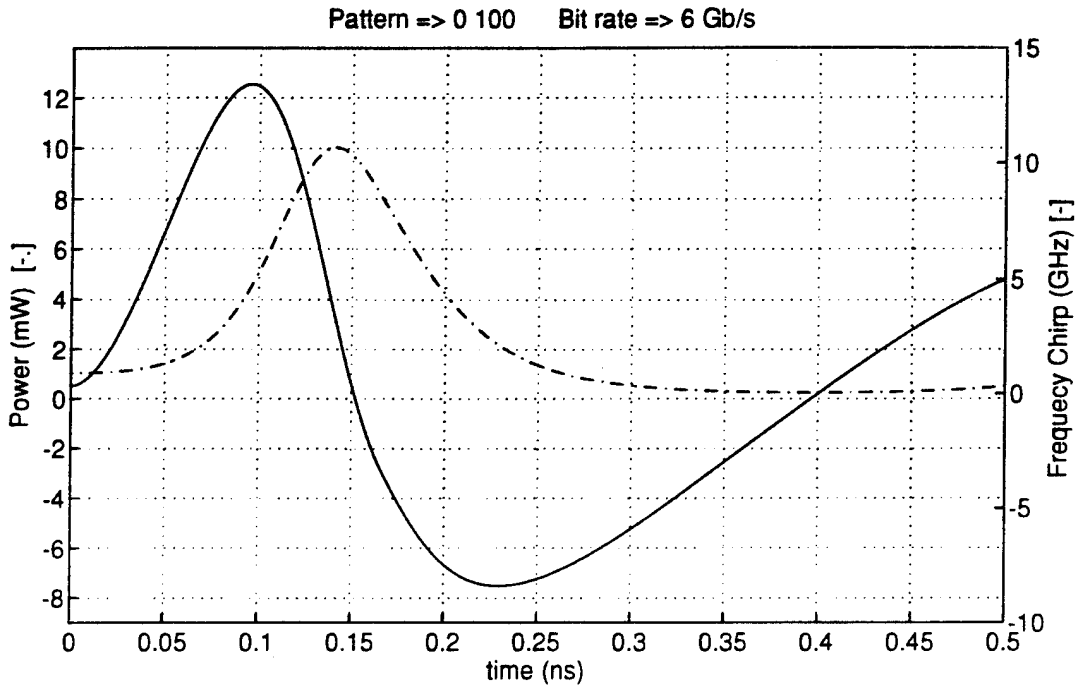

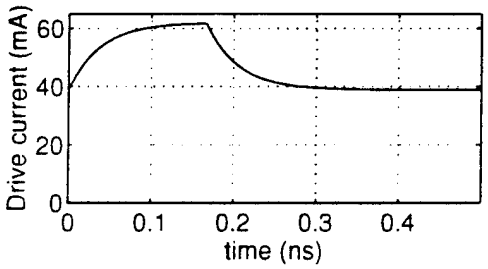

r = 0.1882
Max chirp freq excursion 13.42 GHz
Min chirp freq excursion -8.404 GHz
I_thresh = 0.0335 mA
I_off = 38.86 mA
I_on = 61.98 mA
Case 37

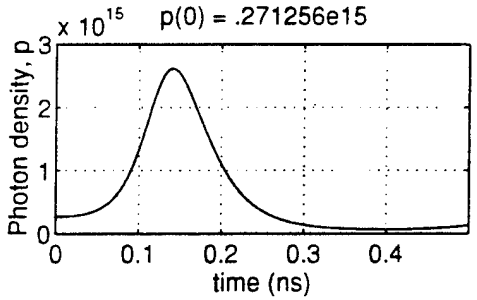

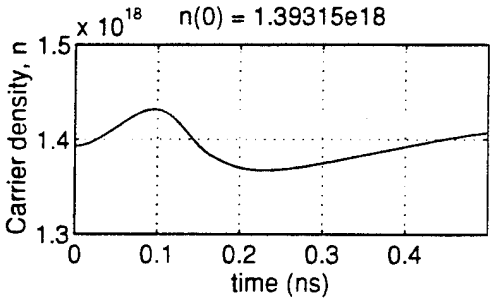

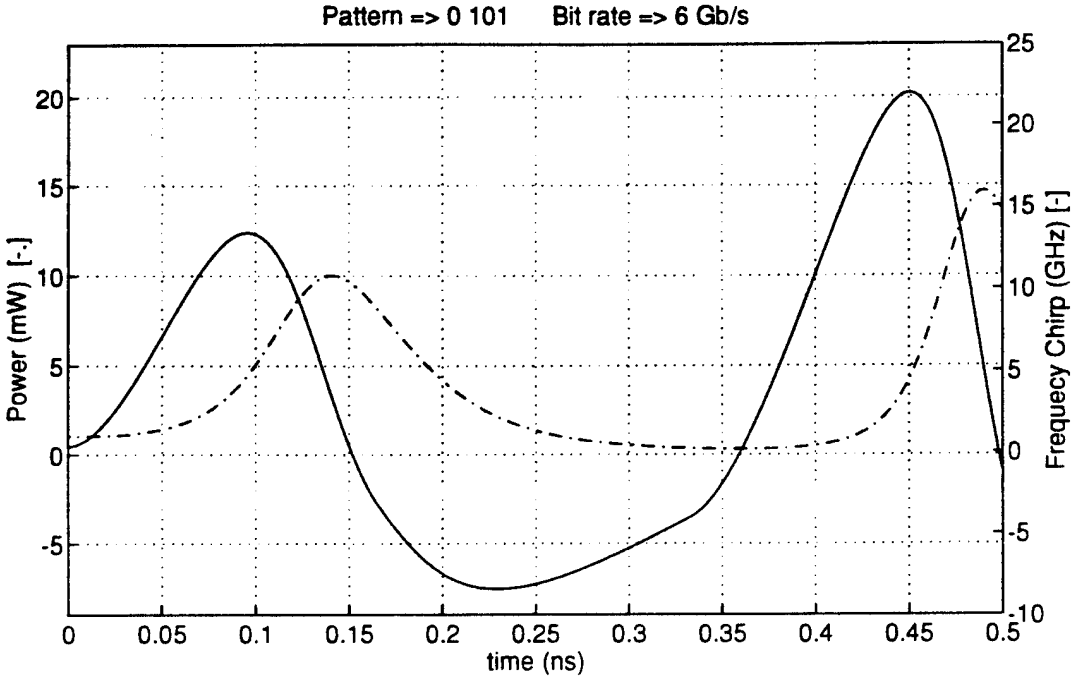

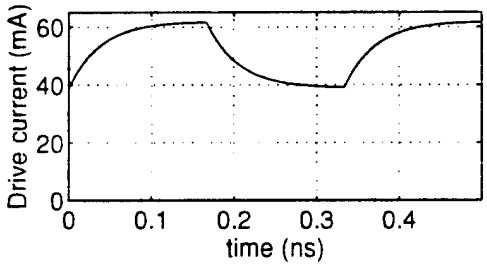

r = 0.1882
Max chirp freq excursion 21.95 GHz
Min chirp freq excursion -8.404 GHz
I_thresh = 0.0335 mA
I_off = 38.86 mA
I_on = 61.98 mA
Case 38

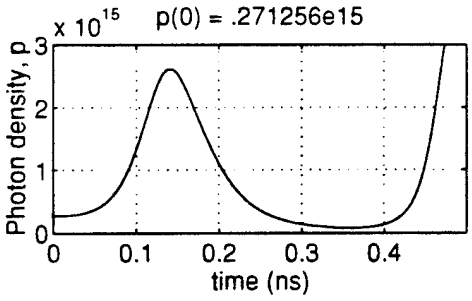

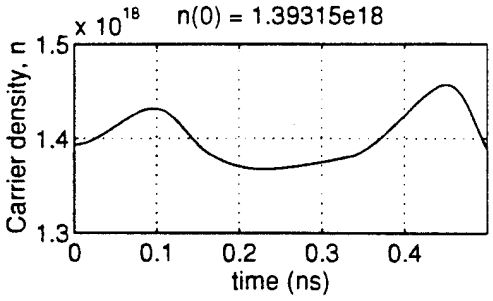

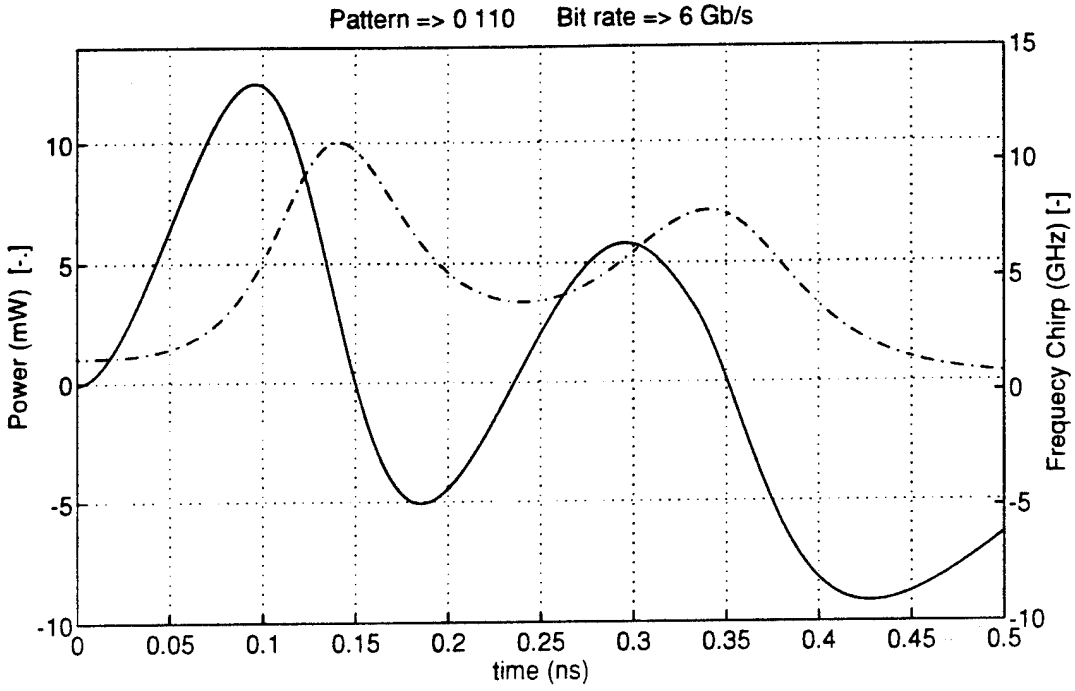

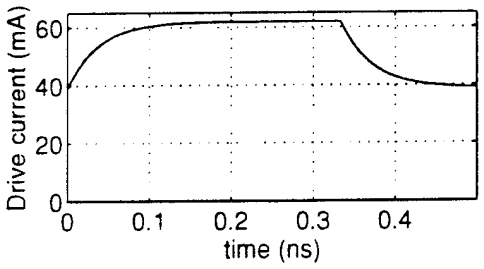

r = 0.1882
Max chirp freq excursion 13.42 GHz
Min chirp freq excursion -9.11 GHz
I_thresh = 0.0335 mA
I_off = 38.86 mA
I_on = 61.98 mA
Case 39

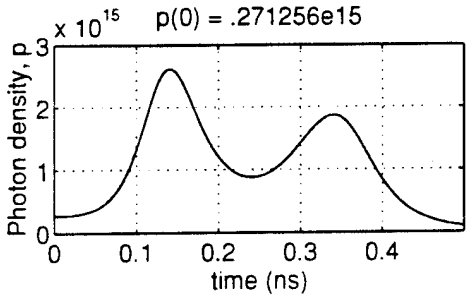

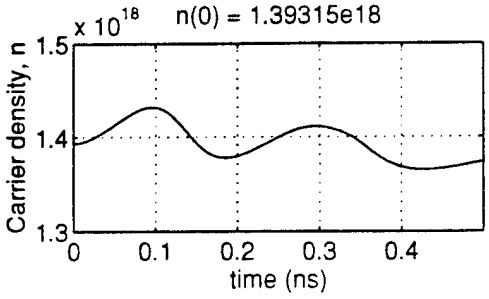

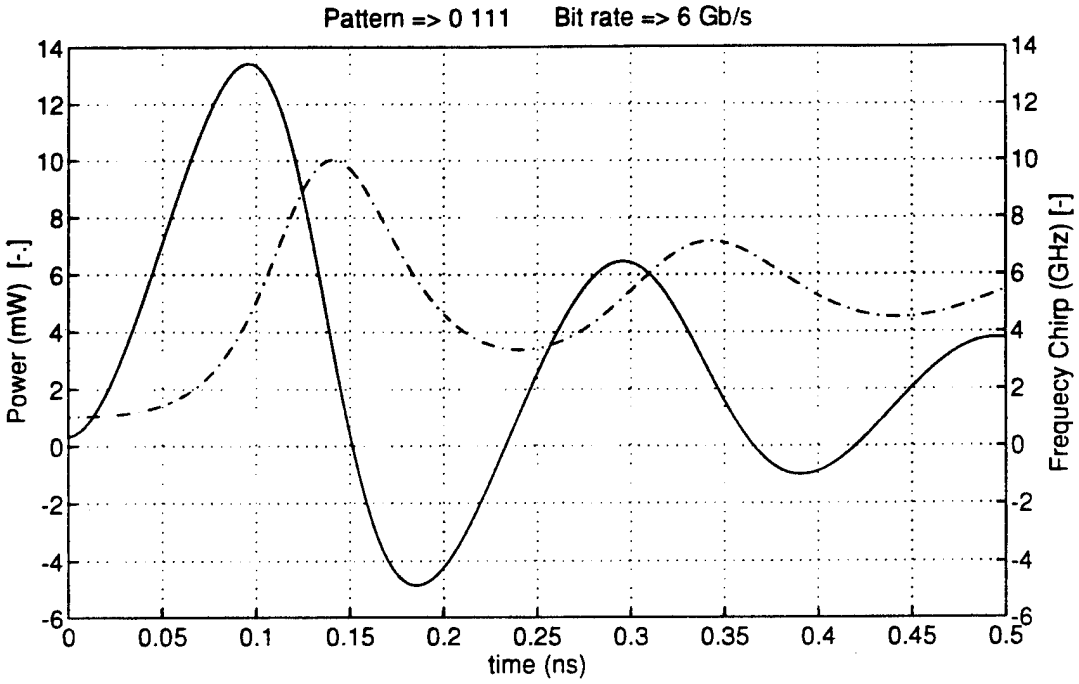

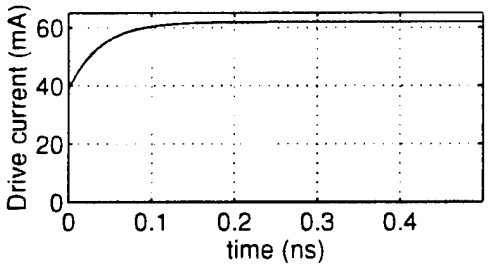

r = 0.1882
Max chirp freq excursion 13.42 GHz
Min chirp freq excursion -4.861 GHz
I_thresh = 0.0335 mA
I_off = 38.86 mA
I_on = 61.98 mA
Case 40

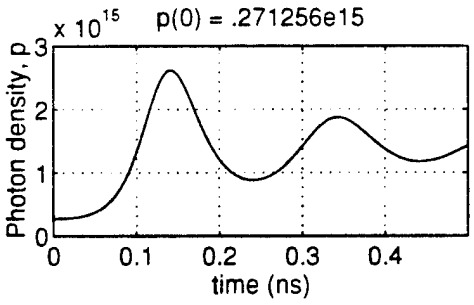

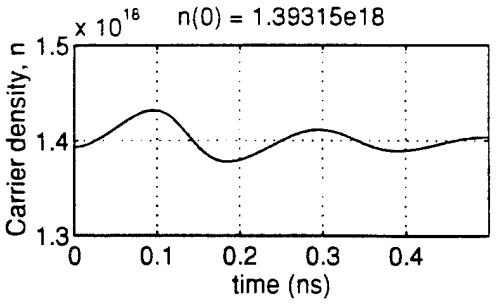

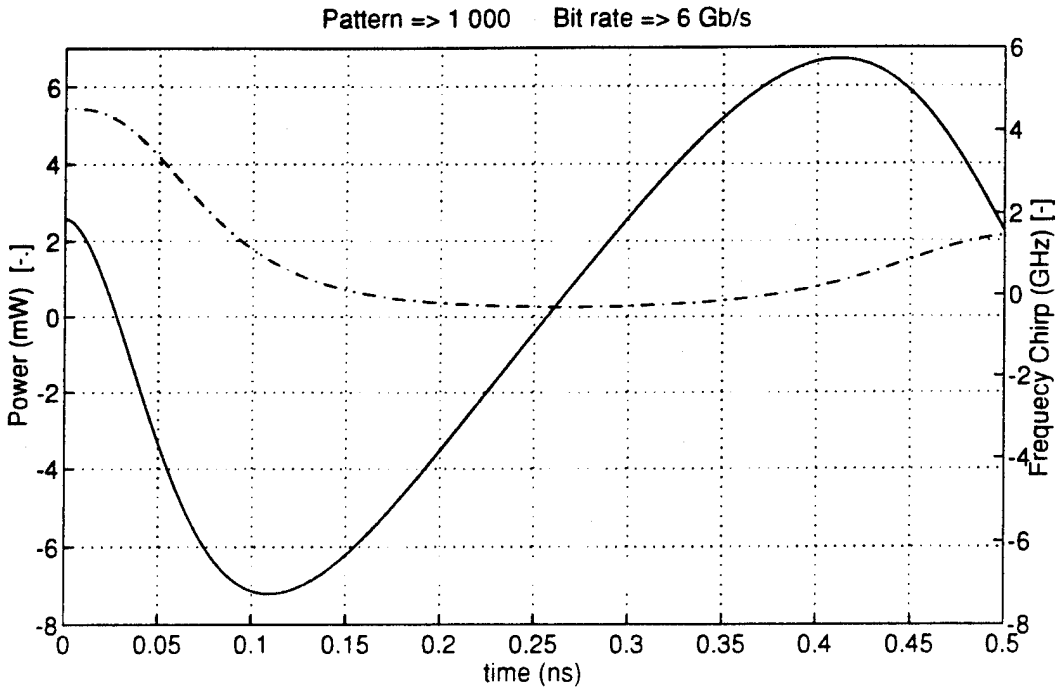

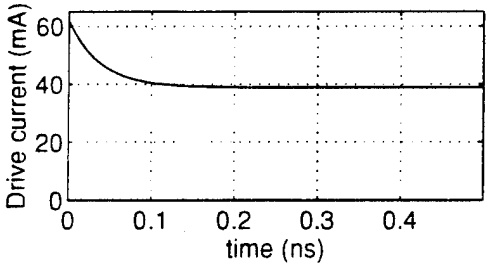

r = 0.1882
Max chirp freq excursion 5.728 GHz
Min chirp freq excursion -7.257 GHz
I_thresh = 0.0335 mA
I_off = 38.86 mA
I_on = 61.98 mA
Case 41

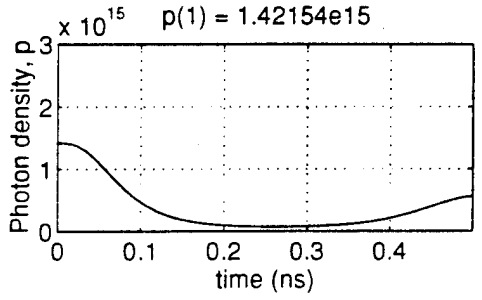

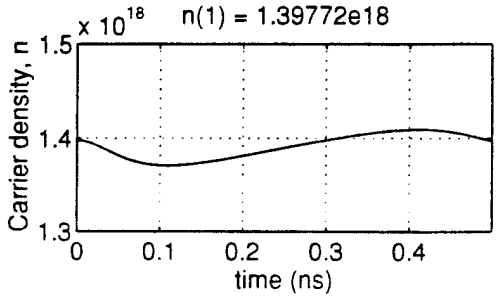

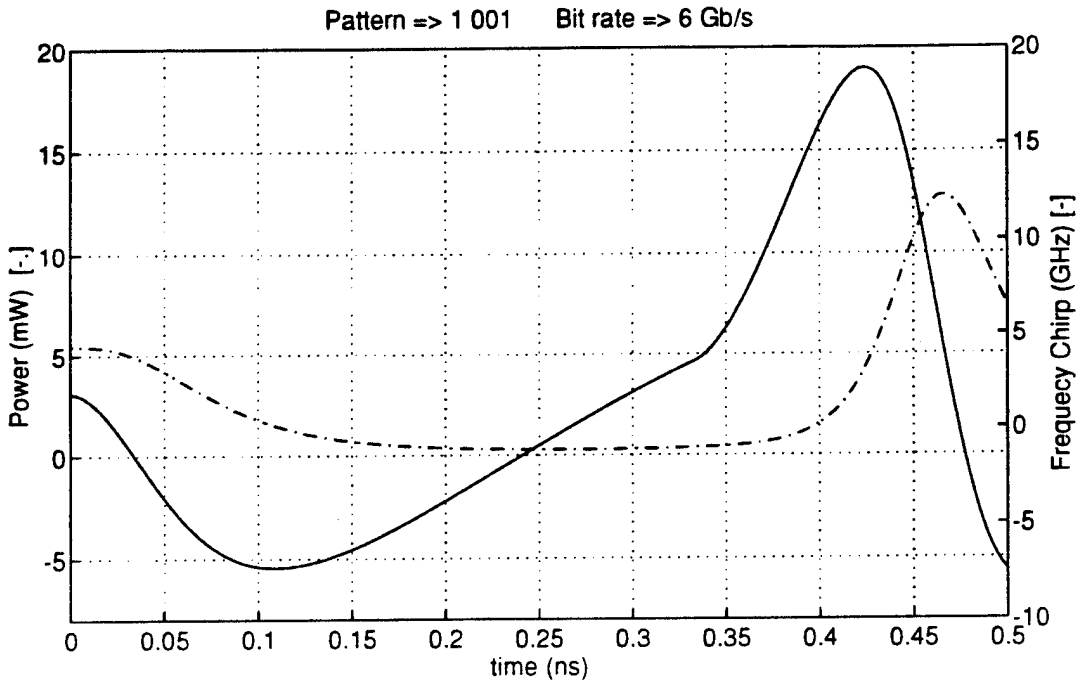

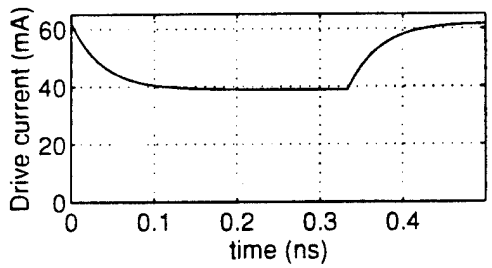

r = 0.1882
Max chirp freq excursion 18.93 GHz
Min chirp freq excursion -7.409 GHz
I_thresh = 0.0335 mA
I_off = 38.86 mA
I_on = 61.98 mA
Case 42

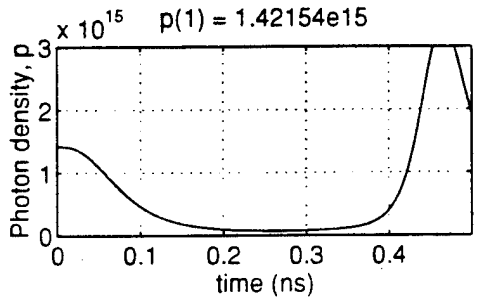

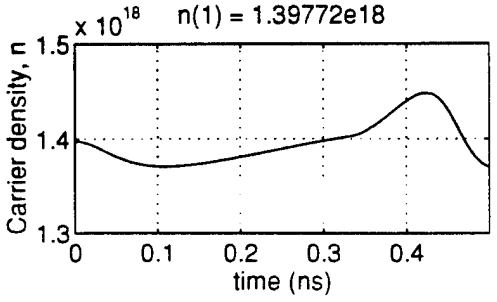

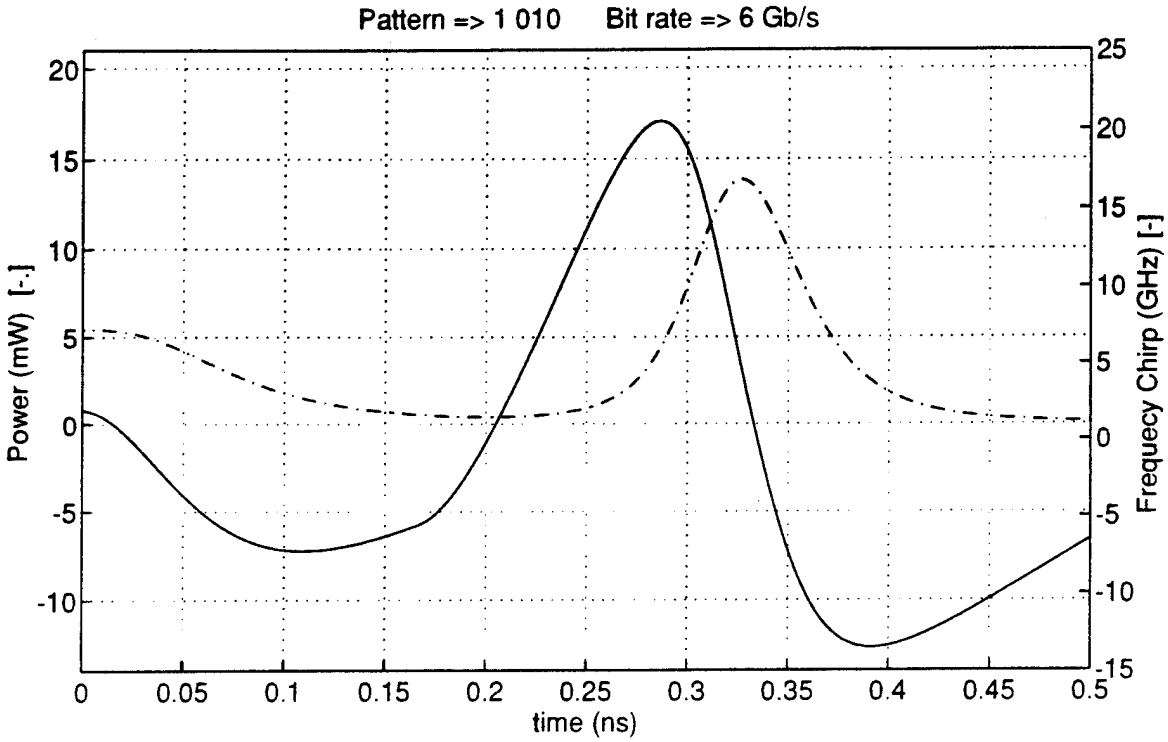

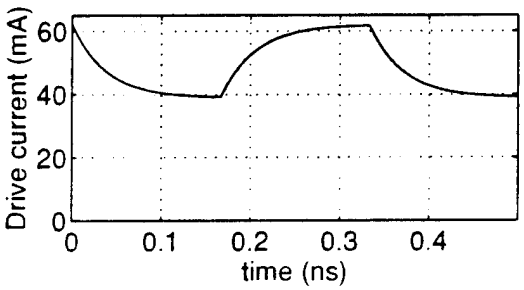

r = 0.1882
Max chirp freq excursion 20.5 GHz
Min chirp freq excursion -13.5 GHz
I_thresh = 0.0335 mA
I_off = 38.86 mA
I_on = 61.98 mA
Case 43

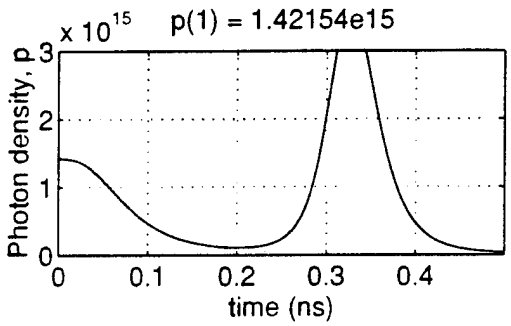

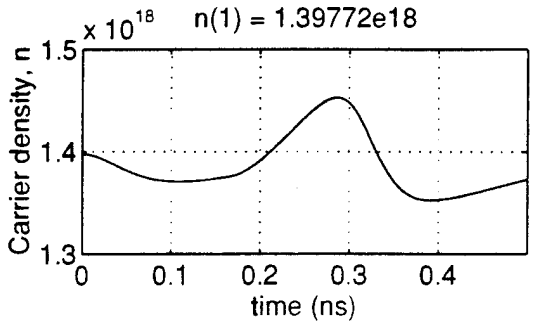

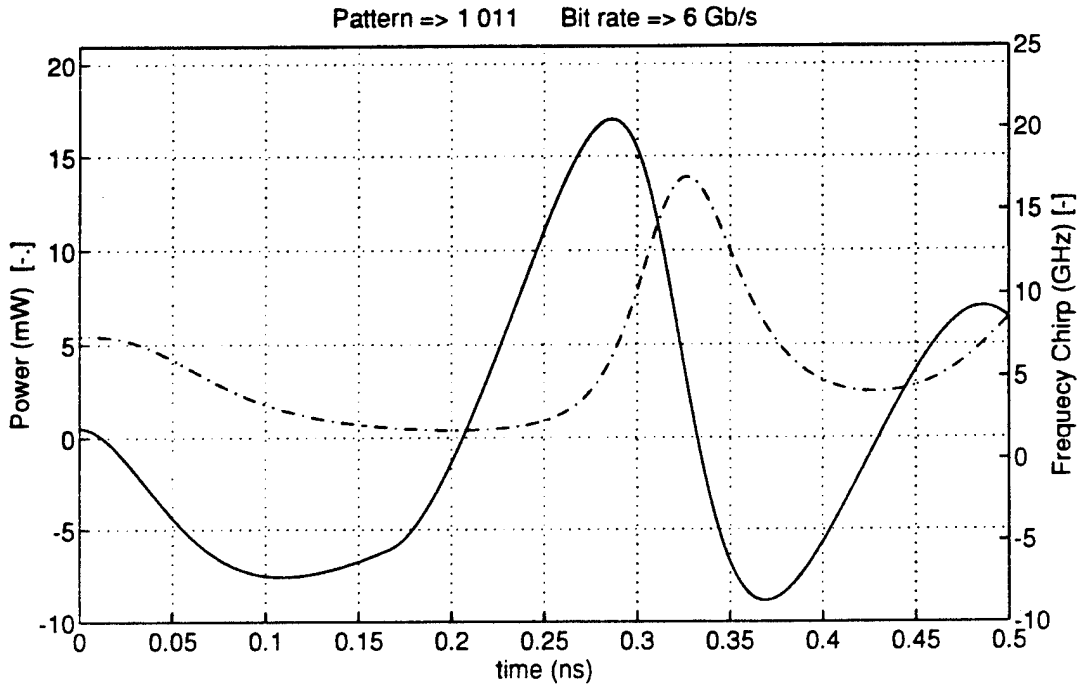

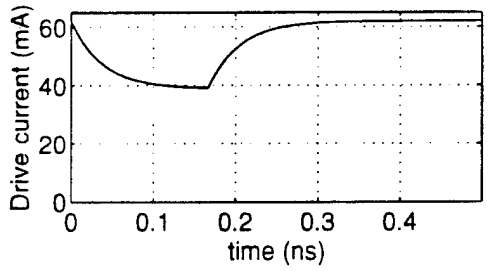

r = 0.1882
Max chirp freq excursion 20.5 GHz
Min chirp freq excursion -8.715 GHz
I_thresh = 0.0335 mA
I_off = 38.86 mA
I_on = 61.98 mA
Case 44

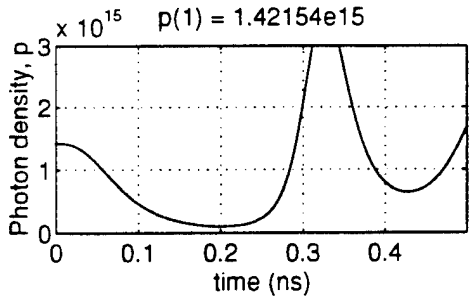

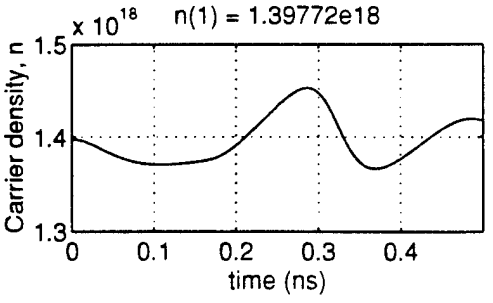

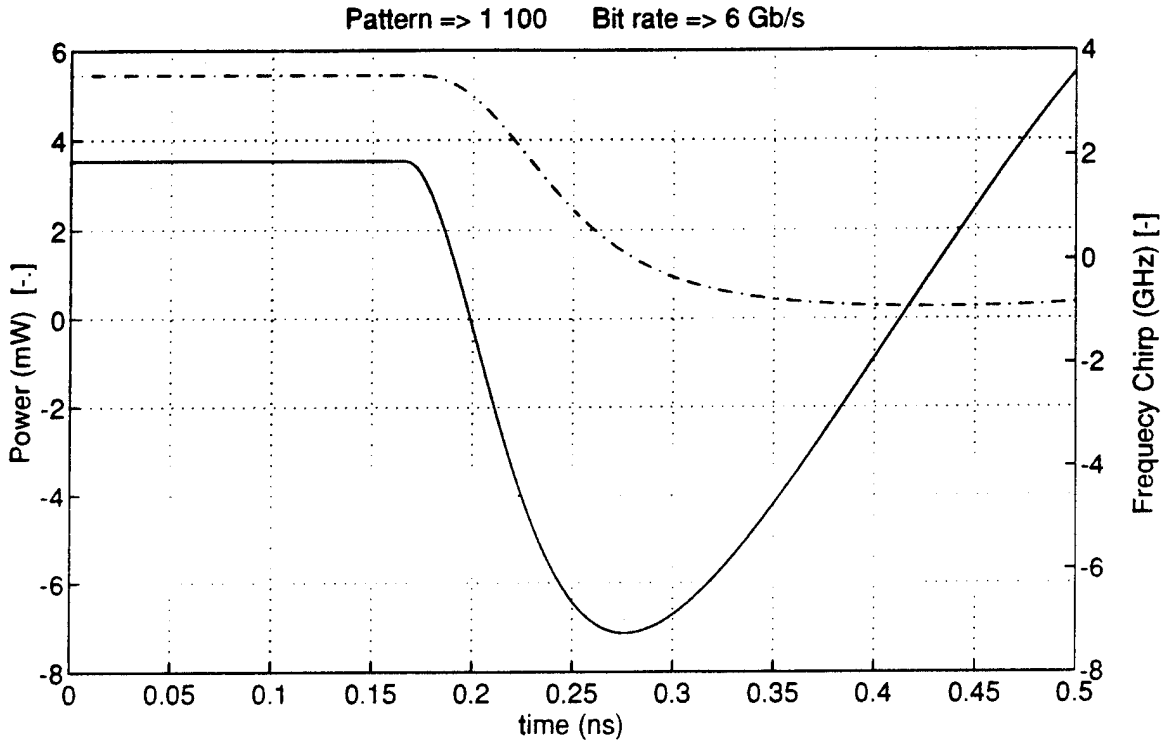

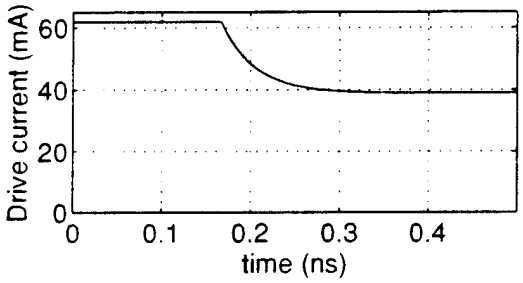

r = 0.1882
Max chirp freq excursion 3.571 GHz
Min chirp freq excursion -7.256 GHz
I_thresh = 0.0335 mA
I_off = 38.86 mA
I_on = 61.98 mA
Case 45

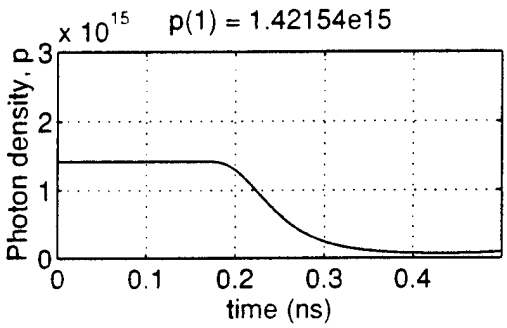

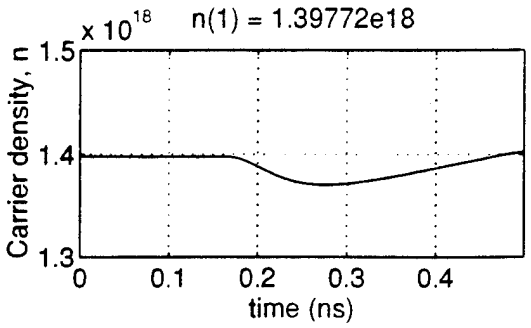

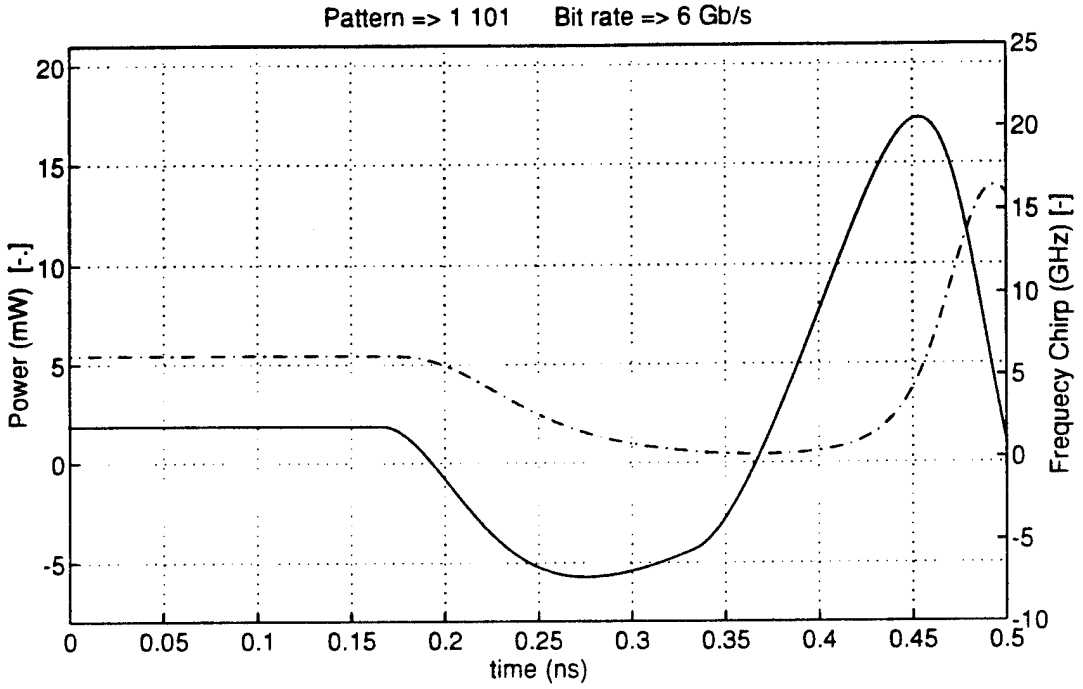

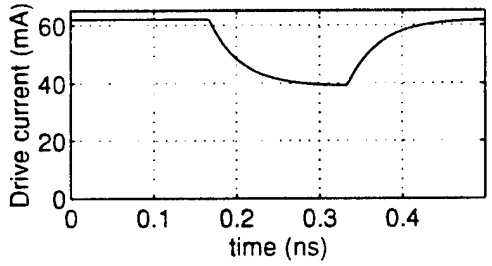

r = 0.1882
Max chirp freq excursion 20.49 GHz
Min chirp freq excursion -7.256 GHz
I_thresh = 0.0335 mA
I_off = 38.86 mA
I_on = 61.98 mA
Case 46

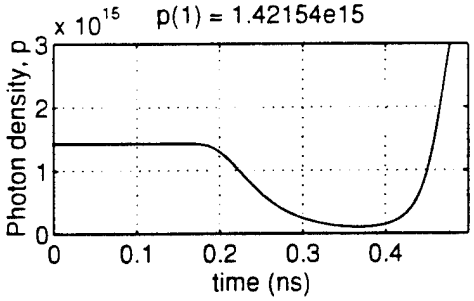

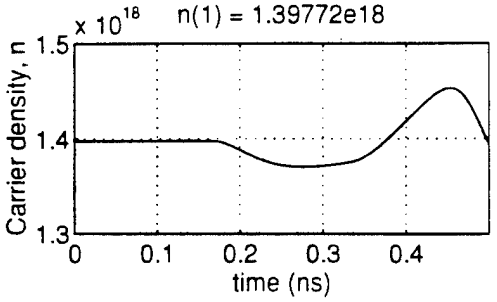

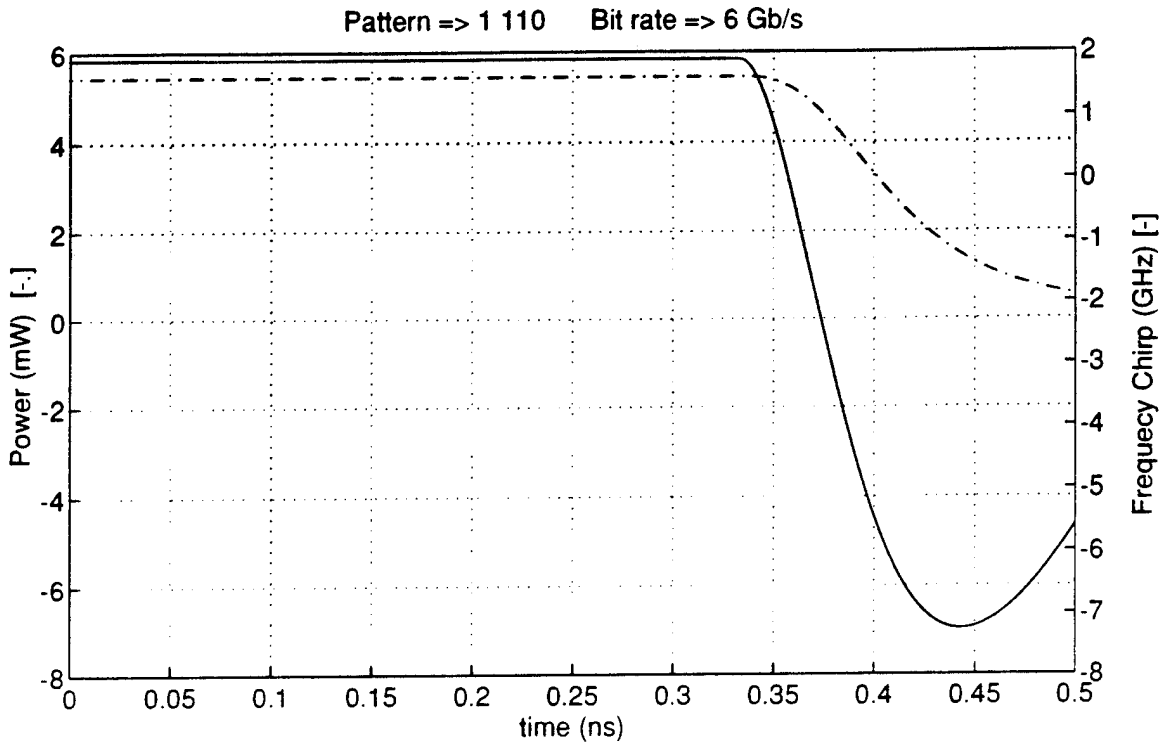

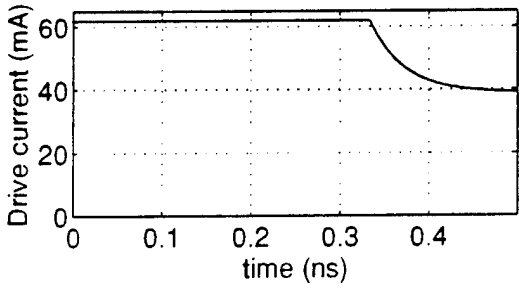

r = 0.1882
Max chirp freq excursion 1.882 GHz
Min chirp freq excursion -7.256 GHz
I_thresh = 0.0335 mA
I_off = 38.86 mA
I_on = 61.98 mA
Case 47

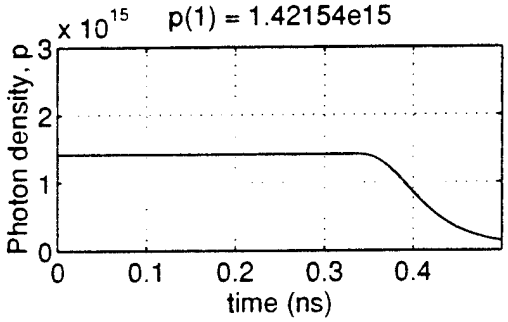

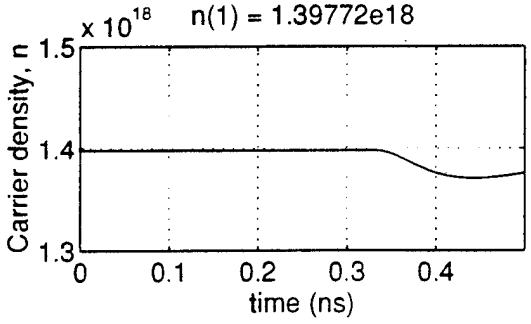

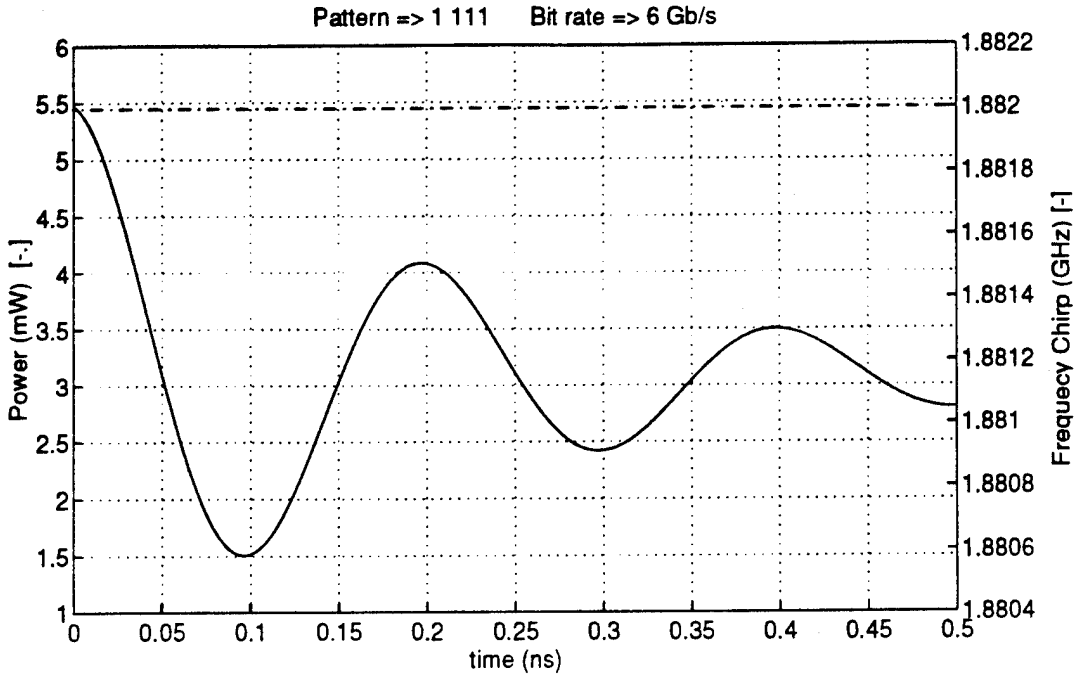

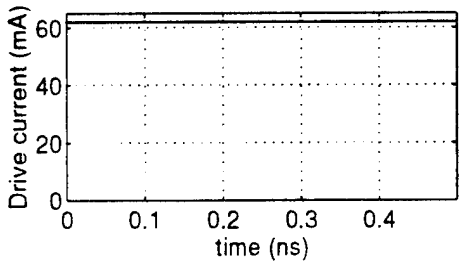

r = 0.1882
Max chirp freq excursion 1.882 GHz
Min chirp freq excursion 1.881 GHz
I_thresh = 0.0335 mA
I_off = 38.86 mA
I_on = 61.98 mA
Case 48

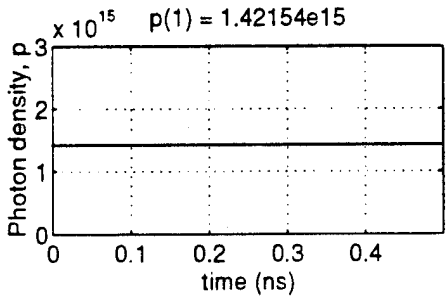

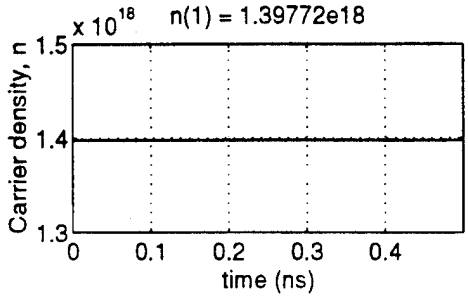

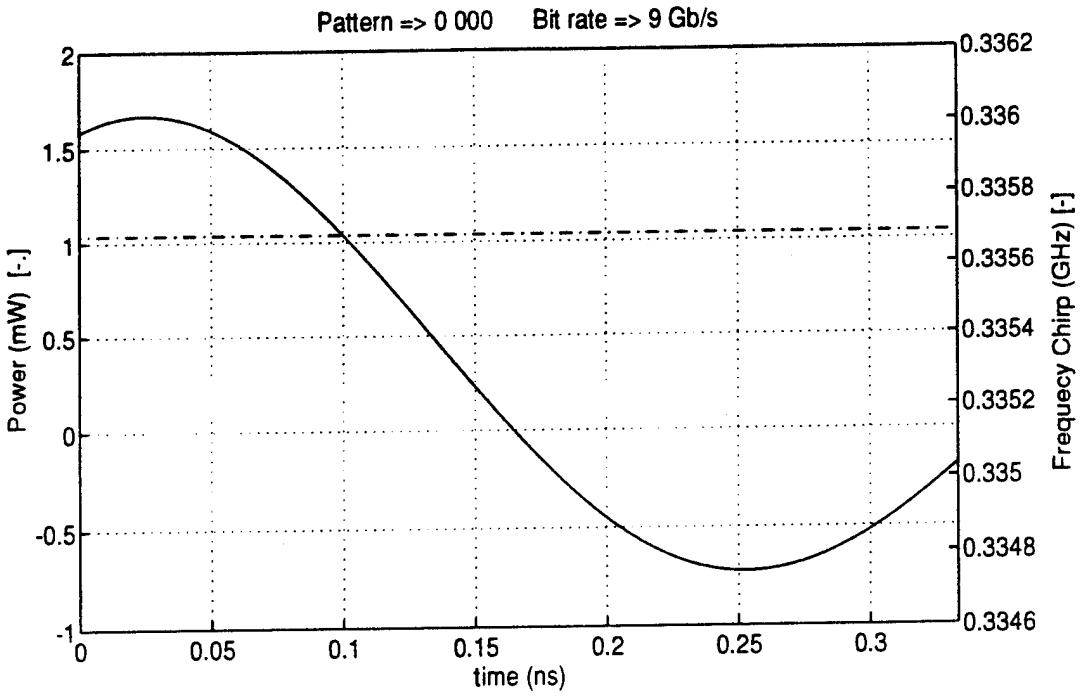

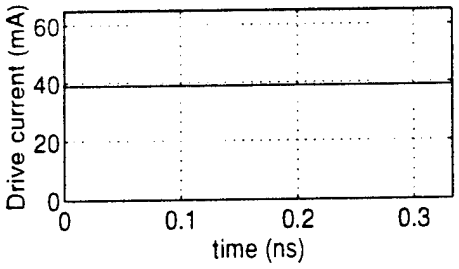

r = 0.1882
Max chirp freq excursion 0.336 GHz
Min chirp freq excursion 0.3347 GHz
I_thresh = 0.0335 mA
I_off = 38.86 mA
I_on = 61.98 mA
Case 49

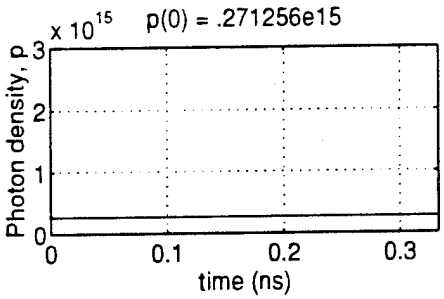

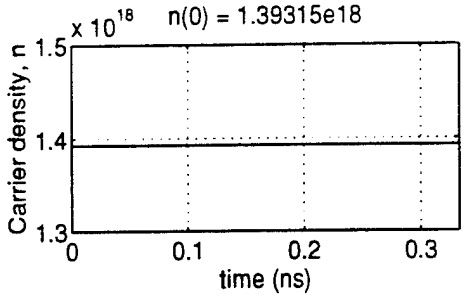

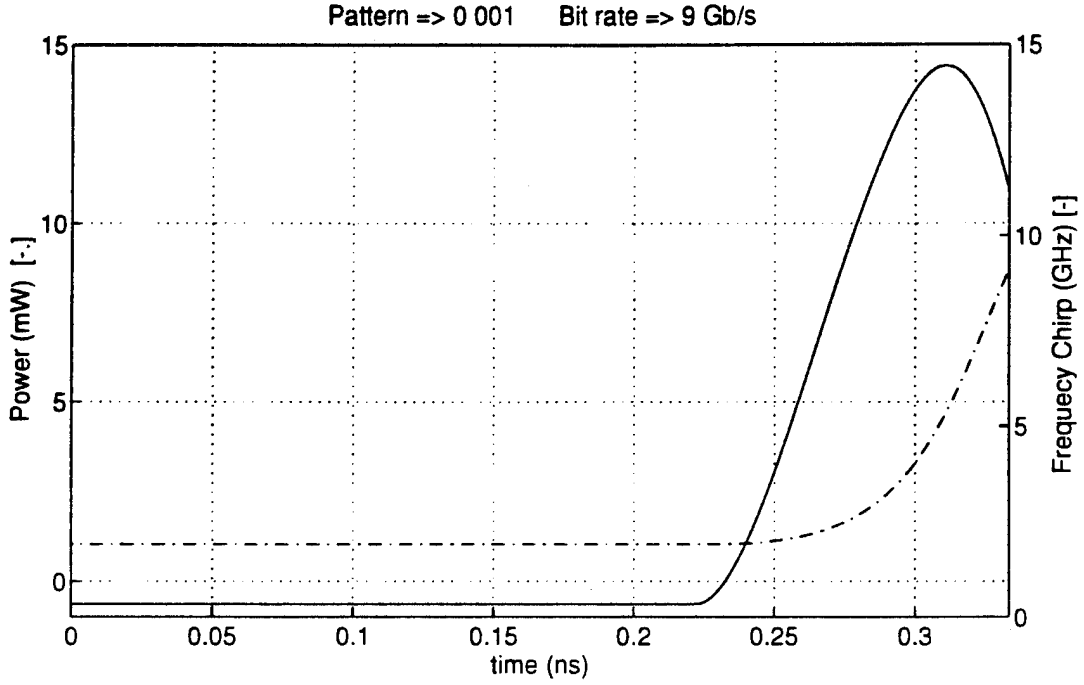

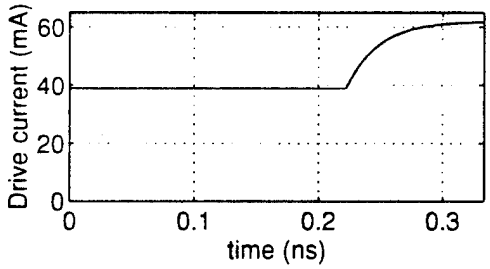

r = 0.1882
Max chirp freq excursion 14.45 GHz
Min chirp freq excursion 0.3348 GHz
I_thresh = 0.0335 mA
I_off = 38.86 mA
I_on = 61.98 mA
Case 50

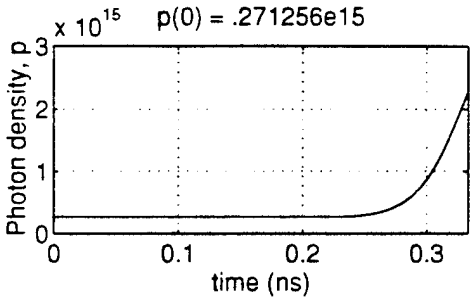

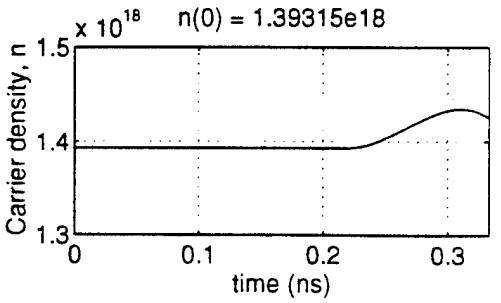

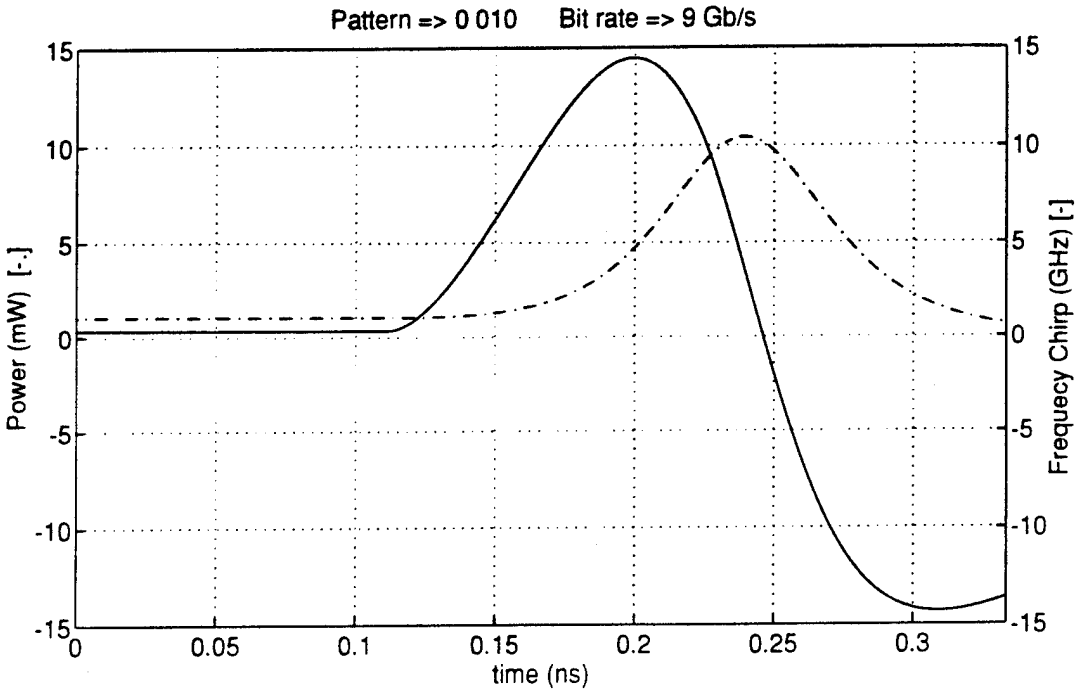

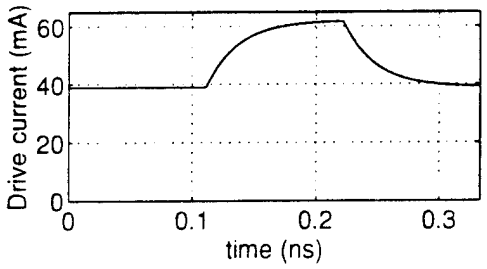

r = 0.1882
Max chirp freq excursion 14.45 GHz
Min chirp freq excursion -14.31 GHz
I_thresh = 0.0335 mA
I_off = 38.86 mA
I_on = 61.98 mA
Case 51

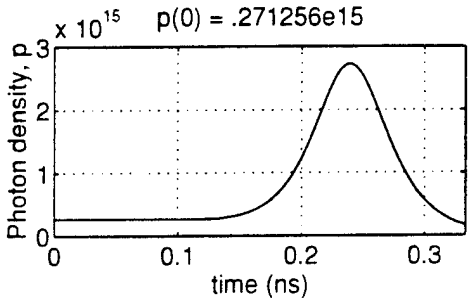

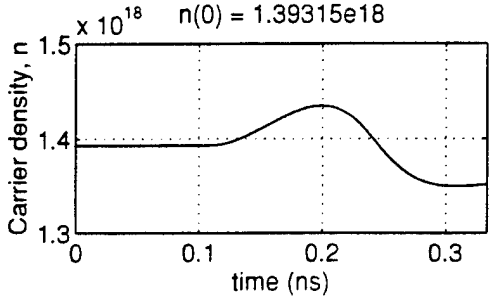

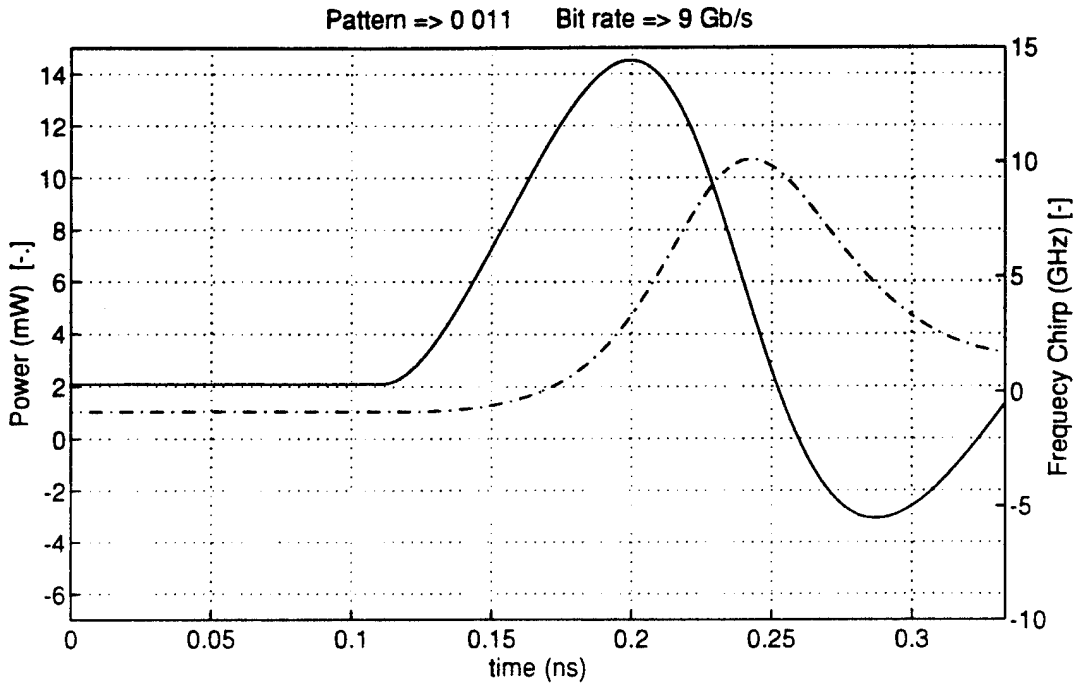

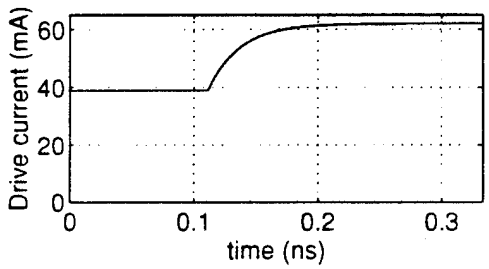

r = 0.1882
Max chirp freq excursion 14.45 GHz
Min chirp freq excursion -5.542 GHz
I_thresh = 0.0335 mA
I_off = 38.86 mA
I_on = 61.98 mA
Case 52

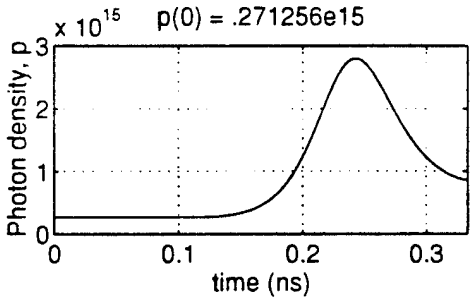

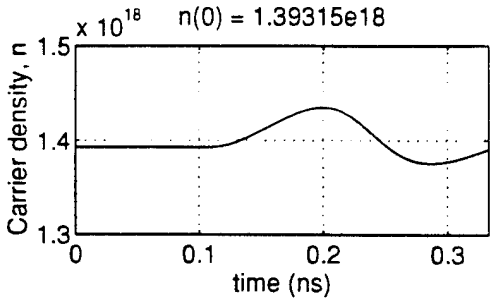

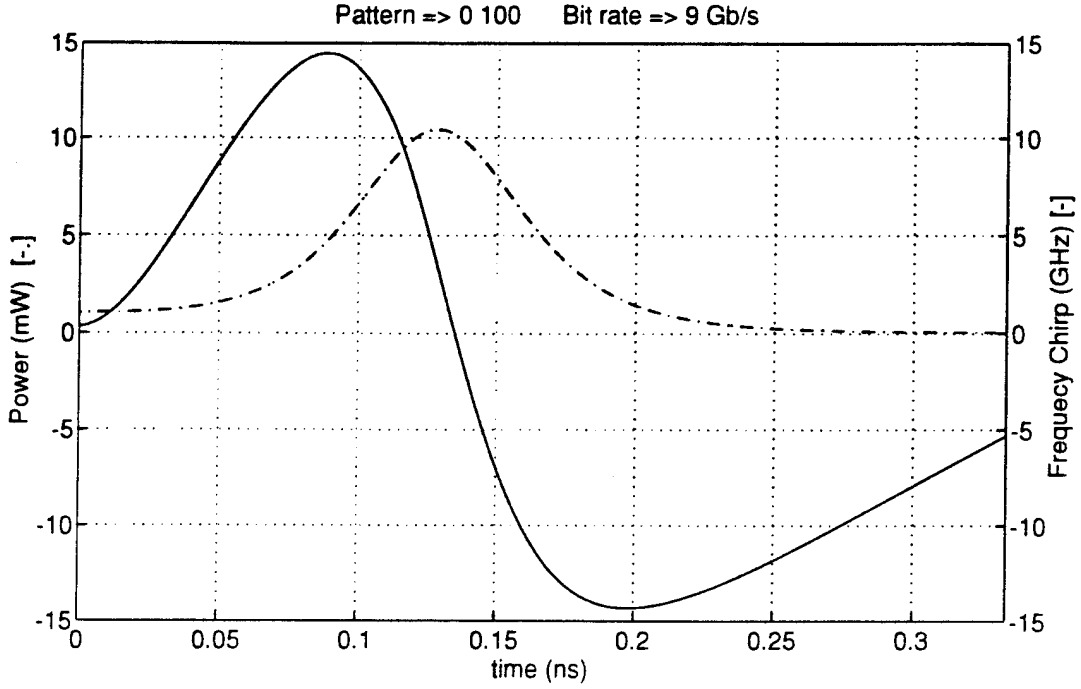

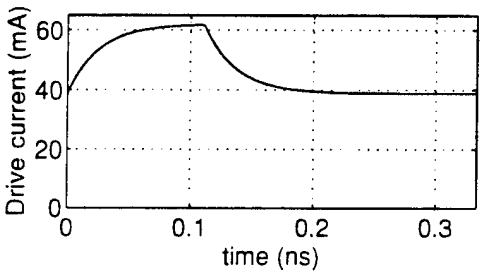

r = 0.1882
Max chirp freq excursion 14.45 GHz
Min chirp freq excursion -14.31 GHz
I_thresh = 0.0335 mA
I_off = 38.86 mA
I_on = 61.98 mA
Case 53

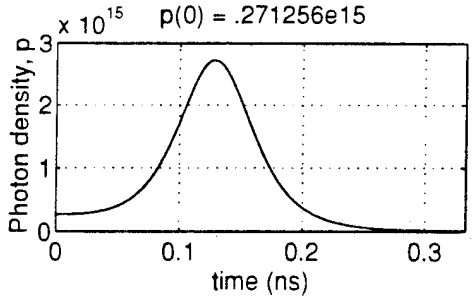

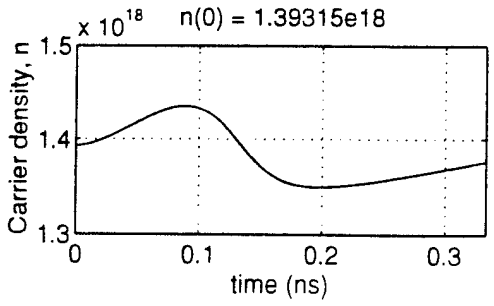

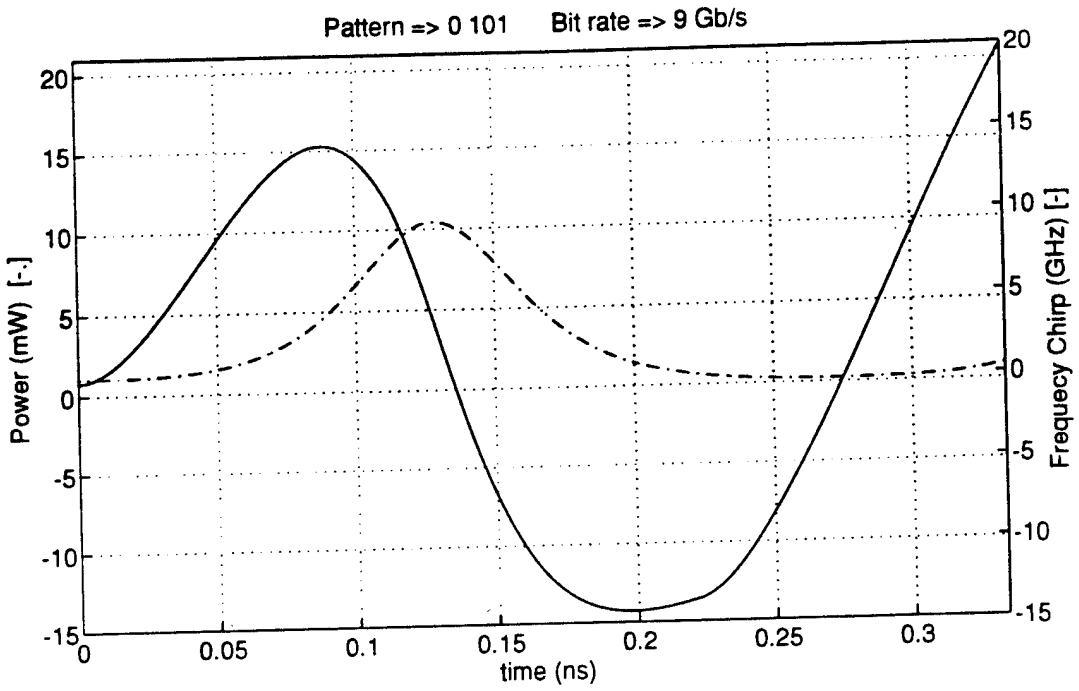

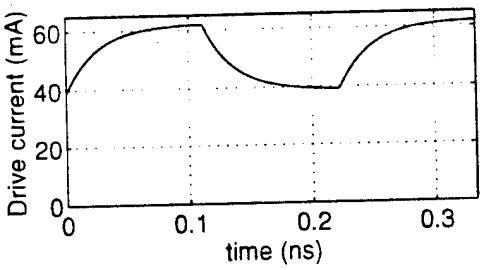

r = 0.1882
Max chirp freq excursion 19.87 GHz
Min chirp freq excursion -14.31 GHz
I_thresh = 0.0335 mA
I_off = 38.86 mA
I_on = 61.98 mA
Case 54

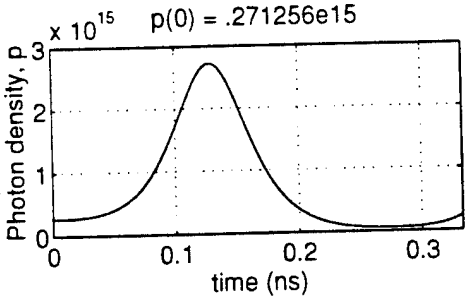

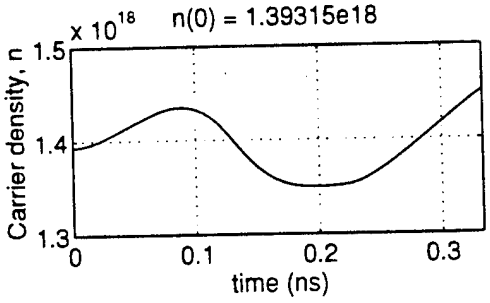

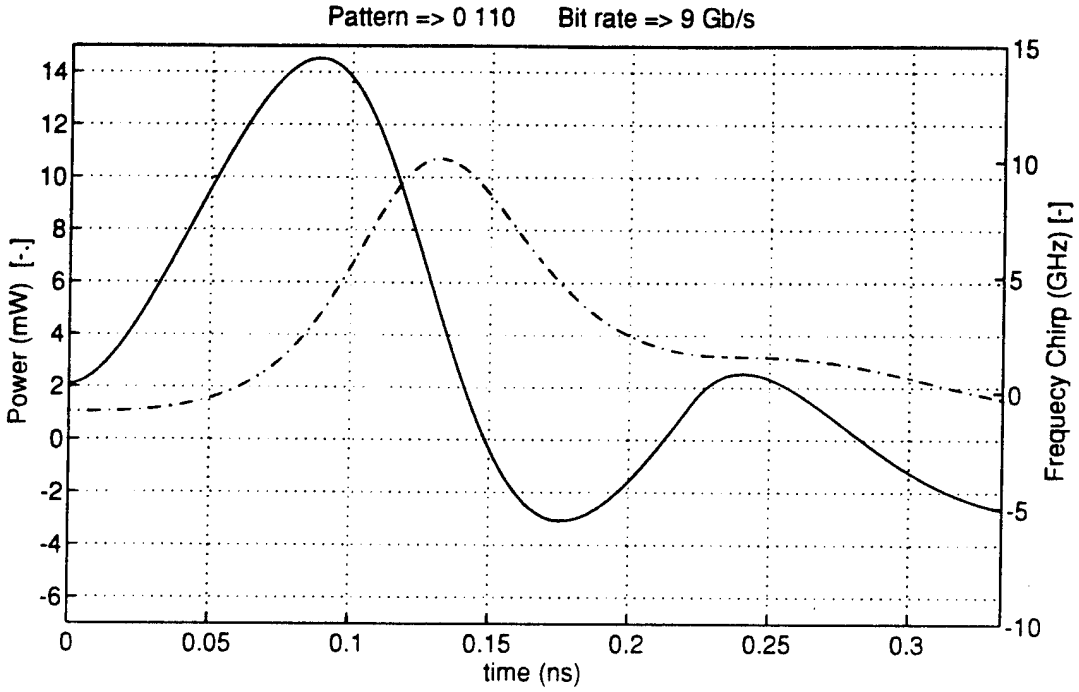

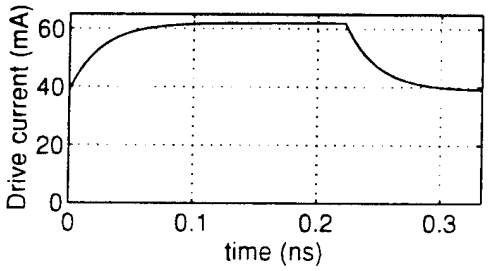

r = 0.1882
Max chirp freq excursion 14.45 GHz
Min chirp freq excursion -5.543 GHz
I_thresh = 0.0335 mA
I_off = 38.86 mA
I_on = 61.98 mA
Case 55

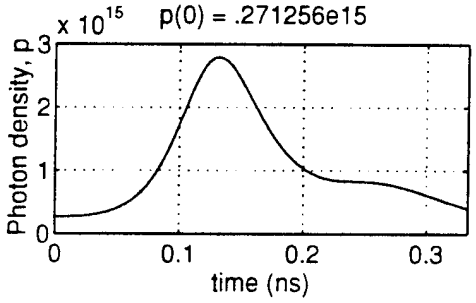

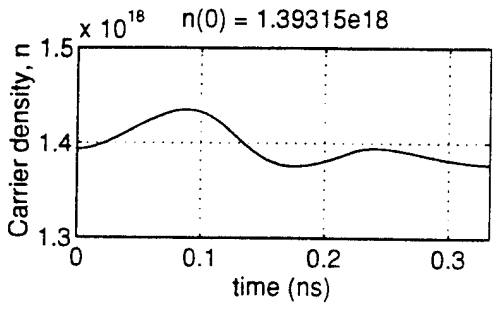

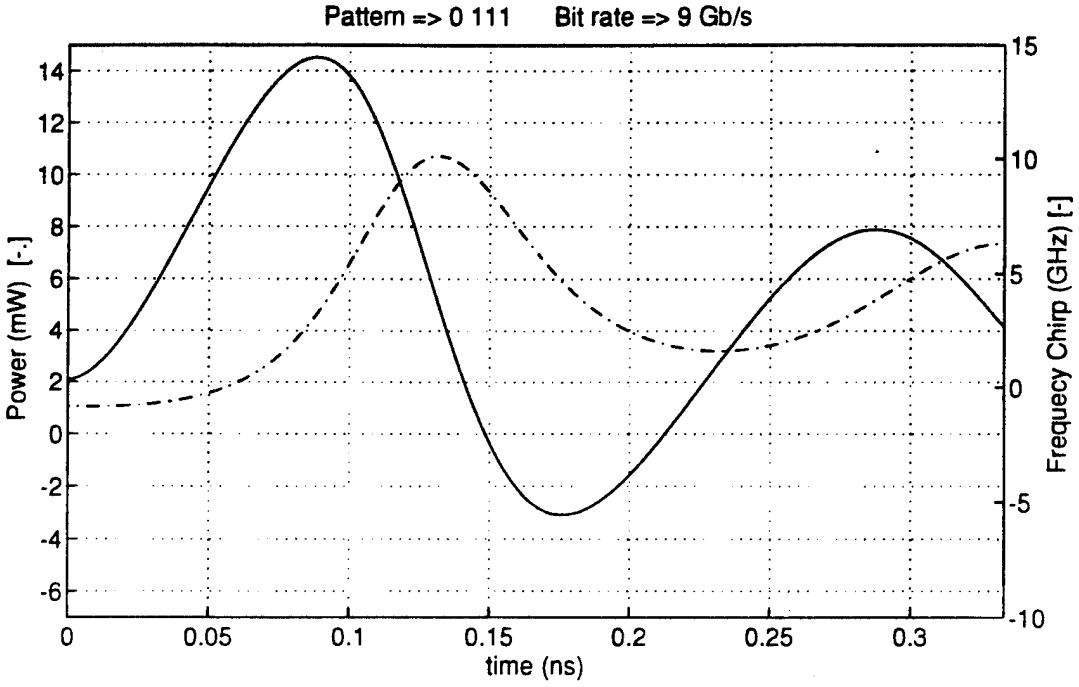

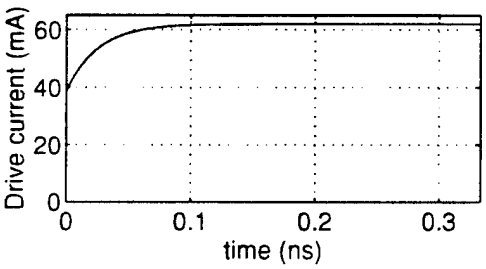

r = 0.1882
Max chirp freq excursion 14.45 GHz
Min chirp freq excursion -5.543 GHz
I_thresh = 0.0335 mA
I_off = 38.86 mA
I_on = 61.98 mA
Case 56

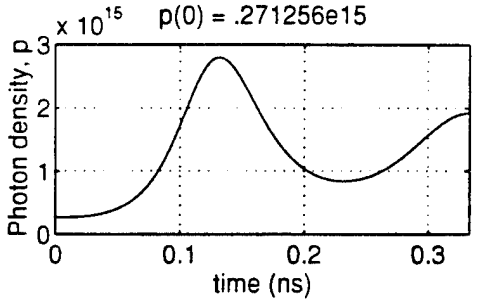

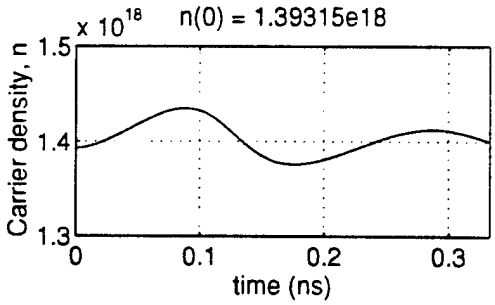

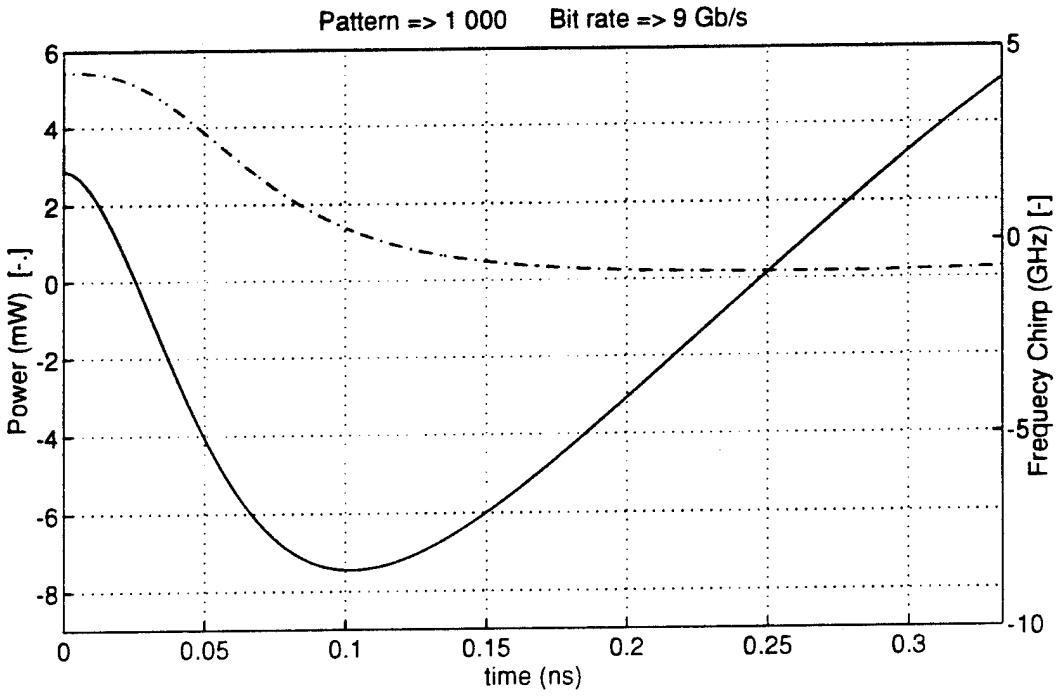

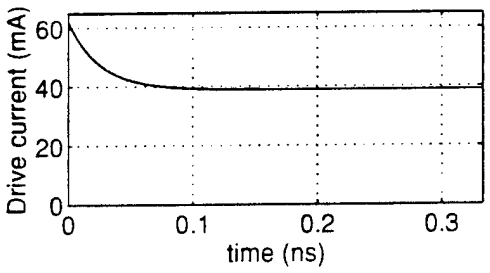

r = 0.1882
Max chirp freq excursion 4.151 GHz
Min chirp freq excursion -8.441 GHz
I_thresh = 0.0335 mA
I_off = 38.86 mA
I_on = 61.98 mA
Case 57

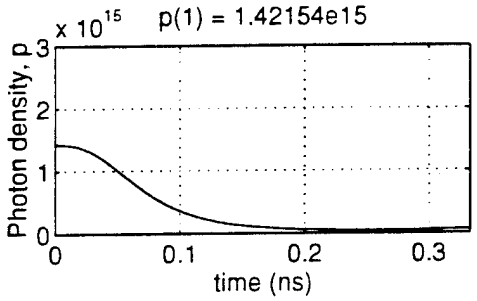

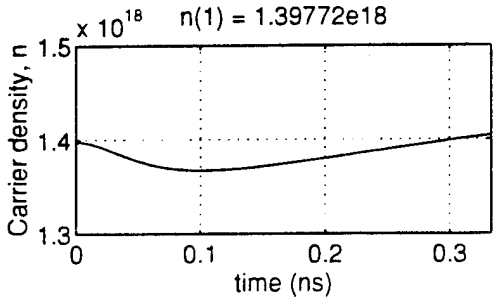

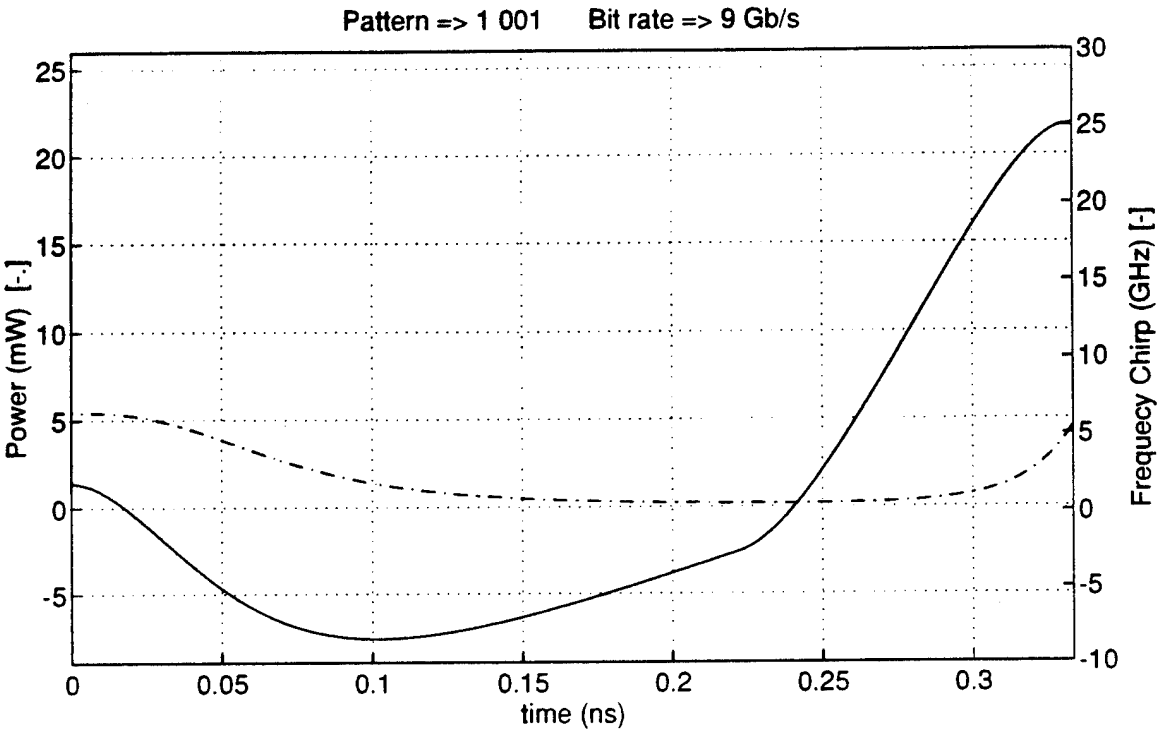

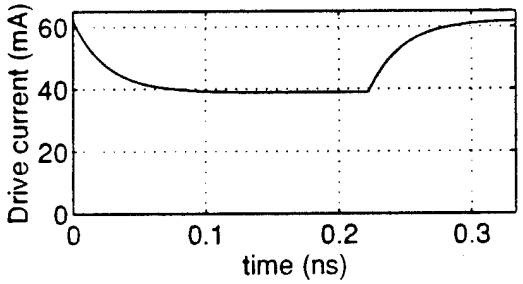

r = 0.1882
Max chirp freq excursion 25.1 GHz
Min chirp freq excursion -8.441 GHz
I_thresh = 0.0335 mA
I_off = 38.86 mA
I_on = 61.98 mA
Case 58

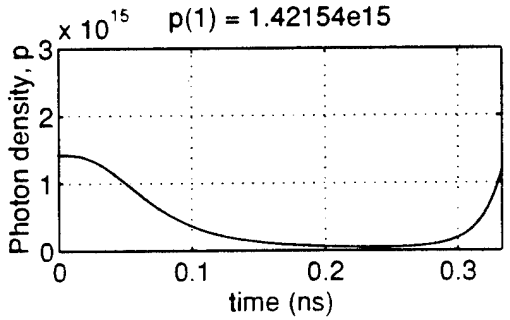

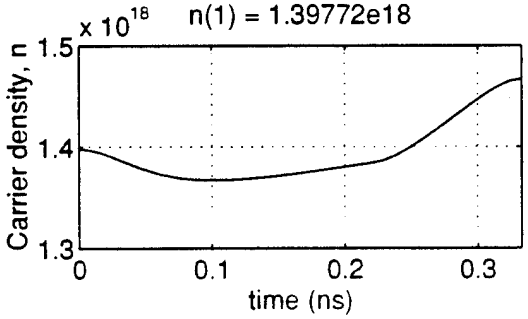

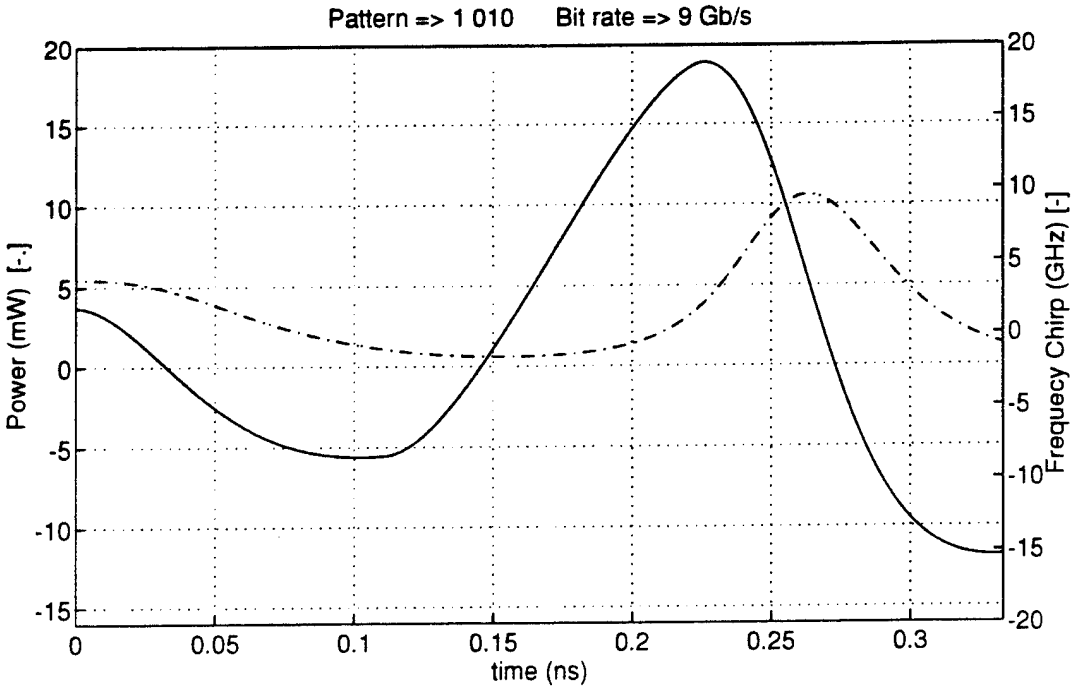

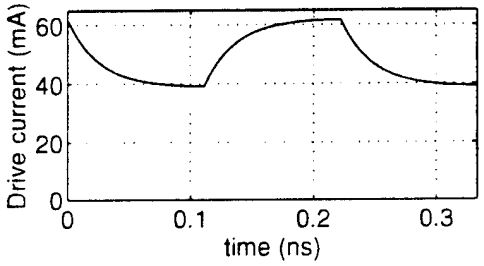

r = 0.1882
Max chirp freq excursion 18.78 GHz
Min chirp freq excursion -15.35 GHz
I_thresh = 0.0335 mA
I_off = 38.86 mA
I_on = 61.98 mA
Case 59

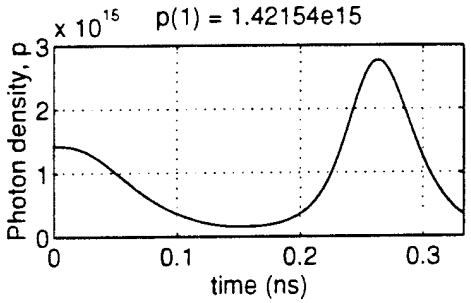

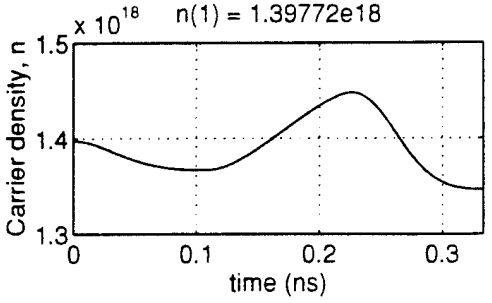

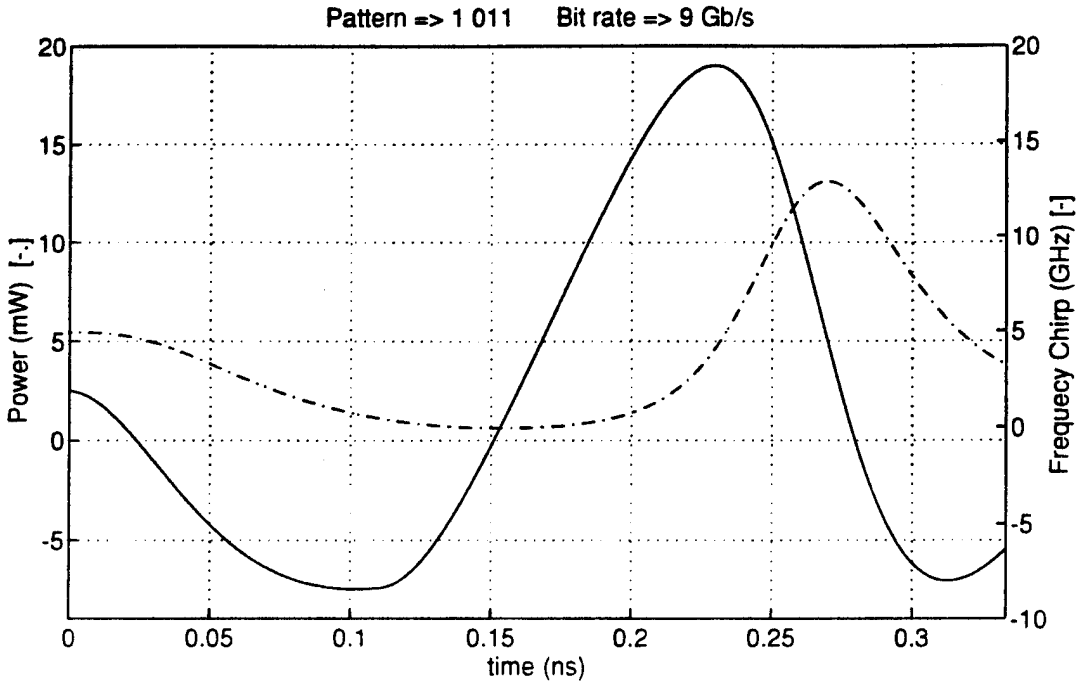

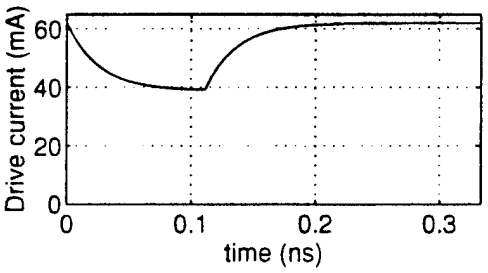

r = 0.1882
Max chirp freq excursion 18.96 GHz
Min chirp freq excursion -8.441 GHz
I_thresh = 0.0335 mA
I_off = 38.86 mA
I_on = 61.98 mA
Case 60

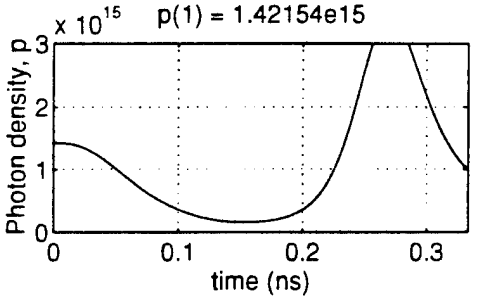

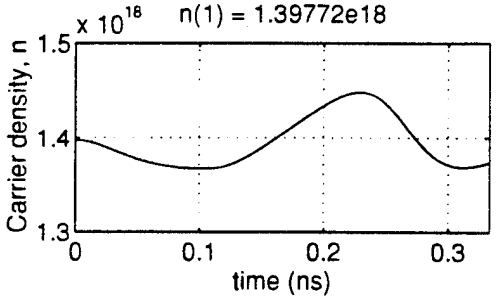

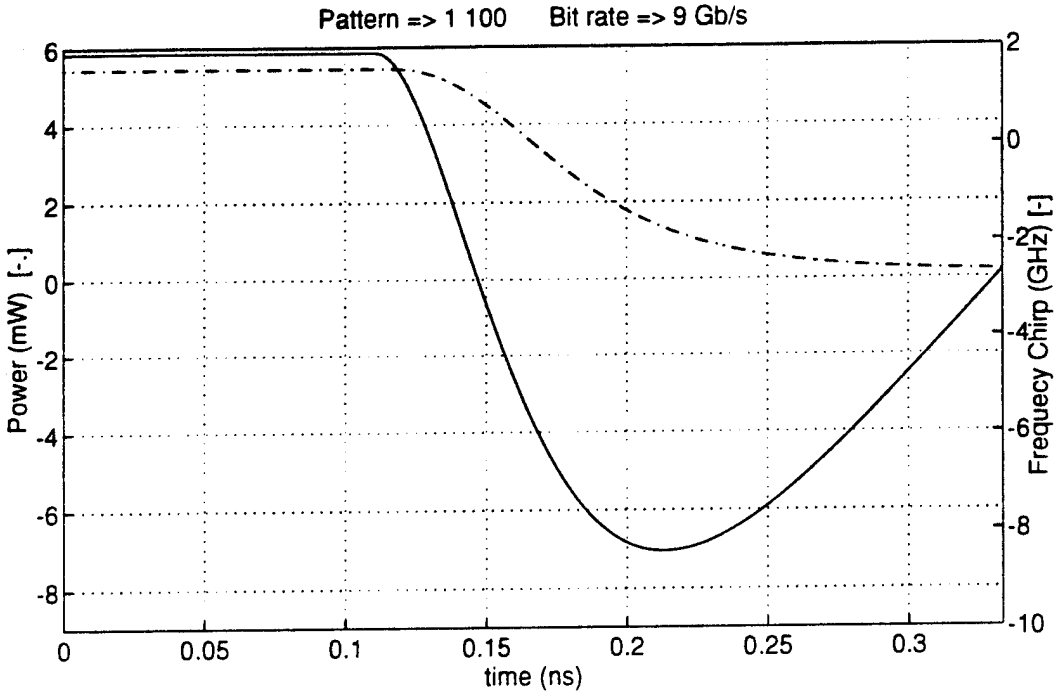

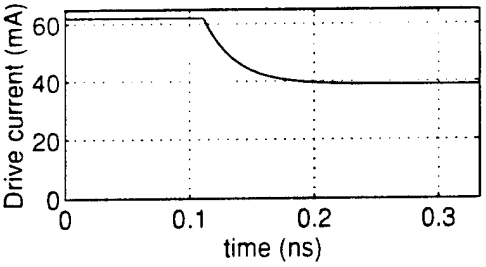

r = 0.1882
Max chirp freq excursion 1.882 GHz
Min chirp freq excursion -8.44 GHz
I_thresh = 0.0335 mA
I_off = 38.86 mA
I_on = 61.98 mA
Case 61

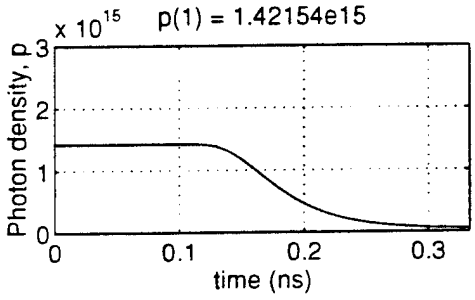

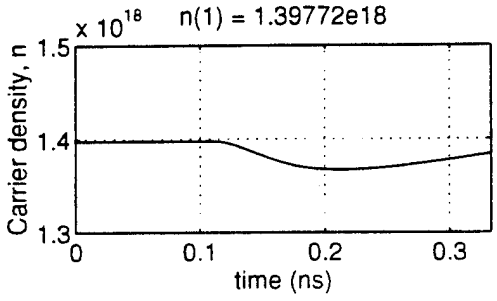

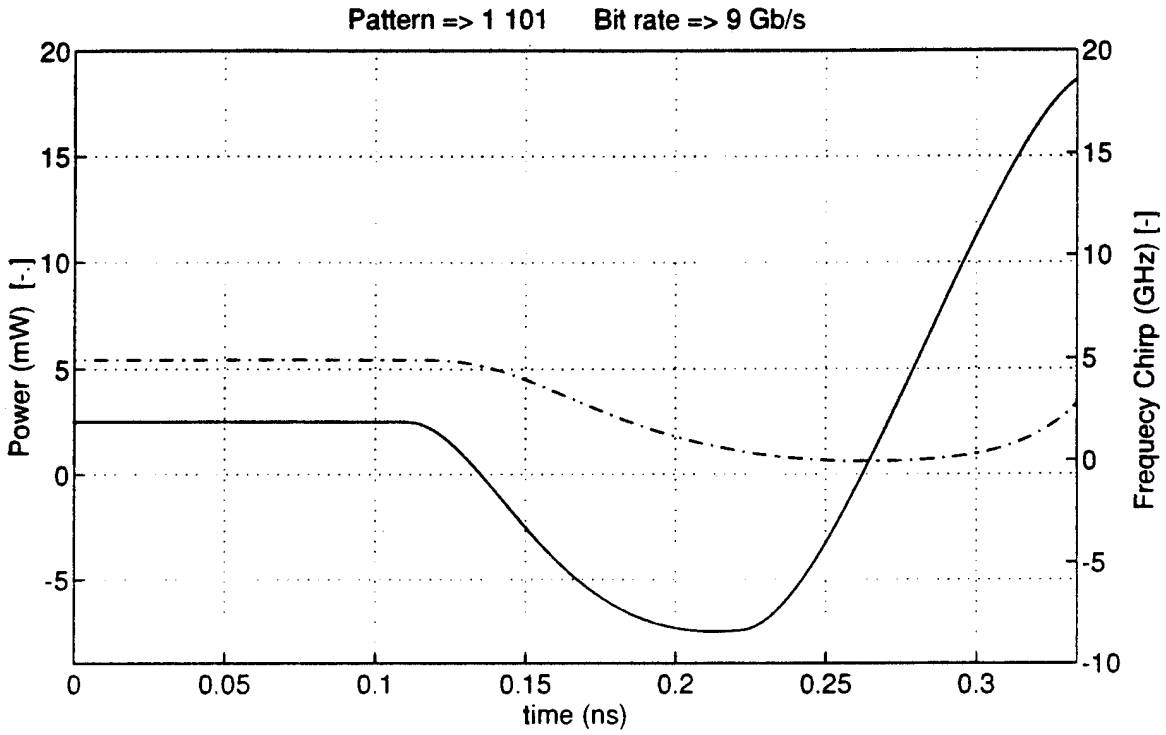

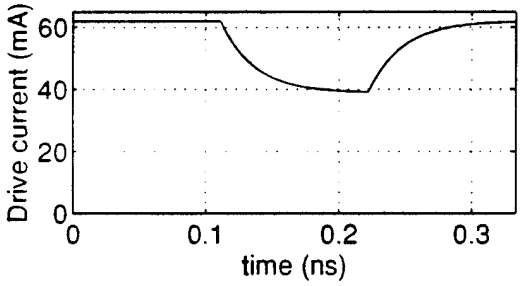

r = 0.1882
Max chirp freq excursion 18.57 GHz
Min chirp freq excursion -8.44 GHz
I_thresh = 0.0335 mA
I_off = 38.86 mA
I_on = 61.98 mA
Case 62

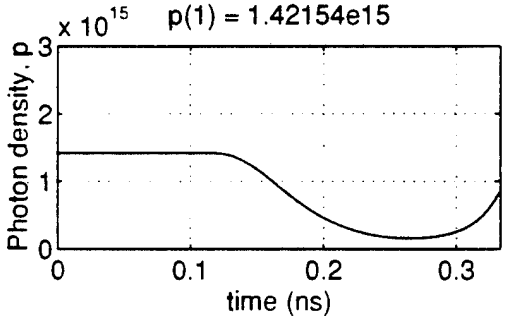

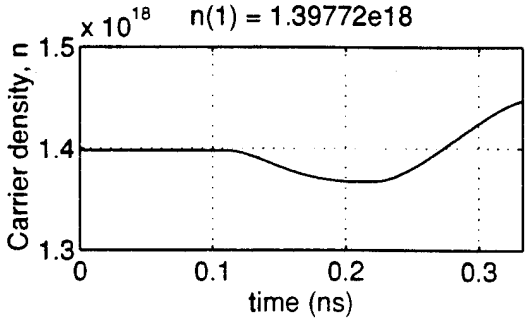

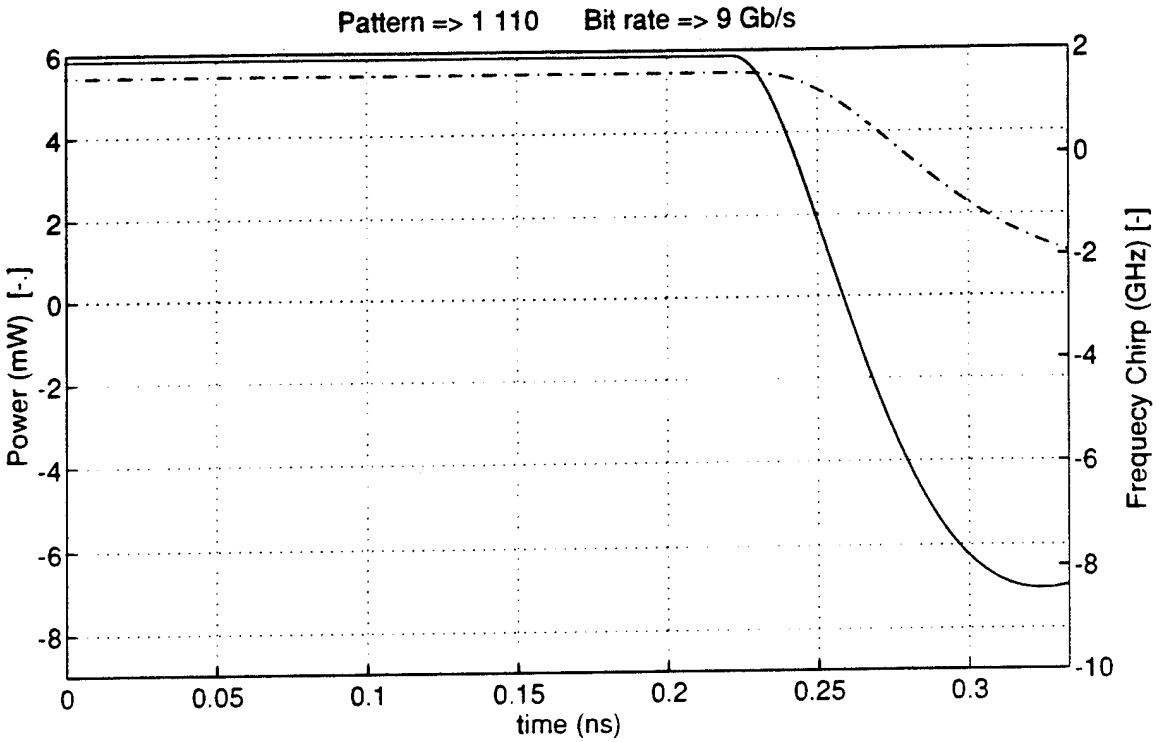

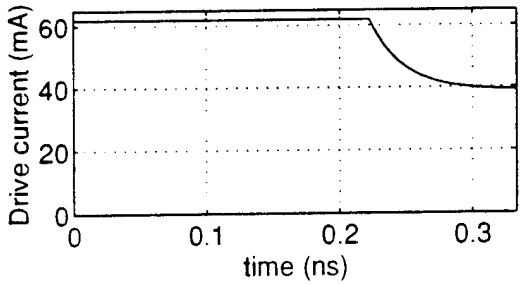

r = 0.1882
Max chirp freq excursion 1.882 GHz
Min chirp freq excursion -8.44 GHz
I_thresh = 0.0335 mA
I_off = 38.86 mA
I_on = 61.98 mA
Case 63

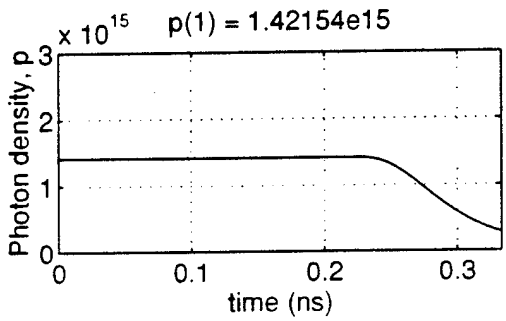

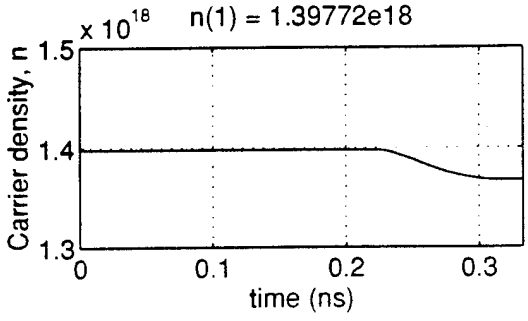

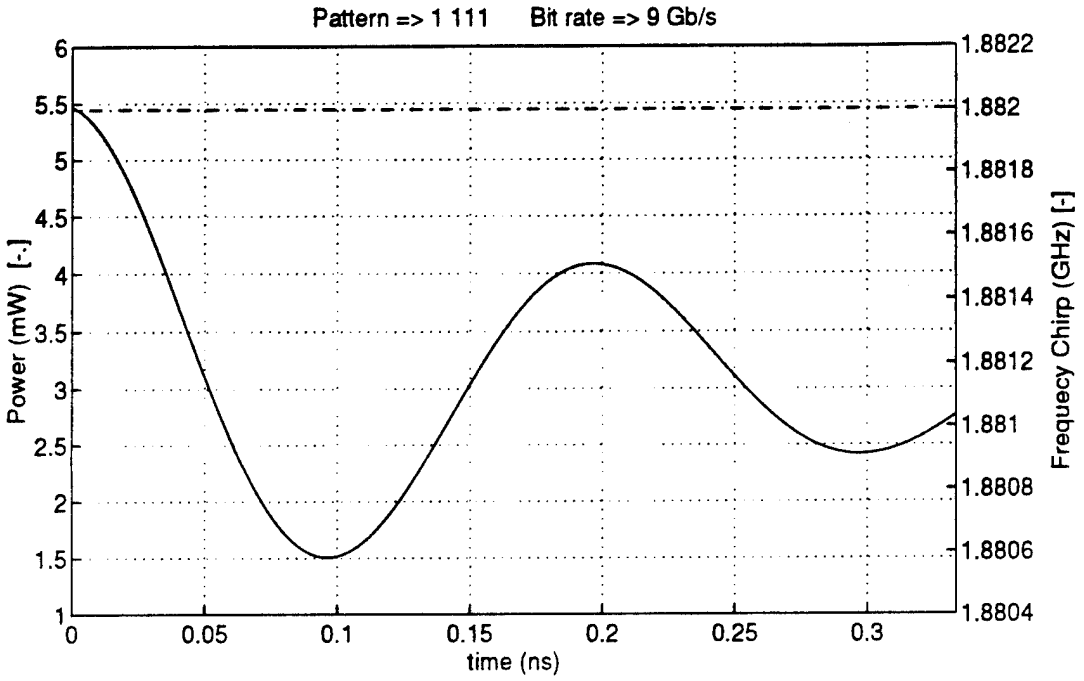

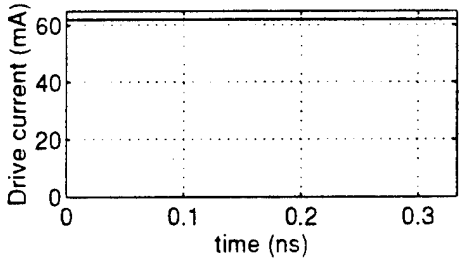

r = 0.1882
Max chirp freq excursion 1.882 GHz
Min chirp freq excursion 1.881 GHz
I_thresh = 0.0335 mA
I_off = 38.86 mA
I_on = 61.98 mA
Case 64

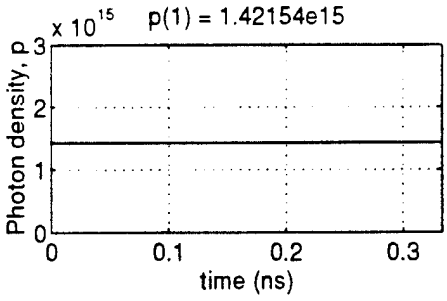

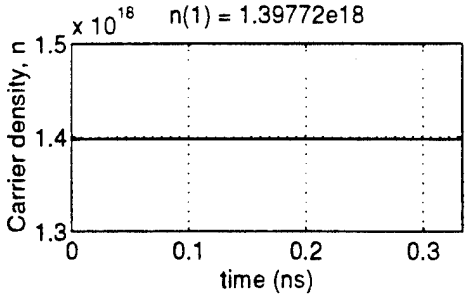

APPENDIX C. EXTINCTION RATIO PLOTS

This appendix contains the maximum frequency excursion versus extinction ratio plots produced from the second set of simulations.

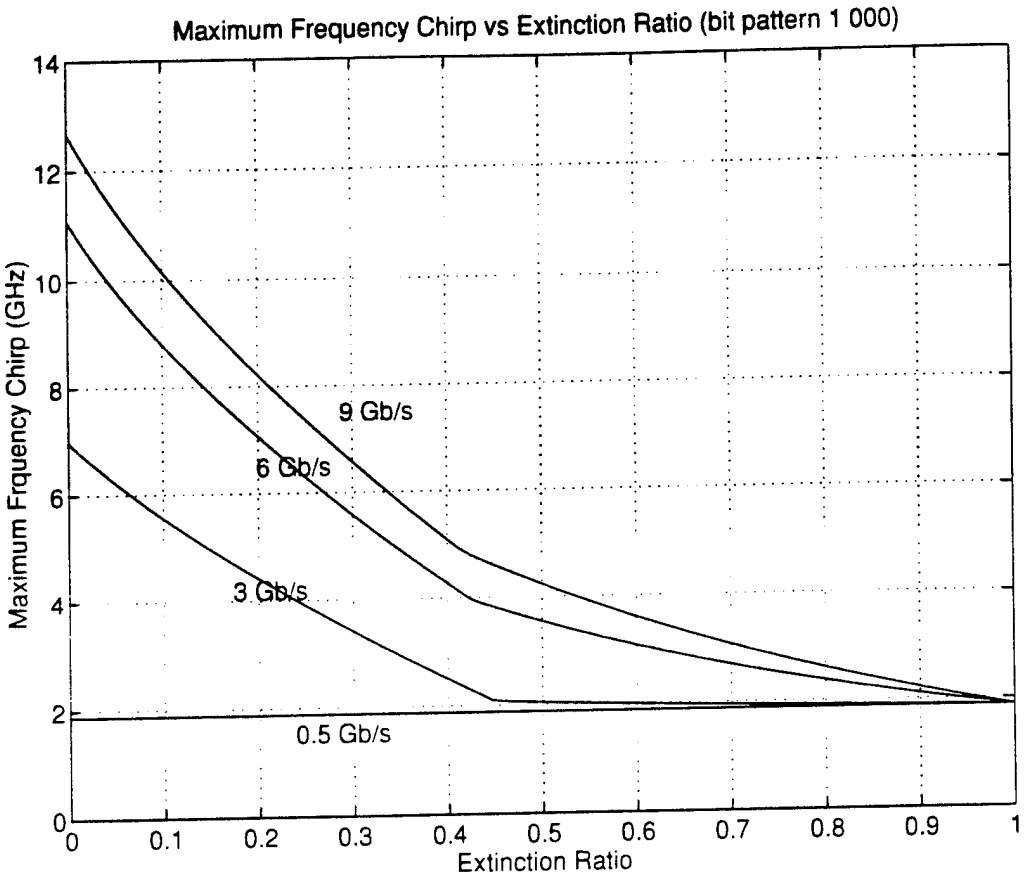
Maximum Frequency Chirp vs Extinction Ratio (bit pattern 1 000)
Maximum Frquency Chirp (GHz)
Extinction Ratio
9 Gb/s
6 Gb/s
3 Gb/s
0.5 Gb/s
0
2
4
6
8
10
12
14
0
0.1
0.2
0.3
0.4
0.5
0.6
0.7
0.8
0.9
1

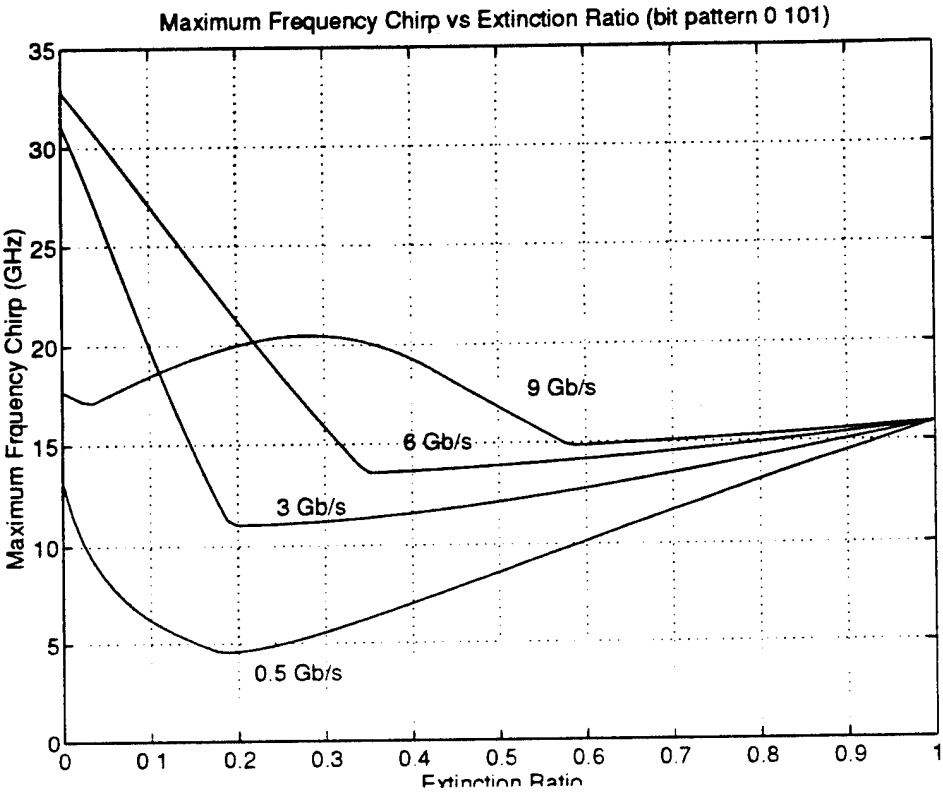
Maximum Frequency Chirp vs Extinction Ratio (bit pattern 0 101)
Maximum Frquency Chirp (GHz)
Extinction Ratio
9 Gb/s
6 Gb/s
3 Gb/s
0.5 Gb/s
0
5
10
15
20
25
30
35
0
0.1
0.2
0.3
0.4
0.5
0.6
0.7
0.8
0.9
1

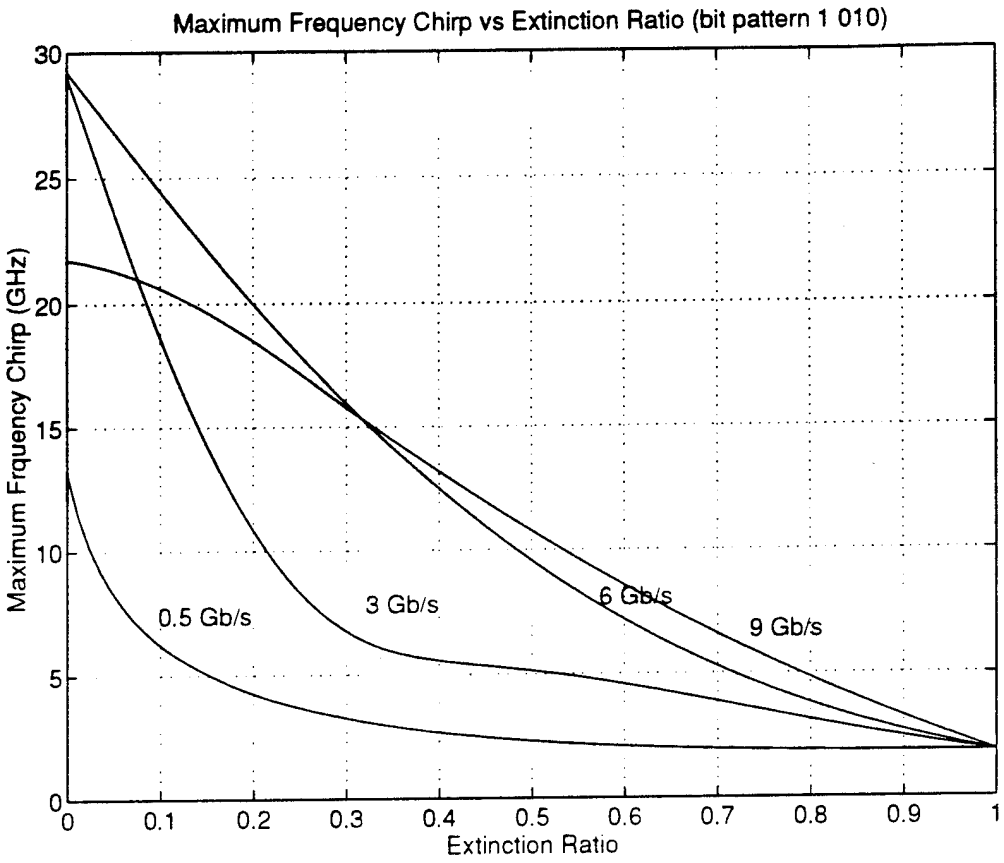
Maximum Frequency Chirp vs Extinction Ratio (bit pattern 1 010)
Maximum Frquency Chirp (GHz)
Extinction Ratio
0.5 Gb/s
3 Gb/s
6 Gb/s
9 Gb/s
0
5
10
15
20
25
30
0
0.1
0.2
0.3
0.4
0.5
0.6
0.7
0.8
0.9
1

LIST OF REFERENCES

1. C-S. Lee, F.F. Tong, K. Liu and D.G. Messerschmitt, "Channel Capacity of Chirp-limited Dense WDM/WDMA Systems using OOK/FSK Modulations and Optical Filters," *J. Light. Technol.*, vol. 10, no. 8, pp. 1148-1161, Aug. 1992.

2. D. Welford, "A Rate Equations Analysis for the Frequency Chirp to Modulated Power Ratio of a Semiconductor Diode Laser," *IEEE J. Quantum Electron.*, vol. 21, no. 11, pp. 1749-1751, Nov. 1985.

3. J.C. Cartledge and G.S. Burley, "The Effect of Laser Chirping on Lightwave System Performance," *J. Light. Technol*, vol. 7, no. 3, pp. 568-573, Mar. 1989.

4. L.D. Westbrook, "Dispersion of Linewidth-broadening Factor in 1.5 μm Laser Diodes, " *Electron. Lett.*, vol. 21, pp. 1018-1019, 1985.

5. K. Kojima. S. Noda, K. Kyuma, and T. Nakayamal, "Measurement of Spectral Linewidth of AlGaAs/GaAs Distributed Feedback Lasers," *Electron. Lett.*, vol. 22, pp. 425-427, Apr. 1986.

6. S. Ogita, Y. Yano, H. Ishikawa, and H. Imai, "Linewidth Reduction in DFB Laser Linewidth by Detuning Effects," *Electron Lett.*, vol. 23, pp. 393-394, Apr. 1987.

7. C.A. Green, N.K. Dutta, and W. Watson, "Linewidth Enhancement Factor in InGaAs/InP Multiple Quantum Well Lasers," *Appl.. Phys. Lett.*, vol. 50, no. 20, pp. 1409-1410, May 1987.

8. Y. Sasai, J. Ohya, and M. Ogura, "Spectral Linewidth and Resonant Frequency Characteristics of InGaAs/InP Multiple Quantum Well Lasers," *IEEE J. Quantum Electron.*, vol. 25, no. 4, pp. 662-667, Apr. 1989.

9. J.P. Powers, *An Introduction to Fiber Optic Systems*, R.D. Irwin, Inc. and Aksen Associates, Homewood, IL, 1993.

INITIAL DISTRIBUTION LIST

1. Defense Technical Information Center.....2
   Cameron Station
   Alexandria, Virginia 22304-6145

2. Library, Code 52.....2
   Naval Postgraduate School
   Monterey, California 93943-5101

3. Chairman, Code EC.....1
   Department of Electrical and Computer Engineering
   Naval Postgraduate School
   Monterey, California 93943-5101

4. Professor John P. Powers, Code EC/Po.....1
   Department of Electrical and Computer Engineering
   Naval Postgraduate School
   Monterey, California 93943-5101

5. Professor Tri Ha, Code EC/Ha 1
   Department of Electrical and Computer Engineering
   Naval Postgraduate School
   Monterey, California 93943-5101

6. Prfessor Randy Borchardt, Code EC/Bt 2
   Department of Electrical and Computer Engineering
   Naval Postgraduate School
   Monterey, California 93943-5101

7. Professor Phillip E. Pace, Code EC/Pa 1
   Department of Electrical and Computer Engineering
   Naval Postgraduate School
   Monterey, California 93943-5101

8. Lt. Burt L. Espe, USN 2
   P.O. Box 2027.
   Bonita, California 91908-2027